Spring 5-10-2013

Molecular Mechanism of Heme Acquisition and Degradation by the Human Pathogen Group A Streptococcus

Mahamoudou Ouattara
Georgia State University

MOLECULAR MECHANISM OF HEME ACQUISITION AND DEGRADATION BY THE HUMAN PATHOGEN GROUP A STREPTOCOCCUS

by

MAHAMOUDOU OUATTARA

Under the Direction of Dr. Zehava Eichenbaum

ABSTRACT

Heme is the major iron source for the deadly human pathogen, Group A Streptococcus (GAS). During infection, GAS lyses host cells releasing hemoglobin and other hemoproteins. This dissertation aims to elucidate the general mechanism by which GAS obtains and utilizes heme as an iron source from the host hemoproteins. GAS encodes a heme relay system consisting of Shr, Shp and the SiaABC transporter. We specifically determine the role of Shr in the heme uptake process, by conducting a detailed functional characterization of its constituent domains. We also undertake to solve the long-standing mystery surrounding the catabolism of heme in streptococci. The studies presented herein established Shr as a prototype of a new family of NEAT-containing hemoproteins receptors. They demonstrate its importance in heme acquisition

by GAS and provide a molecular model for heme scavenging and transfer by the protein. We show that Shr modulates heme uptake depending on heme availability by a mechanism where NEAT1 facilitates fast heme scavenging and delivery to Shp, whereas NEAT2 serves as a temporary storage for heme on the bacterial surface. Finally, we identified and characterized for the first time, a heme oxygenase (HO) in the *Streptococcus* genus which was named HupZ. Sequence comparison between HupZ and several HOs from different structural families indicates that this enzyme is unrelated to any of the previously characterized HOs. However, orthologs of the protein are found in other important pathogens. The structure and the catalytic mechanism of HupZ suggest that it is the representative of a new family of flavoenzymes capable of degrading heme using their reduced flavin cofactor as a source of electrons. Overall, this work contributes significant knowledge to the topic of heme utilization by pathogens and importantly, provides new direct evidence that associates flavins with heme metabolism in bacteria. Thus it sets a new direction in the field and lays the ground for future fundamental and applied discoveries.

INDEX WORDS: Heme acquisition, Heme transfer, Shr, Hemoglobin, Hemoprotein, Kinetics, Protein-protein interaction, Structure/Function, Heme oxygenase, Biliverdin, Bilirubin, *Streptococcus pyogenes*, Iron, UV-visible spectroscopy, Stopped-flow, ELISA

MOLECULAR MECHANISM OF HEME ACQUISITION AND DEGRADATION BY THE HUMAN PATHOGEN GROUP A STREPTOCOCCUS

by

MAHAMOUDOU OUATTARA

A Dissertation Submitted in Partial Fulfillment of the Requirements for the Degree of

Doctor of Philosophy

in the College of Arts and Sciences

Georgia State University

2013

MOLECULAR MECHANISM OF HEME ACQUISITION AND DEGRADATION BY THE HUMAN PATHOGEN GROUP A STREPTOCOCCUS

by

MAHAMOUDOU OUATTARA

Committee Chair: Dr. Zehava Eichenbaum

Committee: Dr. Parjit Kaur

Dr. Chang-Dar Lu

Dr. Adam Wilson

Electronic Version Approved:

Office of Graduate Studies

College of Arts and Sciences

Georgia State University

May 2013

DEDICATION

To my parents and to everyone who directly or indirectly contributed to my education.

"And because all things have contributed to your advancement,

You should include all things in your gratitude."

Wallace D. Wattles

ACKNOWLEDGEMENTS

I express my sincere gratitude to my advisor and mentor Dr. Zehava Eichenbaum for everything and especially for welcoming me in her lab. She is a great person, an excellent scientist, and a wonderful mentor. Her unique mentoring style allowed for creative and independent thinking, while providing great guidance and suggestions. The joyful and friendly working environment in the Eichenbaum lab was created and maintained by the combined efforts of all previous and current lab members. Thank you all for your collaboration and for being good colleagues and friends. I am very thankful to our collaborators that have contributed to this work. In particular, Dr. Dabney Dixon and her lab for helping me understand heme Chemistry, Dr. Giovanni Gadda for allowing us to conduct the stopped-flow experiments. All the kinetic studies were carried out with Dr. Andrea Pennati in Dr. Gadda's lab. I also thank Gadda's lab members for sharing the instruments and for being always helpful. I am thankful to Dr. Irene Weber and to her lab, for helping solve the crystal structure of HupZ. I address a special thanks to Dr. Eric Gilbert for giving me my first research opportunity at GSU, for his kindness, his promptitude to help and for recommending me to Dr. Eichenbaum. I also thank Dr. Gilbert's previous and current lab members, whom I very much enjoyed working with. I thank my committee mebers, Dr. Parjit Kaur, Dr. Chang-Dar Lu and Dr. Adam Wilson, for their advices, suggestions and for the enjoyable committee meetings. Many thanks to the department of Biology, all of the administrative staff and the Biology core facility. I am grateful to the Molecular Basis of Diseases fellowship program for the financial support. I express my heartfelt thanks to my wonderful wife, for her love and support. Finally, I thank my family for its constant encouragement and support in everything I undertake.

TABLE OF CONTENTS

ACKNOWLEDGEMENTS ..... ….. ..v

LIST OF TABLES ix

LIST OF FIGURES x

GENERAL INTRODUCTION…….1

Group A Streptococcus (GAS)……..1

Heme uptake by bacteria……...3

The Sia system……5

Heme oxygenases……6

Research objectives and significance……...9

CHAPTER I: SHR OF GROUP A STREPTOCOCCUS IS A NEW TYPE OF COMPOSITE NEAT PROTEIN INVOLVED IN SEQUESTERING HAEM FROM METHEMOGLOBIN…….....11

Introduction 1……..11

Results 1……...15

Discussion 1…….27

Materials and Methods 1……34

CHAPTER II: MECHANISMS OF INTRA- AND INTER-MOLECULAR HEME TRANSFER BY THE SHR PROTEIN OF GROUP A STREPTOCOCCUS……44

Introduction 2……..44

Results 2……...47

Discussion 2…….55

Materials and Methods 2……62

CHAPTER III: DISCOVERY OF HUPZ, THE FIRST STREPTOCOCCAL HEME OXYGENASE……..68

Introduction 3……..68

Results 3……...71

Discussion 3…….77

Materials and Methods 3……80

GENERAL DISCUSSION……..84

The novel Hb binding motif in Shr NTD…….....84

Significance of heme reduction by Shr…….....85

Basis for the heme degradation by HupZ alone……86

Potential *in vivo* reducing partners of HupZ…….88

HupZ heme degradation products…….89

REFERENCES..... ……135

LIST OF TABLES

Table 1: Primers used in Chapter 1……...42

Table 2. Plasmids used in Chapter 1 43

Table 3: Strains and Plasmids used in Chapter 2…….66

Table 4: Primers used in Chapter 2……...67

Table 5: Strains and Plasmids used in Chapter 3…….83

Table 6: Primers used in Chapter 3……...83

LIST OF FIGURES

Figure 1: Schematic representation of the sia operon and the Shr protein and Heme relay in Group A Streptococcus……...92

Figure 2: Catalytic mechanism of heme oxygenases…….93

Figure 3: Shr proteins in pyogenic Streptococci and *Clostridium novyi*…...…….95

Figure 4: Hemin binding and reduction by rShr……..95

Figure 5: Heme binding by Shr fragments……97

Figure 6: Methemoglobin binding by Shr fragments……..99

Figure 7: Binding of extracellular matrix proteins by Shr……100

Figure 8: Heme transfer from methemoglobin to apoNTD-N1…….101

Figure 9: Growth analysis of *shr* deletion mutants…….102

Figure 10: Heme acquisition from MetHb……..104

Figure 11: Kinetics of heme transfer from metHb to apoNTD-N1……...105

Figure 12: Kinetics of heme transfer from metHb to the full-length Shr…….106

Figure 13: Kinetics of heme transfer from Shr NEAT domains to apoShp…….107

Figure 14: Heme transfer from holoNEAT1 to apoNEAT2……...108

Figure 15: Proposed model of heme acquisition by the *S. pyogenes* Sia system……..109

Figure 16: Heme binding by HupZ……..110

Figure 17: Heme degradation by HupZ without external electron donors……..111

Figure 18: heme degradation by HupZ using CPR-NADPH as reducing equivalent…….112

Figure 19: heme degradation by HupZ with ascorbic acid as a source of electrons……...113

Figure 20: Phylogenetic tree of bacterial heme oxygenases generated from ClustalW2 (EMBL-EBI)……...113

Figure S1: NEAT alignment…….114

Figure S2: UV-visible spectra of hemin chloride……115

Figure S3: Heme reconstitution of NEAT2 protein fragment……...115

Figure S4: Binding of rShr to holo and apo hemoglobin……...116

Figure S5: Heme transfer from methemoglobin to apoNTD-N1.……..117

Figure S6: Growth phenotype of wild type GAS and Shr mutants……...118

Figure S7: Recombinant His-MBP-NEAT1 and Shp-His proteins……...119

Figure S8: Western blot analysis with anti-Hb antibodies of Shr elution fractions……120

Figure S9: Heme reconstitution spectra of MBP-NEAT1 and MBP……121

Figure S10: MetHb binding by Shr fragments……...122

Figure S11: Heme transfer from metHb to Shr fragments……123

Figure S12: Comparative spectra of NTD-N1 and metHb…….124

Figure S13: Spectral differences between metHb and NTD-metHb complex……..125

Figure S14: Gel filtration elution profiles of NTD-N1 and aldolase…….126

Figure S15: The observed rate constants for the third phase of heme transfer from metHb to Shr……...128

Figure S16: UV-visible spectrum of purified holoShp……...129

Figure S17: SDS-PAGE analysis of NEAT2 elution fraction after incubation with NEAT1……130

Figure S18: characterization of the purified recombinant HupZ…….131

Figure S19: UV-visible absorbance spectra of heme bound HupZ and of the heme-pyridine adduct……..132

Figure S20: Characteristic color of HupZ-CPR-NADPH heme degradation reaction……....132

GENERAL INTRODUCTION

Group A Streptococcus (GAS)

Also known as *Streptococcus pyogenes*, GAS is a Gram-positive coccus that grows in chains of variable lengths. When grown on blood agar, the bacterium produces hemolysins, which achieve complete lysis of red blood cells. This is known as β-hemolysis and results in clearing zones around the bacterial colonies. GAS is an important human pathogen that causes a large number of diseases with different clinical manifestations. Repeated GAS infections can also lead to severe immune sequelae such as acute glomerulonephritis and rheumatic fever [1-3]. Cases of non-invasive infections caused by the bacterium worldwide are estimated at 700 million each year. Of these, about 650,000 progress to serious invasive infections resulting in about 25% mortality [1]. Invasive GAS infections often require substantial treatments including surgical procedures. To date no approved commercial vaccine is available against streptococcal infections [4,5]. The *emm* gene encodes the antigenically variable surface M-protein, which serves as a basis for GAS classification into serotypes. More than 100 M-types have been identified [2,6].

The most common disease caused by GAS is pharyngitis or “strep-throat”. It is often associated with symptoms such as sore throat, enlarged and tender lymph nodes in the neck, headache, fever, malaise and sometimes abdominal pain. Several rapid tests based on bacterial surface determinants or throat cultures are used to diagnose GAS infections [2]. Penicillin is the preferred drug for the treatment of GAS pharyngitis, but alternative antibiotics such as amoxicillin, erythromycin or oral cephalosporins are used in case of allergy to penicillin. Other

non-invasive GAS illnesses include the skin infections impetigo and cellulitis, and the acute inflammation of the skin and superficial lymphatic vessels erysipelas [7]. Non-invasive GAS diseases can progress to life-threatening invasive infections, which may also occur as a result of a direct inoculation due to penetrating injuries. One of the most severe invasive GAS infections is the streptococcal gangrene or necrotizing fasciitis, also known as “flesh-eating disease”. The common clinical manifestations of the disease are severe pain at the site of infection even without an obvious sign of skin break, swelling, fever, confusion, stretched and discolored overlying skin. Successful treatment of necrotizing fasciitis dependents on the early diagnosis of the illness and requires timely and intense surgical procedures in conjunction with antimicrobial treatments [7,8].

GAS owes its ability to cause a wide variety of diseases to a multitude of virulence factors. Few examples include the M-protein, which mediates the attachment of the bacteria to host’s epithelial cells and participates in the bacteria resistance to opsonophagocytosis. Escaping phagocytosis is accomplished through binding of molecules such as fibrinogen, C4b-binding protein, immunoglobulin Fc portion and the H factor, which inhibits the complement system [9-11]. A capsule composed of hyaluronic acid, a normal component of human tissue, surrounds invasive GAS strains allowing them to escape the host immune response [12,13]. The streptococcal pyrogenic exotoxins (SPEs) are superantigens that can trigger massive uncontrolled release of cytokines and lead to septic shock. Several enzymes produced by GAS also facilitate the breaking down of DNA, blood clots and proteins including immunoglobulins. GAS exotoxins streptolysins O and S produce pores in the membrane of leukocytes and erythrocytes, causing their lysis and the release of hemoglobin which can serve as a nutrient to the pathogen [14-17].

Heme uptake by bacteria

Iron is an essential micronutrient for nearly all living systems including bacteria. In many enzymes, iron is a catalytic center involved in redox reactions, which carry out vital cellular processes. These include electron transport, DNA and amino acids synthesis, photosynthesis, activation of oxygen and peroxide reduction. Iron is one of the most abundant elements on earth and exists mainly in the oxidized ferric (Fe^{3+}) or the reduced ferrous (Fe^{2+}) forms. Fe^{3+} is highly insoluble and represents the most predominant iron species in aerobic and neutral pH conditions. In contrast, Fe^{2+} is more soluble but is present only in a limited number of anoxic and strongly acidic habitats. Therefore, in spite of its abundance, iron is biologically unavailable in the environments inhabited by the vast majority of microorganisms [18-20].

In mammalian hosts, bacteria are also confronted with iron-restricted environments, where free iron is sequestered in extracellular (transferrin, lactoferrin) and intracellular (ferritin) host proteins with high affinity for the metal. However, the most abundant source of iron in mammals consists of heme, an iron-protoporphyrin IX molecule. It is a hydrophobic tetrapyrrole with an iron center that can partition into membranes, thus impairing lipid bilayers. Free heme also induces non-enzymatic redox reactions which generate toxic amounts of reactive radicals causing severe cell damage [21]. Because of its toxicity, only minute amount of free heme is allowed intracellularly or in the blood. The large majority of heme is sequestered by host proteins, mainly hemoglobin (Hb), a tetrameric protein with two α- and two β-chains. Each subunit of the tetramer binds one heme molecule. Hb is confined in erythrocytes where it serves as the oxygen transporter in its reduced form, oxyhemoglobin. When released from the red blood cells, the tetrameric Hb spontaneously oxidizes to the dimeric methemoglobin (metHb) [22].

The total blood Hb concentration in healthy human adult is estimated between 1.9 and 2.3 mM, suggesting a relative abundance [23]. Though, it remains highly unavailable to pathogens, as free extracellular Hb is readily scavenged by the serum protein, haptoglobin [24].

To survive the hostile iron-restricted conditions they face during infection, pathogens evolved sophisticated machineries to scavenge and import heme from host hemoproteins that are released upon hemolysis and tissue damage. Strategies used by many Gram-negative pathogens involve hemophores, which are extracellular bacterial proteins secreted in the environment to bind free heme or to scavenge heme from host proteins. The heme-bound hemophore subsequently recognizes and delivers its heme to a specific receptor at the cell surface, leading to heme import inside the cell [20,25]. Examples of hemophore-mediated heme uptake mechanisms are described in Gram-negative pathogens *Serratia marcescens*, *Pseudomonas aeruginosa*, *Yersinia enterocolitica* and *Hemophilus influenza* [26-31]. Some Gram-negative organisms also rely on outer-membrane receptors for heme acquisition. Examples include HmbR and HpuA in Neisseria species, ChuA in *E. coli* and *HutA* in Vibrio cholerae [32-36].

The predominant heme uptake mechanism adopted by Gram-positive organisms uses a protein relay. Heme is obtained from host molecules by a surface receptor, then transferred in a cascade manner through the thick peptidoglycan layers to a cognate ABC transporter, which carries it across the cytoplasmic membrane [37,38]. Heme capture and transfer by surface receptors are in the vast majority of cases mediated by a protein domain referred to as NEAT (NEAr-iron Transporter). This protein module is encoded in a variable copy number in the genome of several Gram-positives, in close vicinity of iron ABC transporters. NEAT domains are approximately 125 amino acids long, sharing low primary sequence homology and a

predicted secondary structure of mostly β-strands [39]. Heme acquisition systems that employ NEAT-containing receptors are widely studied in *Staphylococcus aureus*, *Bacillus* species and *Listeria monocytogenes* [37-39]. In addition to these surface receptors, secreted NEAT-hemophores are also found in Gram-positives. Some examples are illustrated by IsdX1 and IsdX2 in *Bacillus anthracis* [40,41]. Recently, heme relays which do not involve NEAT-containing receptors were reported in *Corynebacterium diphteriae* and *Mycobacterium tuberculosis* [42,43].

The Sia system

GAS utilizes heme and host hemoproteins as iron source during infection [44]. The two known heme acquisition pathways in GAS involve of the streptococcal iron uptake (*siu*) and the streptococcal iron acquisition (*sia*) systems [45,46]. The *sia* system consists of a conserved ten-gene operon which is directly repressed by the iron-dependent regulator MtsR [45,47] (fig. 1A). The first gene in the operon encodes Shr (streptococcal hemoproteins receptor), a 145 kDa composite surface protein. Shr contains two NEAT domains, a series of leucin-rich repeats located between the NEAT domains and a unique N-terminus region (NTD) with two copies of a domain of unknown function (DUF1533). Shr C-terminus has a hydrophobic region with a positively charged tail that allows the attachment of the protein to the cytoplasmic membrane. Unlike other NEAT-containing receptors, Shr does not contain a cell wall-anchoring motif, but is exposed to the extracellular environment by protruding through the cell wall. The protein binds a wide range of ligands such as heme, Hb, Hb-haptoglobin complex and the extracellular matrix

(ECM) proteins fibronectin and laminin [45,48]. Shr does not share significant homology to any characterized heme or hemoprotein receptor and its composition and overall domain architecture are unique (fig. 1A). The second gene in the *sia* locus codes for the heme-binding surface protein Shp (streptococcal hemoprotein), which has a NEAT-like domain considered as remotely related to the NEAT family [49,50]. The third, fourth and fifth genes of the *sia* operon express a heme ABC transporter (SiaABC or HtsABC) where SiaA serves as the heme ligand-binding lipoprotein component. Heme coordination in SiaA is mediated by a set of two different axial ligands which were recently identified as Met79 and His229 [51,52]. These two residues also participate in the release of heme from SiaA in a two-step process that involves a conformational change of the protein [52]. From Shr, heme is efficiently transferred to Shp, which in turn gives it to SiaABC where it is carried across the cytoplasmic membrane [53,54] (fig. 1B). The function of the proteins encoded by the remaining genes of the operon is unknown. The importance of heme uptake in GAS virulence was demonstrated in zebrafish and mouse models [46,48,55]. While Shr is proposed to participate in heme acquisition, its direct role in the scavenging and transfer of heme from hemoproteins to Shp has not been established. In addition, the function and importance of the receptor domains are yet to be studied.

Heme oxygenases

Heme imported into the bacterial cytoplasm is incorporated to intracellular proteins as a cofactor, or utilized by the organism as an iron source. In the latter case, the release of iron from the porphyrin ring requires the activity of enzymes such as deferrochelatases [56] or heme

oxygenases (HO) [57]. However, the mode of action of deferrochelatases in iron release from heme is controversial, as contradictory data are provided by different studies [58]. HOs catalyze the oxidative cleavage of the methene (*meso*) carbon bridges of the porphyrin at the positions α, β, γ or δ [59]. There are three known mammalian HOs: the inducible HO-1 [60], the constitutive HO-2 [60] and HO-3 whose functional relevance is unknown [61]. HO-1 is highly induced by chemical agents and a variety of stress conditions and is found in highest concentration in the spleen and liver. HO-2 is unresponsive to exogenous stimuli and is preponderant in the brain and testes [60]. The two isoforms participate in many physiological processes such as neuroprotective activities, iron homeostasis, protection from heme toxicity and oxidative stress [60,62-65].

Heme degradation by HOs requires a source of reducing equivalents, which is provided in mammals by NADPH and cytochrome P450 reductase (CPR). The reaction typically results in equimolar quantities of iron, carbon monoxide (CO) and biliverdin (fig. 2). The heme catabolite, biliverdin is further converted to bilirubin by biliverdin reductase [60,66]. Each of the heme degradation products participates in a number of physiological processes. Iron for example, is necessary for erythropoiesis and participates in oxygen transport. Biliverdin and bilirubin are powerful antioxidants and CO is a vasodilator that is believed to regulate adequate blood flow [63,67-70]. CO is also a signaling molecule that modulates many physiological processes. It was shown to be important for the neovascularization during wound healing and it stimulates the proliferation of endothelial cells. Moreover, CO has been recognized as a neurotransmitter, an immunomodulator and an anti-inflammatory agent [71].

Homologues of the human HO-1 are found in bacteria. The first example of bacterial HO, named HmuO, was identified and characterized in the pathogen *Corynebacterium diphteriae* [72,73]. Ever since, several other bacterial HOs that share sequence homology with HmuO were identified. These include HemO in *Neisseria meningitides* and *Clostridium* species, PigA (also known as pa-HO) and BphO in *Pseudomonas aeruginosa* [74-78]. Structurally, this group of enzymes consists of monomeric α-helices with similar folds. They specifically degrade heme at the α-*meso* carbon, producing α-biliverdin [66]. The only exception in this group is PigA which has an unusual β-*meso* and δ-*meso* regiospecificity, producing a mixture of β- and δ-biliverdins [77]. The fate of the biliverdin produced in bacterial cell is unknown in most cases, since a homologue of mammalian biliverdin reductase has been identified only in cyanobacteria [79,80].

Two bacterial HOs, IsdG and IsdI, distinct in structure from the mammalian HO-1 were found in *Staphylococcus aureus*. These enzymes are part of the *isd* locus which also encodes the NEAT-containing hemoprotein receptors and their cognate ABC transporter. IsdG and IsdI are β-barrel homodimers containing two active sites and catalyze the formation of the atypical product, staphylobilin. This contrasts with the canonical production of biliverdin [81-83]. Homologues of IsdG with similar structural and biochemical features were characterized in *Bradirhyzobium japonicum*, *Mycobacterium tuberculosis*, *Bacillus anthracis* and *Staphylococcus lugdunensis* [84-87]. Additional heme degrading enzymes which do not resemble HO-1 or IsdG-like groups of proteins were also described. ChuS in *Escherischia coli* has a unique structure consisting of two central sets of antiparallel β-sheets, each flanked by two pairs of α-helices [88]. Heme degradation by ChuS in presence of reducing partners produced CO and spectral features that suggest biliverdin production. However, the final products of the reaction were not identified

[88]. HemS, a protein with high sequence homology to ChuS was uncovered in *Yersinia enterocolitica* and *Bartonella henselae* [89,90]. Like ChuS, the products of HemS-catalyzed reaction are undefined [90].

A new family of bacterial HOs with no sequence or structural homologies to previously described groups of HOs has been emerging recently. Members of this class of enzymes include Cj1613c in *Campylobacter jejuni*, HugZ in *Helicobacter pylori* and HutZ in *Vibrio cholerae* [91-93]. These enzymes share weak sequence similarities with FMN-binding proteins and exist as dimers [92-95]. The crystal structures of HugZ and HutZ are almost identical besides a mismatch of one amino acid residue in β6 of HutZ. Both proteins adopt a split β-barrel fold which characterizes FMN-binding proteins, but actual FMN binding by these proteins was not demonstrated [94,95]. Similar to PigA, HugZ cleaves the heme tetrapyrrole at the δ-*meso* carbon, producing δ-biliverdin and HutZ is hypothesized to produce both β- and δ-biliverdin [92,93].

In GAS and all other streptococci, the mechanism by which iron is released from heme is unknown. Homologues belonging to the families of the HOs described above have not been identified in the *Streptococus* genus.

Research objectives and significance

The purpose of this dissertation is to elucidate the general mechanism by which GAS obtains and utilizes heme as an iron source from the host hemoproteins. We specifically determine the role of Shr in the heme uptake process by conducting a detailed functional characterization of the constituent domains of the protein. We also undertake to conduct a

comprehensive kinetic study to establish the intra- and inter-molecular flow of heme in the streptococcal system. Moreover, we aimed to solve the long-standing mystery surrounding the catabolism of heme in streptococci.

The studies presented herein establish Shr as a prototype of a new family of NEAT-containing hemoproteins receptor. They demonstrate the importance of Shr in heme acquisition by GAS and provide a molecular model for heme scavenging and transfer by the protein. This work also brings to light a unique mechanism for the modulation of the heme acquisition process. We have identified and begun characterizing the first heme oxygenase in GAS. This new enzyme seems to represent a novel HO expressed by several streptococcal pathogens. Overall, this dissertation adds a significant knowledge to the blooming topic of heme utilization as an iron source by pathogens and lays the ground for future fundamental and applied discoveries.

CHAPTER I

SHR OF GROUP A STREPTOCOCCUS IS A NEW TYPE OF COMPOSITE NEAT PROTEIN INVOLVED IN SEQUESTERING HAEM FROM METHEMOGLOBIN

Introduction 1

Acquisition of iron from host sources is of vital importance to many pathogenic bacteria during the course of infection. Mammalian hosts limit the availability of free extracellular iron to levels around 10^{-18} M [96] by producing iron-chelating proteins such as lactoferrin and transferrin or by storing it in ferritin within the cells. However, nearly 75% of the iron in the human body is found in the form of heme, where it is incorporated into the protoporphyrin ring and serves as a prosthetic group of hemoglobin, myoglobin, and some enzymes [97,98]. The process of obtaining heme from the host by Gram-positive pathogens often involves binding of heme or hemoproteins by bacterial receptor proteins which then deliver the heme to a membrane-bound ABC transporter for translocation to the cytoplasm [20,98]. The first Gram-positive heme transporter to be described was the *hmu* (hemin/hemoglobin utilization) system of *Corynebacterium diptheriae* [99]. The *hmuTUV* genes share homology with Gram-negative heme-ABC transporters such as found in *Yersinia pestis* [100,101]. HmuT, which is localized to the cell membrane, binds hemin or hemoglobin directly; HmuU and V are the membrane permease and the ATPase, respectively. Two membrane anchored heme-receptors, HtaA and HtaB, encoded by the *hmu* chromosomal locus were recently described and hypothesized to work

in conjunction with the HmuTUV transporter in heme acquisition and transport across the cell envelope [102]. Inside the *Corynebacterium* cytoplasm, a heme-oxygenase enzyme, HmuO, degrades the heme and releases the iron for use by the pathogen [73,103].

The heme uptake system studied in the most detail in Gram-positive bacteria is that from *Staphylococcus aureus* and is termed the Isd (iron-regulated surface determinants) system. In the Isd system, the IsdA, B and H (HarA) proteins are covalently attached by the SrtA sortase enzyme to the cell wall, where they interact with a variety of ligands including heme, hemoglobin, hemoglobin-haptoglobin complex, fibrinogen, and fibronectin [104-107]. These proteins obtain heme and deliver it across the cell wall and the cell membrane in a cascade fashion *via* IsdC and the IsdEF ABC-transporter [82,83,108]. Unlike the surface exposed Isd receptors, IsdC is embedded deep in the cell wall by a dedicated sortase, SrtB [106,109,110]. Ligand binding by IsdA, B, C, and H (HarA) is mediated by NEAT (Near transporter) domains, which are found in one or more copies in each of the receptor proteins.

The NEAT domain is a protein motif first identified in 2002 that is encoded in variable copy number near ABC iron transporter genes in the chromosomes of several Gram-positive bacterial species [39]. It is approximately 125 amino acids long with low primary sequence homology and a predicted secondary structure of mostly β strands [39]. Expressed in recombinant form, the isolated NEAT domains of IsdA, IsdC, IsdH (HarA) and the second NEAT domain of IsdB (IsdBN2) have been studied and manifest different ligand preferences. The IsdA NEAT domain has fibrinogen binding ability [104] and binds heme [111]. The IsdC NEAT domain binds heme but not proteins such as hemoglobin, fibrinogen or fibronectin [112-114]. The third NEAT domain of IsdH (IsdHN3) is also exclusively a heme-binding domain

[115,116] and IsdBN2 binds heme as well [117]. In contrast, the two N-terminal NEAT domains of IsdH (HarA) have demonstrated binding to hemoglobin and hemoglobin/haptoglobin, respectively [105,118,119]. Secreted or cell wall anchored NEAT proteins which are central to heme acquisition pathways were identified in other Gram-positive pathogens including *Listeria monocytogenes* [120], *Bacillus anthracis,* [121,122], and *Bacillus cereus* [123].

Heme uptake has also been studied in Group A Streptococcus, a β-hemolytic pathogen that uses host heme-containing proteins as an iron source [44]. One system involves a 10 gene iron-regulated operon that has been termed Sia (Streptococcal iron acquisition) [45]. Genes three through five in the cluster (*siaABC* or *htsABC* [53]) encode an ABC transporter that shares significant homology with heme or siderophore transporters found in other bacterial species [45]. The second gene in the operon, *shp,* encodes a surface protein with β-sandwich fold similar to that of NEAT domains and is considered a distal member of the NEAT family [49]. Shp protein has been reported to bind heme at the cell surface and transfer it to SiaA (HtsA), the lipoprotein component of the ABC transporter [53]. The heme coordination of SiaA has recently been elucidated by further biophysical studies and is described as six-coordinate and low-spin, employing methionine and histidine as axial ligands [51]. The first gene in the *sia* operon encodes the Shr (streptococcal hemoprotein receptor) protein. Shr is a large (145kDa) hydrophilic protein that does not share significant overall homology with known heme or hemoprotein receptors [45]. The first studies of Shr revealed that it plays a role in iron acquisition. It was observed to bind hemoglobin and hemoglobin-haptoglobin complex [45]. The transfer of heme from Shr to the protein Shp has also been described [54]. Shr was recently demonstrated to bind the extracellular matrix proteins fibronectin and laminin, suggesting that it

also acts as an adhesin [48]. A null *shr* mutant is attenuated for virulence in a zebrafish model for necrotizing fasciitis, underscoring the importance of Shr to the infection process *in vivo* [48].

Shr has two NEAT domains, but its overall domain architecture, which includes a unique N-terminal domain and a series of leucine-rich repeats, is different from any of the characterized heme and hemoprotein-binding receptors, including the NEAT-containing Isd proteins of *S. aureus.* Shr also lacks a cell wall anchoring motif typical of the Isd receptor proteins of *S. aureus*; at the C terminus, Shr has a hydrophobic segment with a positively charged tail that threads the protein through to the cytoplasmic membrane. It was recently demonstrated that Shr spans the cell wall and is exposed to the extracellular environment [48]. Shr is proposed to participate in the acquisition of heme by GAS and its delivery to Shp and/or the SiaABC transporter. The uptake of heme from hemoproteins by Shr or its direct role in iron acquisition has not been shown, however. In this study we establish the function of Shr in hemoglobin use and heme uptake by GAS. We analyze the functional domains of this receptor protein and present evidence that the mechanism of heme uptake by Shr is different from that of the characterized Isd proteins. We suggest that Shr is a prototype of a new group of NEAT proteins involved in heme uptake.

To distinguish between the two NEAT domains in Shr, the closest NEAT domain to the amino group will be referred to as NEAT1 and the second NEAT domain from the amino group will be referred to as NEAT2.

Results 1

Shr is a composite NEAT protein found in pyogenic streptococci and C. novyi

NEAT domains are key ligand-binding domains used by receptor proteins involved in heme acquisition and translocation in Gram-positive bacteria. We recently reported that the GAS Shr protein has two NEAT domains that are separated by an LRR region [48]. Additional sequence examination also identified an EF-hand motif between the first NEAT domain of Shr and the LRR segment (residues 532 and 544) and two copies of a short domain with unknown function, DUF1533 (residues 61-123 and 203-269) in the N- terminal region of Shr (Fig. 3). *In silico* analysis using the web based SMART tool [124,125], reveals that there are about 160 NEAT domains in 80 proteins encoded by Gram-positive bacteria from the Firmicutes phylum. Most of these NEAT-proteins are Isd-like molecules, which contain one or more copies of NEAT domains, a leader peptide, and in some cases a sortase recognition signal or other type of cell-wall binding region. A few proteins consist of an LRR segment in addition to export signals and NEAT domain(s); these include the heme uptake protein of *B. cereus,* IlsA [123], and the following hypothetical proteins A0PYT7 (*C. novyi*), O6HLL6 & O6HNR0 (*B. thuringensis*), and 073BH4 (*B. cereus*). Shr appears to be the first characterized protein with DUF1533 domains. An examination of the database demonstrated that DUF1533 is found in duplication in putative proteins with unknown function from the Clostridia class and in two species of *Paenibacillus*. Therefore, the domain architecture of Shr is different and more complex than most of the previously described NEAT receptors or the hypothetical NEAT-proteins found in bacterial

genomes. The complex domain arrangement of Shr is intriguing and suggests that it evolved by joining several domains found separately in bacterial proteins of Firmicutes. Shr orthologues, which share identical or nearly identical domain architecture, are found in *C. novyi* as well as in the pyogenic streptococci *S. equi zooepidemicus* and *S. dysgalactiae* (Fig. 3). A *shr* orthologue is found in the genome of *S. equi* subsp. *equi* as well; however, a frame shift mutation results in a truncated protein [126]. All streptococcal Shr orthologues are closely related in their primary amino acid sequence (58-86% identity) while the *C. novyi* orthologue shares fewer identical residues (~30%). Intriguingly, the *shr* gene in all the streptococci is part of a 10-gene cluster which is homologous to the *sia* operon of GAS. The *shr* gene in *C. novyi* on the other hand, is found in a genomic locus that encodes only a putative LRR-NEAT protein (A0PYT7). Together these observations suggest that Shr may represent a new type of composite NEAT protein family.

Shr obtains heme from solution and reduces ferric heme to ferrous heme

Shr binding to hemoproteins *in vitro* and its genomic location in the *sia* operon together with the heme binding protein, Shp, and the SiaABC heme-transporter, suggest that Shr is involved in heme acquisition and transport by GAS [45]. This hypothesis was recently supported by the observation that purified Shr transfers heme to Shp [54]. The sequestering of heme from host proteins by Shr was not previously demonstrated, however, and the mechanism of heme and hemoprotein binding has not been investigated. To characterize heme uptake by Shr, a histidine-tagged recombinant protein (rShr) [45] was prepared and analyzed (Fig. 4A). Shr is readily

reduced following treatment with dithionite or oxidized by ferricyanide, producing the corresponding absorption spectra with maxima around 410 nm for the bound ferric heme or 430, 540 and 560 nm for the ferrous heme [54]. In this study we found that the spectral properties of rShr after ferricyanide treatment were almost identical to those without treatment, with Soret bands at 412 and 414 nm (Fig. 4B green and blue lines, respectively). On the other hand, the addition of D, L-dithiothreitol (DTT) resulted in a shift in the absorption peak to 427 nm (Fig 4B red line) and the production of more resolved peaks at 536 and 566 nm, spectral characteristics of ferrous heme-protein complexes [127]. Therefore, our data indicate that rShr was purified from *E. coli* as mostly ferric heme complex. In the course of Shr purification, we observed that heme-bound rShr was considerably more stable than the heme-free protein, and that the addition of hemin to the *E. coli* culture prior to harvesting the cells resulted in a higher production of intact rShr.

Heme binding by rShr was investigated further by monitoring the changes in the UV-visible spectrum following the addition of increasing amounts of hemin (heme with ferric iron) to the protein solution. The addition of free hemin resulted in a concomitant increase in rShr-bound hemin, as was indicated by the growing absorbance at 414 nm (Fig. 4C). Surprisingly, the UV-visible spectrum of rShr following the hemin addition also revealed growing absorption peaks at 427 and at 540 and 564 nm as well (Fig. 4C insert). Removing the free heme by dialysis did not lead to changes in the spectrum (data not shown). The growing peaks at 427, 540 and 564 nm indicate a simultaneous increase in rShr-bound ferrous heme. The addition of hemin to rShr was done under aerobic conditions (using an open tube and vigorous mixing) and in the absence of reducing agents. Therefore, the observed rise in rShr-bound heme suggests that Shr reduces

the added hemin. The addition of ferricyanide to the protein solution following titration with 20 μM hemin resulted in a shift of the absorption peak from 427 back to 410 nm. The 410/280 absorbance ratio that is indicative of the ferric heme load in Shr [54] was changed from 0.59 to 0.75. Oxidation with ferricyanide also eliminated the peaks at 540 and 564 nm (Fig. 4D). Therefore, ferricyanide was able to oxidize the ferrous iron of the Shr bound heme, confirming that the changes in Shr spectrum seen following the addition of free hemin were due to a reversible reduction of the protein-bound hemin. It was previously reported that Shr could be purified from *E. coli* as a mixture of ferric and ferrous iron heme [54]. Our observations suggest that Shr has an inherent ability to reduce the ferric heme and to provide a stable environment for the produced ferrous complex. The autoreduction activity is a very intriguing characteristic of Shr. To the best of our knowledge, it is the first report of heme reduction by a bacterial heme receptor.

NEAT1 and NEAT2 are both heme-binding domains in Shr

Heme binding by the Isd proteins is imputable to their NEAT domains [128]. However some NEAT domains have been reported to not bind heme. For example, IsdH NEAT3 domain binds heme [115-117], whereas IsdH NEAT1 and IsdH NEAT2 domains interact only with hemoglobin and haptoglobin [116]. Isd NEAT domains hold the heme within a hydrophobic pocket through several conserved residues including two invariant tyrosines, one of which coordinates the iron (Tyr 166 in IsdA) and a second residue (Tyr 170 in IsdA) that interacts with both the heme pyrrole ring and the coordinating tyrosine [111]. Sequence analysis revealed that

not all of the conserved residues in the Isd heme binding sites are found in Shr NEAT domains (Fig. S1); most significantly, both of the NEAT domains in Shr are missing the iron-coordinating residue Tyr 166, and only NEAT1 has the Tyr 170. Interestingly, the second heme binding protein coded by the *sia* operon, Shp, does not use tyrosine residues to coordinate the heme iron, and instead utilizes two methionines [49].

To investigate heme acquisition by Shr, several recombinant proteins containing one or more of the component domains of Shr were constructed with an N-terminal fusion to the *Strep*-Tag epitope. These Shr variants include recombinant proteins with the amino terminal domain of Shr (NTD) or the amino terminal domain through NEAT1 (NTD-N1), the NEAT1 domain, and the NEAT2 region (Fig. 5A). The recombinant proteins were overexpressed, purified by FPLC using a *Strep*-Tactin column, and analyzed. The protein containing only the NEAT1 region turned out to be highly insoluble and was therefore excluded from further investigations. SDS-PAGE analysis confirmed the production and purification of the recombinant Shr protein fragments, revealing protein bands at the expected size for each construct: 61 kDa (NTD-N1), 42 kDa (NTD), and 23 kDa (NEAT2, Fig 5B).

The Shr protein variants that contained the first NEAT domain (NTD-N1) or the second NEAT domain (NEAT2) both had red color when purified and a UV-visible spectrum consistent with bound heme. The purified NTD-N1 protein showed a significant absorbance at 410 nm indicating that it was co purified with ferric heme (Fig. 5C). In contrast, the optical spectrum of the purified NTD fragment showed no band at the Soret region indicating that it did not contain heme (Fig. 5D). To test the heme binding ability by Shr's N-terminal region, the recombinant NTD protein was incubated with increasing concentrations of hemin. The optical spectrum of the

protein after incubation showed no absorption at the Soret region. Instead, similar to the spectrum of free heme (Fig. S2), a broad peak at 390 nm was formed as increasing amounts of hemin were added, indicating an accumulation of unbound heme in the NTD protein solution (Fig. 5E). Therefore, the NEAT1 domain contained within the NTD-N1 protein is responsible for the ferric heme binding observed by this protein fragment.

Unlike the ferric-heme load of the NTD-N1 protein, the optical spectrum of the purified NEAT2 protein suggests that it is purified with a mixture of ferric and ferrous heme. NEAT2 spectra consistently had a significant Soret band at 428 nm along with sharp peaks at 535 nm and 564 nm. However, variations in the intensity of absorbance at 410 and 428 nm (indicating different ratio of the protein bound ferrous and the ferric forms) were observed in the spectrum of NEAT2 from different protein preps (Fig. 5F and the blue line in Fig. S3). To further investigate heme binding by NEAT2, the protein was titrated with increasing concentrations of free hemin and the UV-visible spectrum was monitored (Fig. S3). As observed with the full length Shr, the addition of free hemin resulted in concomitant increase of absorption at around 410 nm as well as 428, 535 and 564 nm. NEAT2 was then treated with ferricyanide and the UV-visible spectrum was taken after 5 and 30 min intervals and after 24 h. Within 5 min after addition of ferricyanide (Fig. 5G red line), the absorbance at ~410 nm increased compared to NEAT2 without ferricyanide (Fig. 5G blue line), and the bands at ~ 428, 535, 564 nm were almost gone, indicating that the NEAT2 protein was mostly in the oxidized form. The spectra did not change significantly at 30 min (data not shown). After 24 h (Fig. 5G green line), a red shoulder on the Soret band was seen, and the absorbance at 428, 535 and 564 nm had increased. Together these observations indicated that the NEAT2 protein autoreduced slowly.

Methemoglobin binding is mediated by the N-terminal domain of Shr, which specifically recognizes the holo form

Following erythrocyte lysis, the $\alpha_2\beta_2$ heterodimeric hemoglobin converts to methemoglobin, in which the heme is found in the ferric form. This is largely an $\alpha\beta$ heterodimer [129,130]. Methemoglobin is likely to be a physiologically relevant heme source for the hemolytic GAS. To investigate Shr interactions with methemoglobin, we developed and used an ELISA. rShr and the recombinant Shr fragments NTD-N1, NEAT2, and NTD, were used to coat the wells of microtiter plates and allowed to interact with increasing concentrations of methemoglobin (Fig. 6A). Ligand binding by the immobilized proteins was detected using hemoglobin antiserum. Wells coated with BSA and uncoated wells were used as controls for non-specific interactions. rShr bound methemoglobin in a dose dependent and saturable manner, while only low background binding (OD 405 $\leq$ 0.1) of the hemoglobin antiserum to the control wells was observed. The recombinant Shr fragments NTD and NTD-N1 bound methemoglobin with binding profiles that were similar to the full length Shr, and methemoglobin binding appeared saturated at a concentration of 10 nM (Fig. 6A). The observation that the full length Shr, NTD-N1 and NTD alone equivalently bind methemoglobin indicates a preponderant role for the NTD in hemoglobin binding. In contrast, no methemoglobin binding by the NEAT2 protein was detected. Therefore, unlike IsdA, IsdB, and IsdH proteins, which use NEAT domains to bind hemoglobin, an uncharacterized protein pattern found in the N-terminal domain of Shr interacts with hemoglobin.

We hypothesize that Shr interacts with methemoglobin to acquire heme from the host. We therefore asked whether Shr could differentiate between the apo and the holo forms of

hemoglobin. Heme was removed from methemoglobin according to Asakura *et al*, [131] and the formation of the apoprotein was confirmed by the UV-visible spectrum, which revealed no absorption at the Soret region. The binding of NTD to immobilized apohemoglobin was tested by ELISA. In contrast to its interactions with holoprotein, no binding of NTD to apohemoglobin was observed (Fig. 6A, red line). Similar to the NTD, the full length Shr did not bind apohemoglobin (Fig. S4). A control ELISA performed with immobilized holo and apohemoglobin demonstrated that the hemoglobin-specific antibody was able to detect both forms of hemoglobin similarly over the range of hemoglobin concentrations studied (Fig. 6B). Therefore, the absence of binding of apohemoglobin in the experimental ELISA shown in Fig. 6A (red line) was not due to a lack of ability of the hemoglobin antiserum to recognize the apoprotein. In conclusion, these experiments demonstrate that Shr differentiates between the holo and the apo forms of hemoglobin and binds only to heme-loaded protein.

The NEAT 2 domain in Shr mediates most of its binding to ECM

We have recently observed that in addition to its interactions with hemoproteins, Shr also functions as an adhesin and binds fibronectin and laminin [48]. To determine the domains involved in the ability of Shr to bind these proteins components of the extracellular matrix (ECM), immobilized rShr, NTD, NTD-N1, and NEAT2 were allowed to react with the ECM components using ELISAs. Ligand binding was detected with antibodies specific for fibronectin or laminin. When fibronectin was added in increasing concentrations to the immobilized proteins, rShr as well as the recombinant fragments NTD-N1 and NEAT2 bound it in a

concentration-dependent and saturable manner (Fig. 7A). The NEAT2 protein demonstrated the highest binding to fibronectin, while only low level binding was seen with NTD-N1. No interactions with fibronectin were demonstrated by the immobilized NTD protein. These observations suggest that NEAT regions mediate the observed Shr binding to fibronectin. Similar observations were made with laminin; as shown on Fig. 7B, rShr, and NEAT2 proteins bound laminin, while no significant binding to laminin was observed by the NTD or NTD-N1. Together, these observations indicate that while both Shr NEAT domains are able to interact with some ECM components, the NEAT2 domain plays a more significant role in this activity of Shr.

The NTD-NEAT 1 region of Shr is sufficient for heme acquisition from methemoglobin

We next asked if the NTD-N1 fragment of Shr, which contains the hemoglobin-binding region and the heme-binding NEAT1, is sufficient for heme acquisition from methemoglobin. Heme was removed from the purified NTD-N1 [131], and the formation of apo NTD-N1 was confirmed by UV-visible spectrum analysis (Fig. 8A). The heme transfer assay was done over a *Strep*-Tactin column with immobilized apoNTD-N1 protein. Methemoglobin in equimolar amounts to the immobilized apoNTD-N1 protein was flowed through the column. The bound hemoglobin was removed by extensive washes with salt containing buffer (see Materials and Methods), and the NTD-N1 protein was then eluted with desthiobiotin. Western blot analysis of the fractions collected during this procedure revealed that the hemoglobin containing fractions also included low amounts of NTD-N1 in addition to methemoglobin (lane 3, Fig. 8B),

suggesting that some methemoglobin/NTD-N1 complexes were washed from the column. The NTD-N1 fraction that was eluted with desthiobiotin, however, did not contain a detectable amount of hemoglobin (lane 4, Fig. 8B). The optical absorbance of NTD-N1 after the methemoglobin passage showed a sharp peak at 411 nm, indicating that the apoNTD-N1 acquired heme from methemoglobin (red line, Fig. 8A). To confirm that the observed absorbance at 411 nm resulted from NTD-N1/heme complex and not from trace amounts of methemoglobin, we analyzed the absorbance of 0.7 μM methemoglobin solution, a concentration which is above the detection level of the hemoglobin antibody utilized in the assay (lane 6, Fig. 8B). This analysis revealed that methemoglobin, at the tested concentration, had a significantly lower Soret band than in the NTD-N1 fraction.

A similar experiment was done with immobilized NTD-N1 with hemin chloride solution (in 4-fold molar excess) instead of methemoglobin in the mobile phase. The optical analysis of NTD-NEAT1 after passage of free hemin also revealed that it acquired heme as indicated by the peak at 412 nm (blue line Fig. 8A). However the peak at the Soret region of NTD-N1 after the passage of methemoglobin was significantly higher than that after contact with the hemin chloride solution. This observation suggests that the NTD-N1 protein acquires more heme from hemoglobin than from the hemin solution, supporting heme transfer from methemoglobin directly to the immobilized NTD-N1. Heme acquisition by apoNTD-N1 was also investigated using an alternative assay in which the NTD-N1 was allowed to interact with methemoglobin in solution at room temperature. The UV-visible spectrum of the NTD-N1 protein after its separation from methemoglobin (using *Strep*-Tactin column) revealed a sharp peak at 410 nm (Fig. S5), demonstrating heme transport from methemoglobin to the NTD-N1 protein.

Interestingly, the absorption intensity at the Soret region following 5 min of co-incubation was about 80% of that seen following 75 min, indicating rapid heme sequestering by the NTD-N1 protein.

Shr is required for GAS growth using hemoglobin as the sole iron source

To determine the importance of the heme binding domains to the function of Shr *in vivo*, several GAS mutants containing in frame deletions of various regions in *shr* were constructed. These include a mutant with NEAT1 deletion mutant (ΔNEAT1), a mutant with a deletion that spans the distal part of the LRR and most of the second NEAT domain (ΔNEAT2), and a mutant with a large deletion that includes both NEAT domains and the region in between (ΔNEAT1-2, Fig. 9A). The production of *shr* alleles in the expected size in the genome of each of the mutants and of the corresponding Shr proteins was confirmed by PCR and Western blot analyses (Fig. 9B and 9C). This analysis also confirmed the production of the wild type Shr when the ΔNEAT1-2 was complemented. Successful complementation of the null *shr* mutant was previously shown [48]. RT-PCR analysis with primers specific for *siaA*, which is located downstream of *sh*r, verified that the *shr* mutations were not polar and did not affect the expression of the downstream genes in the *sia* operon (Fig. 9B).

The ability of wild type, a *shr* null mutant [48], and the isogenic mutant strains described above to use hemoglobin as a sole source of iron was investigated using a growth assay that is based on iron-depleted chemically defined medium (CDM). The wt strain and all of the *shr* mutants grew well in complete CDM medium containing 20 μM of free iron (Fig. 9D). On the

other hand, CDM that was prepared without iron and contained 2 mM of the ferric chelator 2, 2-dipyridyl did not support significant growth of any of the tested GAS strains (Fig. 9E). The addition of 20 μM of methemoglobin to the iron-depleted CDM restored growth of the wt strain to the level obtained with CDM containing 20 μM iron (Fig. 9F), lower hemoglobin concentration however, did not support growth of any of the strains in the iron depleted medium (Fig. S6 A & B). These observations demonstrate that iron is indeed the limiting factor for GAS growth in the 2,2-dipyridyl CDM and that GAS is able to use hemoglobin to satisfy its iron needs as we previously reported [44]. No significant growth differences were observed between the *shr* mutants containing a deletion of NEAT1 (ΔNEAT1) or of NEAT2 (ΔNEAT2) and the wt strain in the 2, 2-dipyridyl-CDM supplemented with methemoglobin. Therefore, the ΔNEAT1 and the ΔNEAT2 *shr* mutants are not affected in their ability to use hemoglobin as a source of iron. On the other hand, the growth of the *shr* null mutant and to a lesser extent that of the mutant that was missing both of the NEAT domains (ΔNEAT1-2) was impaired (Fig. 9F). The growth phenotype demonstrated by the *shr* mutants was reversed by complementation with the *shr* gene (Fig. 9G). These findings establish that Shr is required for hemoglobin utilization *in vivo* and suggest that Shr function requires at least one of the heme binding NEAT domains. The addition of methemoglobin in higher concentration (60 μM) supported better growth of the tested GAS strains (Fig. S6C). Thus, the Shr-dependent pathway for hemoglobin utilization in GAS may be of high affinity. However, additional pathways for acquisition of iron from hemoglobin also exist, as previous findings suggest [46].

Discussion 1

During the infection process, the β-hemolytic GAS can tap into the intracellular heme reservoir due to the potent hemolysins it produces and satisfy its needs for iron with hemoglobin, hemoglobin-haptoglobin, and other heme-containing proteins [44,132]. Previous observations implicated the surface-exposed NEAT protein, Shr, in the first step of heme acquisition from host proteins by GAS [45,54]. In this work we have provided the first direct support for this proposition by demonstrating that Shr can obtain heme from methemoglobin and by establishing that Shr function is important for GAS ability to use methemoglobin as an iron source. GAS use of Shr in heme acquisition is reminiscent of NEAT-containing receptors such as the Isd proteins in *S. aureus* and related proteins from other Gram-positive bacteria. In this study, however, we demonstrate that GAS Shr structure and function are different from that of previously characterized NEAT proteins and suggest that Shr represents a new type of protein family with a different mode of hemoglobin binding and heme acquisition.

Shr represents a family of composite NEAT proteins

Shr is a complex NEAT protein that consists of a unique combination of domains and protein motifs (Fig. 3). The database contains many secreted or surface proteins with NEAT domain(s); a few also carry LRR region(s) including IlsA of *B. cereus* [123]. LRR are commonly involved in protein recognition and protein-protein interactions [133]. It is possible that the LRR may help facilitate the intra-molecular communications that are likely to take place in Shr or its interactions with the other transport components such as Shp. DUF1533 is a domain of unknown

function found in hypothetical proteins that contain secretion or export signals and sometimes other functional regions including LRR. The combination of two DUF1533, a LRR region and two NEAT domains is seen for the first time in Shr, however. Interestingly, Shr seems to be the first characterized NEAT protein that has an EF-hand motif (located between the NEAT1 and the LRR regions, Fig. 3). The EF-hand motif is a calcium-binding domain that is ubiquitous among eukaryotic calcium-binding proteins such as calmodulin, but is also found in bacterial sequences [134-136]. As with other bacterial proteins with EF-hands, the functional significance of this motif is yet to be determined. Further *in silico* analysis identified several orthologues of Shr in *C. novyi*, *S. equi sub spp zooepidemicus*, *S. equi sub spp equi,* and *S. dysgalactiae*. These Shr-like proteins share with Shr significant sequence homology and domain architecture, suggesting that GAS Shr is a representative of a small family of NEAT proteins that evolved by combining domains found in surface or secreted proteins encoded by bacteria from Phylum Firmicutes.

Shr is the only NEAT protein to show ferric heme reduction

We isolated rShr with ferric heme (Fig 4B), indicating that this protein can sequester heme from *E. coli*. It was previously reported that Shr could be isolated from *E. coli* apoprotein with a mixture of ferric and ferrous heme [54]. When we titrated the protein with free hemin, the increase in the absorption around 414 nm demonstrated that Shr can also acquire ferric heme from solution (Fig. 4C). The concurrent rise in absorption at 427, 540 and 564 nm indicated increasing amounts of rShr-bound ferrous heme and was reversed by oxidation (by ferricyanide, Fig. 4D). This increase in bound ferrous heme following the addition of ferric heme to the

purified rShr strongly suggests that Shr autoreduces the heme, even in air. Shr clearly provides a stable environment for the bound ferrous heme. This is the first demonstration that Shr can obtain heme from solution and reduce it to ferrous heme. Heme reduction is a unique property of Shr that to our knowledge has not been reported for any other NEAT protein.

The iron oxidation state in protein-bound heme can have a significant impact on the heme fate and its environment. For example, reduction of the ferric heme in IsdC NEAT domain results in the loss of the heme from the protein [112]. On the other hand, the full length IsdA and its single NEAT domain can bind both ferric and ferrous heme. The reduction to ferrous heme, however, changes the iron axial ligand from tyrosine to histidine and renders it accessible to small anionic ligands such as CO. Based on these observations, it is suggested that iron oxidation/reduction lead to subsequent conformational changes with closing/opening of the heme-binding pocket in IsdA [112,137]. Our *in vitro* study of rShr shows that the full-length protein is able to bind the heme group in both the ferric and the ferrous forms as well. It seems possible that, as in IsdA however, iron oxidation/reduction may be accompanied by structural changes that influence the heme location within the protein (i.e., binding to first or the second NEAT domain) or the subsequent *in vivo* steps in the heme trafficking such as the heme transfer to Shp or SiaA.

Functional and sequence analysis show that both NEAT domains in Shr are divergent from one another and from the NEAT domains of the Isd protein family

The optical spectrum of the Shr variants NTD-N1 and NEAT2 demonstrate that they both complex heme, while the NTD protein, in contrast, did not show any heme binding. Sequence alignment demonstrated that only a few of the residues that contact the heme in Isd NEAT domains are conserved in the putative heme biding sites of NEAT1 and NEAT2 in Shr [128], (Fig. S1). Most noticeably, both of the NEAT domains in Shr are missing the potential iron-coordinating residue, Tyr 166, a heme ligand in other NEAT proteins, and only NEAT1 has Tyr 170 (proposed to regulate heme binding and release) (Fig. S1). Therefore, the heme-binding region in both Shr NEAT domains is quite different from that of Isd-like heme-binding NEAT domains and the heme iron may not be coordinated by a tyrosine, at least in the NEAT2 domain of Shr. These observations suggest that Shr NEAT domains have different mechanism for interactions with heme. Likewise, Shp, which can acquire heme from Shr, has a unique iron coordination involving two methionines within the single Shp molecule that function as axial ligands [49]. Additional work is needed to determine the heme axial ligands of the NEAT domains in Shr. Future investigations of the evolutionary relation between Shr NEAT domains and Shp, which represents a more remote member of the NEAT family, are warranted.

Both of the NEAT domains in Shr bind heme. The optical spectra of NTD-N1 and NEAT2 proteins as isolated from *E. coli* indicate that NEAT1 is complexed with ferric heme, and that NEAT2 is bound to both ferric and ferrous heme (Fig. 5C and 5F). Like with the full-length Shr, titration of NEAT2 with increasing concentration of hemin resulted in raising amounts of bound ferric and ferrous heme (Fig. S3). Over time some of the ferric heme in

NEAT2 (produced by oxidation with ferricyanide) was reduced to ferrous heme (Fig. 5G). Together these observations suggest that the NEAT2 domain in Shr is capable of autoreduction. Functional differences between NEAT1 and NEAT2 were also found in their interaction with non-heme ligands. While Shr NEAT2 interacts with both fibronectin and laminin molecules, NEAT1 binding to fibronectin is significantly weaker and it does not demonstrate significant binding to laminin (Fig. 7).

A unique site in Shr N-terminal region mediates binding to methemoglobin

We demonstrated in this study, using ELISA with immobilized Shr variants, that the full-length rShr, the NTD, and the NTD-N1 all bound methemoglobin similarly. The NEAT2 protein, on the other hand, did not interact with methemoglobin (Fig. 6A). Therefore, it appears that an unspecified region within Shr NTD mediates its binding to methemoglobin. While this manuscript was in preparation Meehan *et al* [138] reported that like GAS NTD, the truncated Shr molecule produced by *S. equi* sub spp *equi* (consisting mostly of Shr NTD) binds hemoglobin and hemoglobin-haptoglobin complex. The finding that the interaction of Shr with methemoglobin is not mediated by NEAT domains distinguishes Shr from the previously studied Isd receptors. Domain analysis of IsdA and IsdH demonstrated that binding to host hemoproteins is carried out by the single NEAT domain in IsdA and two of the NEAT domains of IsdH [104,116]. Site directed mutagenesis localized the binding to a conserved aromatic motif also found in the first NEAT domain of the IsdB [116], which binds hemoglobin and hemoglobin/heptoglobin complex [107]. Consistent with the results of the ELISA experiments,

both of the Shr NEAT domains are missing the hemoglobin binding sites identified in the Isd proteins. Additional work is required to identify the region within Shr NTD that is involved in hemoglobin binding. The sequence of the Shr N-terminal region is unique, and besides the two copies of DUF1533, it shares sequence homology only with Shr orthologues. Therefore, hemoglobin binding is mediated by a new protein motif in Shr.

Hemoglobin binding by bacterial receptors is not fully understood. In this work we show that the Shr N-terminal domain binds only heme-containing hemoglobin (Fig. 6A). The functional significance of this observation is that Shr may release the bound hemoglobin after sequestering all the heme. It is not clear how Shr differentiates between the apo and the holo forms of methemoglobin. Recognition of the heme moiety does not seem to be part of Shr binding to methemoglobin as NTD does not bind heme and the heme is mostly buried within hemoglobin [139]. We hypothesize, therefore, that Shr recognizes a tertiary structure in the holoprotein that is disrupted when heme is lost, rather than recognizing a linear region within the α or β polypeptides of hemoglobin.

The NTD and NEAT1 in Shr are sufficient for heme acquisition from methemoglobin in vitro

It was previously demonstrated that purified Shr transfers heme directly to apoShp *in vitro* [54], while the direct movement of heme from methemoglobin to Shp was not observed. Therefore it was hypothesized that Shr is involved in the first step of heme sequestering from hemoglobin. In this study we used the column-immobilized apoNTD-N1 to ask if it could obtain heme following transient interactions with methemoglobin or free heme (Fig. 8). Spectral

analysis done with NTD-N1 following the passage of methemoglobin showed that it obtained heme. In a separate assay, co-incubation of apoNTD-N1 with methemoglobin in solution demonstrated that the heme transfer from methemoglobin is fast. NTD-N1 was also able to receive heme from solution, but to a lesser extent. These experiments imply that heme is transfered directly from methemoglobin to the NTD-N1 protein. Further investigations are required to determine if NEAT2 can obtain heme from NEAT1 and/or from methemoglobin, and to find out which of the Shr domains are required for the subsequent step in heme trafficking.

Shr is needed for heme uptake from methemoglobin in vivo

The growth of the *shr*$^{-}$ and ΔNEAT1-2 mutants in iron-depleted medium supplemented with hemoglobin was impaired in comparison to that of the wild type GAS strain (Fig 9F). The mutant growth phenotypes were reversed by complementation with the *shr* gene, establishing the role of Shr in hemoglobin utilization *in vivo*. The residual growth of the ΔNEAT1-2 in low hemoglobin concentration and the full growth of both mutants observed when higher amounts of hemoglobin were added (Fig. S6C) are consistent with a previous report suggesting that additional hemoglobin utilization pathways are found in GAS [46]. Since the *shr* mutants required a high concentration of hemoglobin to restore growth than the wild type strain, we suggest that Shr mediates a high affinity pathway. It is noteworthy, however, that the deletion of a single NEAT domain (as in the ΔNEAT 1 and ΔNEAT 2 mutants) did not have significant growth defect. These findings indicate that either one of the NEAT domains is sufficient for

heme uptake from hemoglobin *in vivo*, suggesting that despite the differences found between Shr NEAT domains, they have some functional redundancy.

In conclusion, this study establishes the role of Shr in heme acquisition from hemoglobin, and demonstrates that the streptococcal receptor is a representative of a structurally and functionally distinct NEAT protein family found in *C. novyi* and pyogenic streptococci. We have begun to elucidate the functional domains of Shr, although additional investigations are required to fully understand the mechanism of heme uptake mediated by this intriguing protein.

Materials and methods 1

Strains, media, and growth conditions

Escherichia coli (*E. coli*) DH5α and XL1 blue were used for cloning and gene expression. The GAS strain used in this study was NZ131, an M type 49; ZE4912 an isogenic strain with a non polar, null mutation in *shr* (*shr::aad9*) [48]; ZE4924, a merodiploid strain, which contains both the *shr::aad9* and the wild type alleles of *shr* in the chromosome [48]. *E. coli* cells were grown aerobically in Luria Bertani (LB) medium at 37 ºC. GAS cells were grown statically at 37 ºC in Todd-Hewitt broth with 0.2% w/v yeast extract (THY, Difco Laboratories) or Chemically Defined Medium (CDM; SAFC Biosciences) as described in Montañez *et al* 2005 [46]. When necessary, 100 μg/ml ampicillin, 100 μg/ml spectinomycin, 70 or 300 μg/ml kanamycin (for *E. coli* and GAS respectively) was added to the medium.

DNA manipulations

Chromosomal and plasmid DNA extraction and DNA manipulations, including restriction digest, cloning, and DNA transformation into *E. coli* or GAS, were done according to the manufacturer's recommendations and with standard protocols as previously described [140,141]. PCR for cloning was performed using the High Fidelity AccuTaq LA DNA Polymerase (Sigma). PCR products were purified with the QIAquick PCR Purification Kit (Qiagen). DNA ligation was done with using Fastlink ligation kit (Epicentre). For RNA extraction and analysis, GAS cells were harvested at the logarithmic growth phase and total RNA was prepared using the RiboPure-Bacteria Kit (Ambion). RNA was quantified spectrophotometrically, and its integrity was examined by agarose gel electrophoresis. For RT-PCR cDNA was produced by Superscript III reverse transcriptase (Invitrogen) according to the manufacturer's specification. The oligonucleotide primers used in this study are listed in Table S1. Table S2 lists and describes the construction of the plasmids used in this work.

Strain construction

The following isogenic mutant series was constructed in NZ131 background: ZE4925 (in frame deletion of NEAT1 in *shr,* ΔNEAT1), ZE4926 (in frame deletion of the LRR 3' and most of the NEAT2 in *shr,* ΔNEAT2), and ZE4929 (in frame deletion of the region between NEAT1 up to and including NEAT2 in *shr,* ΔNEAT1-2). Alleles with unmarked and in frame deletions in the *shr* gene with about 1 Kb of flanking sequence were cloned into the temperature sensitive shuttle vector pJRS700, as described in Table S2. The mutations were then introduced into GAS

chromosome by transforming NZ131 cells with each of the recombinant vectors and selecting for Kanamycin resistance at 30 °C. The transformants were then passed in antibiotic free medium at 37 °C. Mutants in *shr* gene, generated by allelic replacement *via* double homologous recombination were identified by screening for plasmid loss (kanamycin sensitivity). The formation of each mutation was confirmed by PCR and Western blot analysis (Fig. S5). The GAS strains ZE4925, ZE4926, and ZE4929 were engineered using plasmids pXL2, pXL13, and pXL3 respectively. The strain ZE4935 is a merodiploid containing both the wt and the ΔNEAT1-2 *shr* alleles in the chromosome. For ZE4935 construction, the temperature sensitive plasmid pXL14 was introduced into ZE4929 cells and vector integration into the chromosome (*via* homologous recombination) was selected on Kanamycin at 37 °C; strain construction was confirmed by PCR and Western blot analysis (Fig. S5 and data not shown).

Overexpression and Purification of Recombinant Shr, NTD, and NTD-N1 and NEAT2

The expression of *Strep*-tag Shr (pEB2), *Strep*-tag Shr NTD (pEB10), Strep-tag NTD-N1 (pEB11), or *Strep*-tag NEAT2 (pHSL2) was induced with 200 ng/ml anhydrotetracycline, overnight at 27 ºC. Cells were harvested, resuspended in lysis buffer (100 mM Tris/HCl pH 8, 500 mM sucrose, 1 mM EDTA) with the addition of 0.5 mg/ml lysozyme, β-D glucopyranoside final concentration 0.5% and Complete, mini-EDTA-free protease inhibitor cocktail tablets (Roche) then lysed by sonication. The cells pellet was centrifuged and the cleared lysate was then applied to a *Strep*-Tactin Superflow column (IBA) with a 5 ml bed volume and purified using FPLC. A step gradient program was used and *Strep*-tag proteins were eluted with 5 column

volumes of 100 mM Tris-HCl pH 8.0, 150 mM NaCl, 1 mM EDTA, 2.5 mM desthiobiotin. A cation exchange column (4 ml bed volume Hi-trap SP HP, GE Healthcare) was used for further purification of *Strep*-tag Shr by FPLC. The *Strep*-tag Shr directly after elution from the *Strep*-Tactin Superflow column was diluted 1:5 in 50 mM acetic acid pH 4.8, applied to the Hi-trap SP HP column and eluted with 50 mM acetic acid pH 4.8 plus 1M $NaCl_2$.

His-tagged Shr was expressed (pCB1) and purified as described previously [48] with the following exceptions: when necessary, hemin in dimethyl sulfoxide was added to give a final concentration of 1 μM hemin in the cell culture one hour before cell disruption by sonication and sonication was increased to include ten cycles.

All proteins were prepared in Laemmli sample buffer and separated by sodium dodecyl sulfate-10% polyacrylamide gel electrophoresis (SDS-10%). Western Blot analysis was performed with polyclonal antibodies against Shr raised in rabbit as described previously [45]. Total protein concentration was measured using a Lowry assay (Pierce Biotechnology, Inc). Each elution fraction was stored in 15% glycerol with 200 μl protease inhibitor cocktail (Complete, mini-EDTA-free, Roche). Fractions used for further study underwent buffer exchange to 20 mM Tris-HCl, 15% Glycerol, pH 8.0 and were stored at -20 °C.

Enzyme-linked Immunoabsorbent Assays (ELISA)

An enzyme-linked immunoabsorbent assay (ELISA) was used to analyze the ability of *Strep*-tagged Shr, NTD, NTD-N1 and NEAT2 to bind to various ligands. ELISA plate wells

(Costar, Corning, inc.) were coated with a 50 µl solution containing the desired concentrations of bait proteins. Wells coated with BSA and uncoated wells were used as controls for non-specific interactions. The bait proteins were diluted in PBS buffer (10 mM phosphate-buffered saline, 100 nM NaCl, pH 7.4) and included rShr, NTD, NTD-N1, NEAT2 and BSA. After the bait proteins were incubated overnight at 4 ºC, the wells were washed with PBS-Tween (0.05%) buffer and blocked with 200 µl 5% soy infant formula (Nestle)-PBS-Tween for 1 hour at 37 ºC then washed again to remove blocking solution. For apohemoglobin preparation, heme was removed from methemoglobin according to Asakura *et al.* [131]. The desired concentrations of human apo/holomethemoglobin (Sigma), human fibronectin (BD) or mouse laminin (BD) in 5% soy/PBS-Tween were then added to each well (50 µl / well). The wells were then washed PBS-Tween/well to remove unbound protein. Fifty µl of a 1:15,000 dilution of polyclonal rabbit anti-hemoglobin (sigma), rabbit anti-fibronectin (abcam) or rabbit anti-laminin (abcam) antibodies in blocking buffer were subsequently added to each well and incubated at 37 ºC for one hour, and the wells were then washed. Fifty µl of goat anti-rabbit IgG conjugated to alkaline phosphatase (Sigma) at 1:6000 dilution in blocking buffer was added to each well and incubated at 37 ºC for 1h. Interactions between recombinant Shr, NTD, NTD-N1 or NEAT2 and the ligands were then detected by adding pNPP substrate and developing the chromogenic reaction (KPN). Plates were read at 405 nm on an automated ELISA reader for intervals up to one hour after development. An assay to assess the ability of a variety of blocking buffers to diminish nonspecific binding was also performed as described above except the ELISA wells were uncoated.

rShr, NTD, NTD-N1 and N2 UV-visible spectra

The spectrophotometric analysis of samples from 250 to 700 nm was carried out using a Varian Cary 50 Bio spectrophotometer. Absorption spectra of the purified proteins were measured on the spectrophotometer in a quartz cell with an optical path length of 10 mm. All absorption spectra shown in this study are representative of multiple experiments done with at least three biological replicas.

Heme titration assays

A stock solution of hemin chloride in DMSO was prepared. The absorbance of a 1:1000 dilution of the stock solution at 404 nm was recorded and the concentration of hemin chloride in the stock solution was calculated using Beer's law (A= εbc where hemin in DMSO ε_{404}=188,000 $m^{-1}cm^{-1}$ [142,143]. Protein samples were diluted in *Strep*-tag elution buffer to 3 μM. Absorbance from 250-700 nm was recorded before addition of hemin chloride. Hemin chloride was added to 1 ml aliquots of 3 μM protein to a final hemin chloride concentration of 1 μM, incubated with stirring at 4° C for 1 h and the absorbance from 250-700 nm was scanned and recorded. This was repeated for hemin chloride concentrations of 3 μM, 5 μM, 10 μM and 20 μM. *Strep*-tag elution buffer alone was similarly incubated with 1 μM, 3 μM, 5 μM, 10 μM and 20 μM of hemin chloride. These heme-containing buffer solutions were scanned as blanks for the UV-visible spectra of the protein solution containing corresponding concentrations of hemin chloride. The total volume of DMSO added to the protein solutions or the blank solutions ranged from 0.15 μl to 3 μl. Thus, the final DMSO concentration in the sample was $1.5x10^{-4}$ to $3x10^{-3}$ v/v.

Ferricyanide and DTT treatment were done in sealed tubes with incubation at room temperature. Ferricyanide was then removed by dialysis.

Heme transfer from methemoglobin

Heme transfer from methemoglobin to Shr fragment NTD-N1 was done using FPLC. ApoNTD-NEAT1 was prepared according to the method described by Asakura *et al* [131] and 100 nmoles of the protein in 2 ml *Strep*-tag wash buffer were attached to a *Strep*-Tactin Superflow column. Equivalent moles of methemoglobin (100 nmoles) were flowed through the immobilized NTD-N1. The bound methemoglobin was removed by washing several times (10 column volumes) with a wash buffer (100 mM Tris-HCl pH 8.0, 250 mM NaCl, 1 mM EDTA). Subsequently, the immobilized NTD-N1 was eluted with *Strep*-tag elution buffer (100 mM Tris-HCl pH 8.0, 150 mM NaCl, 1 mM EDTA, 2.5 mM desthiobiotin). Methemoglobin flow-through and NTD-N1 elution samples were collected and analyzed by Western blot using anti-Shr and anti-hemoglobin antibodies. Protein concentration in the different fractions was determined by Modified Lowry assay, and Spectroscopic analysis (250 - 700 nm) of 10 μM apoNTD-N1 before and after passage of methemoglobin, was carried out using a Varian Cary 50 Bio spectrophotometer.

Culture in microplate

All GAS strains were grown in CDM supplemented with 3 mM of L-cysteine, 15 mM of sodium bicarbonate, 2.5 mM of magnesium sulfate, 44 μM of calcium chloride, 15 μM of zinc chloride, 20 μM of manganese and either 20 μM of metal iron or a range of concentrations of human hemoglobin. In the latter case, 2 mM of 2, 2-dipyridyl was added to the supplemented CDM to completely chelate residual metal iron prior to the addition of Hb. The prepared media were inoculated to final OD_{600} = 0.005. The inocula consisted of cells grown overnight at 37 °C on blood agar and suspended in iron-free CDM. Bacterial suspensions at OD_{600} = 0.5 were diluted 1:100 into the corresponding medium, which was then dispensed in 200 μl triplicates in a 96 well microplate (Costar 3595, Corning Inc.) at 37 °C for 24 h. The experiments were performed in triplicates and were done at least twice for each strain. Kanamycin (150 μg/ml) was added to the medium for the growth of the complemented strain ZE4924 and ZE4935.

In silico analysis

The following accession numbers were utilized for the NEAT domain-containing proteins examined in this study: *S. aureus* IsdA ABX29083, *S. aureus* IsdC ABX29084, *S. aureus* IsdB YP_001332074, *S. aureus* IsdH Q6G8J7, *S. equi subs. zooepidemicus* YP_002122760, *C. novyi* NT YP_877540, *S. dysgalactiae subs*. *equisimilis* YP_002997560, *S. pyogenes* Shr MGAS5005 ABW80932. Identification of all protein domains was conducted by SMART analysis except the EF-hand domain, which was identified by PROSITE. Multiple sequence alignment the NEAT domains were executed using the ClustalW program.

Table 1: Primers used in this study

Name	Sequence	Source
204A-FW	5'-GCTATGATGCTGTTAAGCGTGTGG	*siaA*
204A-Rev	5'-TCTGGAATGGCATGAGCTGTTC	*siaA*
Y-His-Fwd	5'-CCCCGAATTCAAATCACAAGAGCCTTTAGT	*shr*
Strep-shr-rev	5'-CCCCTCGAGTTATTTAAATAATGTCTTTGCACC	*shr*
ZE1	5'-CCCCGAATTCAAATCACAAGAGCCTTTAGTT	*shr*
ZE58	5'-ATCCCTCGAGGTCGACCTGCAGG	*shr*
ZE59	5'-CCCCTCGAGAACCTCACCTGCTTGATAAGAC	*shr*
ZE60	5'-TTTCTCGAGCCCAACCCCTTTTTCTTTATCATCAG	*shr*
ZE50	5'-AAAGGATCCACTGATGATAAAGAAAAAGGG	*shr*
ZE51	5'-AAAGGATCCAACCTCACCCTGCTTGATAAG	*shr*
ZE139	5'-CCCCGAATTCTTAAATCAAAAACAATTGCGTG	*shr*
ZE106	5'-TTGTAGAGGAATTCTTTTATCAGAGATATCCTC'	*shr*
ZE126	5'-GTAACCTTTGTGATTTGCTGAG'	*shr*
ZE140	5'-AAAAGGTACCTTAGACAACCTTTGCCTTCTCTG	*shr*
ZE168	5'- CCCCCCATCGATTCACAAGAGCCTTTAGTTCAGTCAC	*shr*
ZE169	5'-CCCCCCATCGATCTTATTTAAATAATGTCTTTGCACC	*shr*
ZE170	5'-TTTTTTATCGATTTAGCTCTTGCTGACTAG	*shr*
ZE171	5'-TTTTTTATCGATGGAAGCTTCAAGTTTTGCAA	*shr*
ZE172	5'-CCCCGGTACCTTAGGCTACCTTGGTGAATTGAGCTATTC	*shr*
ZE173	5'-TTTTGGTACCTGATGTTAGAGGCTCTAGCGCT	*shr*
ZE215	5'-TTTTTTATCGATGATCTAGATCCGACTCAAGCAAGTAAG	*shr*

Table 2: Plasmids used in this study

Name	Description	Cloning method	Reference
pASK-IBA-12	Step-Tag expression vector		IBA
pEB2	Strep-tag Shr	A PCR fragment was amplified from GAS chromosome with Y-His-fwd/Strep-shr-rev primer set, cut with *Eco*RI & *Xho*I and ligated into pZSK-IBA-12	This study
pEB10	Strep-tag NTD	A PCR fragment was amplified from pEB2 using ZE58/ZE59 primers cut with *Xho*I and self-ligated	This study
pEB11	Strep-tag NTD-N1	A PCR fragment was amplified from pEB2 using ZE58/ZE60 primers cut with *Xho*I and self-ligated	This study
pHSL2	Strep-tag NEAT2	A PCR fragment was amplified from GAS chromosome using ZE139/ZE140 primer set, cut with *Kpn*I and ligated into pZSK-IBA-12	This study
pCB1	Express His-tag Shr		[45]
pJRS700	Tm sensitive shuttle vector		[46]
pXL2	Carries the *shr* ΔNEAT1 allele	A PCR fragment was amplified from pEB8 using ZE168/ZE169 primer set, cut with *Cla*I and ligated into pJRS700.	This study
pXL3	Carries the *shr* ΔNEAT1-2 allele	A PCR fragment was amplified from pXL2 using ZE171/ZE172 primer set, cut with *Kpn*I and self-ligated	This study
pXL5	Carries the *shr* wt gene	APCR fragment was amplified from GAS chromosome with ZE160/ZE170 primer set, cut with *Cla*I and ligated into pJRS700	This study
pXL13	Carries the *shr* ΔNEAT2 allele	A PCR fragment was amplified from pXL5 using ZE171/ZE172 primer set, cut with *Kpn*I and self-ligated	This study
pXL18	Carries *shr* fragment with upstream region	A PCR fragment was amplified from GAS chromosome with ZE215/ZE170 primer set, cut with *Cla*I and ligated into pJRS700	This study
pXL14	Tm sensitive plasmid expressing the wt *shr* gene		[48]

CHAPTER II

MECHANISMS OF INTRA- AND INTER-MOLECULAR HEME TRANSFER BY THE SHR PROTEIN OF GROUP A STREPTOCOCCUS

Introduction 2

Hemoglobin (Hb) and other hemoproteins that are released from lysing host cells are major iron sources for pathogenic bacteria. Upon erythrocyte lysis, the serum carrier haptoglobin forms a complex with Hb. Free in the blood, Hb spontaneously oxidizes to methemoglobin (metHb) and free heme is sequestered by the plasma hemopexin. To take advantage of these molecules, pathogens compete for the heme and transfer it across the cell envelope into the cytoplasm, where the iron is removed or the heme is incorporated in the bacterial machinery [98,144,145]. An emerging theme for heme transport in Gram-positive organisms is the use of a protein relay apparatus, in which heme is obtained from host molecules and delivered in a cascade fashion from the bacterial surface through the peptidoglycan layers to a cognate ABC transporter. The latter then mobilizes the heme across the cytoplasmic membrane [37,38]. A protein domain named NEAT (for NEAr-iron Transporter) often facilitates the capture and transfer of heme by the surface receptors [37-39]. NEAT domains are found in one or more copies in the heme-binding proteins of the different members of the Isd (Iron-regulated surface determinant) family. These receptors are well described in *Staphylococcus aureus, Bacillus*

species and *Listeria monocytogenes* [37-39]. Alternative heme relay apparatuses that use non-NEAT heme-binding modules were recently identified in *Corynebacterium diphtheriae* and *Mycobacterium tuberculosis* [42,43].

Heme sequestering from host proteins in *S. aureus* is achieved by the cell-wall proteins IsdB and IsdH, which transfer the heme to a third receptor in the peptidoglycan, IsdA [107,116,117]. Heme is then passed to IsdC and then to the IsdEF proteins for import across the cell membrane [117,146]. *B. cereus* relies on a surface NEAT-containing receptor (IlsA) that interacts with uncharacterized partner proteins to import heme into the cell [123]. An Isd-like system involving the secreted NEAT-containing hemophores, IsdX1 and IsdX2, is used by *Bacillus anthracis* [40,147]. Similarly to *S. aureus*, heme obtained by IsdX1 and IsdX2 is transferred to IsdC, which conveys the ligand to the cytosol through the IsdEF transporter. In addition to IsdC, IsdX1 also transfers its heme to IsdX2.

Multiple NEAT domains may be found in a single receptor, in which case they are numbered from the N-terminus of the protein. Isolated NEAT domains from various NEAT-containing proteins exhibit major functional differences and contribute differently to the heme acquisition process. Many NEAT domains bind heme and/or hemoproteins [41,51,111-119,148,149], whereas some also bind other ligands, such as extracellular matrix (ECM) components [104,148]. This functional diversity is often illustrated within a single protein harboring several NEAT domains. For example, both IsdX2 NEAT1 and NEAT5 from *B. anthracis* can scavenge heme from Hb, but only IsdX2 NEAT1 can transfer its heme to IsdC [147]. IsdX2 NEAT3 and NEAT4 can bind free heme and transfer it to IsdC, but are unable to obtain heme from Hb. In contrast, IsdX2 NEAT2 does not bind heme, but interacts with Hb.

In Group A Streptococcus (GAS), the conserved ten-gene operon *sia* (streptococcal iron acquisition system) participates in heme uptake [45]. The first gene in the *sia* locus, *shr*, expresses a composite surface receptor. Shr contains two NEAT domains separated by a series of leucine-rich repeats, a unique N-terminus region (NTD) with two copies of the uncharacterized module DUF1533 and a calcium binding EF hand [148,150]. Unlike other NEAT-containing hemoproteins receptors, Shr (and BslK from *B. anthracis*) are not attached to the peptidoglycan. Shr, which protrudes through the cell wall, is anchored to the cytoplasmic membrane by an hydrophobic segment at its C-terminus [48], whereas BslK associates with the S-layer on the bacterial surface [151]. Ligands recognized by Shr include heme, metHb, Hb-haptoglobin complex and some ECM proteins [45,48]. A recent study demonstrated that Shr binds heme through both of its NEAT domains. A separate region in Shr N-terminus mediates stable metHb binding, but possible transient binding by other parts of the receptor are not ruled out [148]. NEAT2 interacts with fibronectin and laminin in addition to heme. The full-length Shr and a protein fragment containing NTD and NEAT1 acquire heme from metHb *in vitro* [54,148]. Heme from Shr is efficiently transferred to the NEAT-like module in Shp, which is encoded by the second gene in the *sia* operon. Heme is then transferred from Shp to the SiaABC (HtsABC) transporter [152].

The *sia* operon is found in several pyogenic streptococci. For example, *S. equi zooepidemicus* and *S. dysgalactiae* code for Shr orthologues with identical domain architecture. The function of these Shr proteins in heme uptake is yet to be studied. A homologue of Shr (SeShr) is also found in the genome of *Streptococcus equi* subsp. *Equi*; however, a frame shift mutation in the *Seshr* gene results in a truncated protein that binds metHb and hemoglobin-

haptoglobin, but not heme or fibronectin [138]. As in GAS, the Shp orthologue (SeShp) binds heme and transfers it to the SiaABC (SeHtsABC) transporter [138,153]. In summary, heme acquisition strategies in *Streptococci* share some similarity with Isd and Isd-like systems, though important differences are found between these systems.

Here we conduct for the first time a comprehensive kinetic study to determine the role of GAS Shr domains in heme acquisition, and we suggest a model for inter- and intra-molecular heme flow in the streptococcal system.

Results 2

NEAT1 is more efficient in acquisition of heme from metHb than NEAT2

We recently showed that NTD-N1, a recombinant fragment of Shr containing the domains that bind metHb and heme (NTD and NEAT1, respectively), acquires heme from metHb *in vitro* [148]. To test whether NTD is essential for heme acquisition by NEAT1, we cloned and purified a recombinant Shr fragment containing the NEAT1 domain alone fused to maltose binding protein (MBP) (fig. S7). The molar extinction coefficient of heme-bound NEAT1 ($\varepsilon_{410\ nm} = 136,\ 670\ M^{-1}\ cm^{-1}$) was determined at 410 nm using the hemochromogen method [154]. ApoNEAT1 was incubated for 5 min on ice with metHb at 2:1 apoNEAT1/metHb molar ratio. The two proteins were then separated by affinity chromatography, allowing a selective binding of the NEAT1 protein. Western blot analysis of the elution fraction confirmed it contains only the NEAT1 protein without metHb contamination (fig S8). The UV-visible absorbance spectrum of the eluted NEAT1 had the typical Soret peak at 410 nm, indicative of

NEAT1-bound heme with ferric iron [148] (fig. 10A). These changes in the NEAT1 spectrum suggest heme acquisition by the apoNEAT1 domain. Control heme reconstitution experiments were carried out using 5 μM NEAT1 as purified from *E. coli* (fig. S9A), 5 μM MBP (fig. S9B) or buffer only, incubated with heme in increasing concentration (fig. S9C). The initial Soret band of NEAT1 (indicative of initial heme bound to the protein) increased significantly with the addition of heme to the protein solution from an absorbance of 0.20 to 0.65 at 20 μM heme. In contrast, when heme was added to MBP, the small and broad band (absorbance ~0.02) that was visible at the Soret region slightly expanded with heme addition and reached a maximum absorbance of only 0.071. These observations established that it is the NEAT1 domain that is readily associating with heme in the MBP-N1 fragment, and that MBP does not contribute significantly to these interactions. Consistent with previous observations, ELISA with immobilized NTD, MBP-N1, MBP and BSA showed the formation of a stable complex between metHb and NTD, and ruled out similar interactions between metHb and MBP (fig. S10).

The ability of isolated NEAT2 domain to obtain heme from metHb was tested using the same methods. The molar extinction coefficient of heme-bound NEAT2 ($\varepsilon_{410\ nm}$ =146, 000 M^{-1} cm^{-1}) was determined at 410 nm. Western blot analysis of the eluted protein showed no metHb contamination (fig. S8). The UV-visible absorbance spectrum of NEAT2 after metHb incubation showed a major peak at 426 nm and peaks at 410, 530 and 560 nm, indicative of bound ferrous and ferric heme (fig. 10B) [54,148]. Therefore, as we previously found for the acquisition of free heme from solution by Shr [148], NEAT2 reduced some of the ferric heme it acquired from metHb. The combined ratio Abs_{426nm}/Abs_{280nm} (0.51) and Abs_{410nm}/Abs_{280nm} (0.32) of apoNEAT2

treated with metHb is lower than the ratio $Abs_{410\ nm}/Abs_{280nm}$ (2.25) of apoNEAT1 upon metHb treatment. This suggests that apoNEAT1 acquired more heme from metHb than apoNEAT2.

The N-terminal domain of Shr facilitates heme transfer from metHb to Shr

To further investigate the transfer of heme from metHb to the different domains of Shr, rapid reaction studies were carried out on a stopped-flow spectrophotometer. The Shr domains in PBS were mixed individually at 25 ºC with different concentrations of metHb in PBS. Time-resolved absorbance data were collected over the entire 340-700 nm wavelength span of the diode-array detector. Alternatively, time-courses of the reaction were collected at the wavelength of maximal change with a monochromator and a photomultiplier detector. The time-courses of the reactions of NTD-N1, NEAT1, NEAT2 and MBP *versus* metHb are shown in fig. S11. Over time, significant changes in absorbance at 414 nm were seen only with the NTD-N1 fragment. Therefore, in the stopped-flow experiments, NTD-N1 was the only tested fragment that efficiently acquired heme from metHb.

Based on the observation described above, a detailed analysis of the heme transfer from metHb to NTD-N1 was carried out. The different spectra of NTD-N1 and metHb in the apo and holo forms are shown in fig. S12. ApoNTD-N1 at 2.5 μM final concentration was mixed with different amounts of metHb in a stopped-flow spectrophotometer equipped with a monochromator. The absorbance variations at 414 nm plotted as a function of time best fitted a triple exponential process at all the concentrations of metHb tested (fig. 11A). The observed rate constants for the fast phase (k_{obs1}) at each concentration of metHb decreased hyperbolically with

increasing metHb concentration (fig. 11B). Both k_{obs2} and k_{obs3} did not show any linear or hyperbolic dependence on metHb concentration, and had average values of 0.034 s^{-1} and 0.003 s^{-1}, respectively (fig. 11C). These three kinetically distinct phases are consistent with the minimal kinetic model that we propose in Scheme 1. In brief, NTD-N1 devoid of heme exists in solution in two populations that are in slow equilibrium, with only one population proving able to form a complex with metHb. Slow equilibrium is defined here as being governed by rate constants for the interconversion of the two populations (i.e., k_1 and k_2 in Scheme 1) being slower than the rate of association of metHb with apoNTD-N1. After rapid association of metHb with apoNTD-N1 to yield a binary protein complex, the heme is transferred from metHb to apoNTD-N1, possibly followed by the slow release of heme in solution or by the slow dissociation of the binary complex to yield holoNTD-N1 and unloaded metHb. The presence of two populations of apoNTD-N1 in slow equilibrium is reminiscent of a proposed kinetic model previously proposed by Zou *et al*. to explain similar inverse concentration dependence kinetics for calcium (Ca^{2+}) binding by the Ca^{2+} sensor, Ca-G1 [155]. Such type of kinetics has been recently reviewed by Vogt *et al*. [156]. The three well-separated phases observed in the stopped-flow spectrophotometer provide unequivocal evidence for the presence of multiple, temporally distinct kinetic steps. The presence of two populations in slow equilibrium and the rapid formation of the initial protein complex are supported by the inverse concentration dependence of k_{obs1}, with fitting of the data to the equation: $k_{obs1} = k_1 + k_2 * (K_{eq} / (K_{eq} + [\text{metHb}]))$ with $R^2 = 0.99$, establishing the values for k_1 (0.1 s^{-1}), k_2 (1.7 s^{-1}) and K_{eq} (32 μM). Conformational changes or interactions with partner proteins have been shown to alter the spectral properties of protein-bound heme in several hemoprotein [157-162].

The first phase of the minimal kinetic model proposed in Scheme 1 suggests that the observed changes in the Soret region reflect the formation of a complex between metHb and NTD-N1. To test whether complex formation (in the absence of heme transfer) could result in spectral perturbations, the UV-visible absorbance spectrum of metHb (3 μM in PBS) was compared to that of metHb in a mixture with NTD (3 and 4.5 μM respectively, in PBS). Unlike NTD-N1, the NTD fragment can only bind to MetHb, but not heme [148]. The Soret peak of metHb slightly decreased and shifted from 406 nm toward 408 nm in presence of NTD (fig. S13A). The UV-visible absorbance spectrum of NTD in PBS is shown in fig. S13B. Then again, the addition of 4.5 μM of MBP (which does not interact with metHb) to 3 μM metHb in PBS did not lead to any change in the UV-visible absorbance spectrum of metHb (fig. S13A). It is conceivable that like with NTD, the association of NTD-N1 with metHb leads to spectral changes in the Soret region as proposed in Scheme 1.

The transfer of heme from metHb to NTD-N1 within the binary protein complex is assigned to the second phase (k_{obs2}) observed in the stopped-flow spectrophotometer, which is defined by an average first-order rate constant of 0.034 s^{-1}. The slowest phase (k_{obs3}) observed in the stopped-flow spectrophotometer had an average first-order rate constant of 0.003 s^{-1}. The value of k_{obs3} is not significantly different from the literature values for the dissociation of ferric heme from the β subunits of human metHb (~0.002 s^{-1}) [163]. Therefore, we suggest the third phase corresponds to the dissociation of heme from metHb in solution that occurs after the heme transfer within the binary protein complex. Alternatively, the third phase may represent the slow dissociation of the holoNTD-N1-apometHb complex.

One possibility for the two populations inferred in resting NTD-N1 by the kinetic analysis is because of different oligomerization states of the protein. Analytical gel filtration was performed to evaluate the oligomerization state of NTD-N1 in solution. The molecular weight (MW) of NTD-N1 was determined by comparing its elution volume with those of known protein standards (aldolase, catalase and bovine serum albumin) on a Superose-6 10/300 column (GE Healthcare) in PBS. Most of the NTD-N1 protein in these experiments was excluded from the column with an elution volume (15.7 ml, fig. S14A) that was similar to that of aldolase (MW of 160 kDa, elution volume 15.4 ml, fig. S14B), thereby establishing a MW of ~140 kDa for NTD-N1, consistent with the presence of NTD-N1 dimers (~142 kDa).

Heme transfer from metHb to the full-length Shr

The kinetics of heme acquisition from metHb by the full-length Shr was carried out and compared to the heme transfer between metHb and the NTD-N1 fragment. Stopped-flow experiments were conducted by mixing various concentrations of metHb in PBS with 2.5 μM apoShr in PBS. The changes in the absorbance at 414 nm recorded over time indicated a triple exponential process (fig. 12A). The observed rate constants of the first and second phases (k_{obs1} and k_{obs2}) increased hyperbolically with increasing metHb concentration (fig. 12B & 12C). The limiting rate constants were determined as the asymptotic estimates at high metHb concentrations, with values of 6.5 ± 0.7 s^{-1} (R^2 = 0.99) for the fast phase, which defines an intercept of 1 s^{-1} on the y axis, and 2.3 ± 0.6 s^{-1} (R^2 = 0.99) for the second phase. The observed rate constants of the third phase (k_{obs3}) did not show an unequivocal dependence on metHb concentration with k_{obs} values that could be fit either with a hyperbolic saturation dependence or

a linear dependence (fig. S15). Each fit returned a rate constant value for k_{obs3} at infinite concentration of metHb of ~0.15 ± 0.07 s^{-1}.

NEAT1 mediates rapid heme transfer to Shp

Heme transfer from Shr to Shp has been previously reported [54]. However, the role of Shr NEAT domains in the process was not studied. To determine whether the two NEAT domains of Shr constitute heme sources for Shp, stopped-flow experiments were carried out. Shp was cloned and the recombinant protein was purified by affinity chromatography (fig. S7). The molar extinction coefficient at 410 nm ($\varepsilon_{410\ nm}$ =116, 000 M^{-1} cm^{-1}) and the UV-visible absorbance spectrum of the heme-bound recombinant Shp were determined (fig. S16). ApoShp at a final concentration of 2.5 μM was mixed in a stopped-flow spectrophotometer with various concentrations of holo NEAT1 or NEAT2, and the spectral changes were monitored over the entire 340-700 nm wavelength range of the diode-array detector. The time course of the reactions for holoNEAT1 *versus* apoShp best fitted a double exponential process (fig. 13A), with both observed first-order rate constants being linearly dependent on the concentrations of holoNEAT1. The second-order rate constants estimated from the slopes of the plots in fig. 13B and 13C were 2.50 ± 0.04 s^{-1} μM^{-1} (R^2 = 0.99) for the fast phase (fig. 13B) and 0.017 ± 0.004 s^{-1} μM^{-1} (R^2 = 0.89) for the slow phase (fig. 13C).

The time course of the reactions for holoNEAT2 *versus* apoShp also best fitted a double exponential process (fig. 13D). The observed rate constants for the fast phase showed a saturation behavior dependent on the concentration of holoNEAT2, with a rate limiting value at

saturating NEAT2 of 0.010 ± 0.001 s^{-1} (fig. 13E). The apparent first-order rate constants for the slow phase were nearly independent of the concentrations of holoNEAT2, with an average observed rate constant of (2.1 ± 0.5) x 10^{-5} s^{-1}.

Heme exchange between Shr NEAT domains

We sought to determine whether NEAT2 could acquire heme from NEAT1. ApoNEAT2 was mixed with holoNEAT1 at 2:1 apoNEAT2/NEAT1 molar ratio for 5 min. NEAT2 was then separated from NEAT1 by affinity chromatography, allowing a selective binding of the NEAT2 fragment. Eluted NEAT2 was analyzed by SDS-PAGE and showed no NEAT1 contamination (fig. S17). The UV-visible spectrum of NEAT2 after incubation with NEAT1 revealed two major peaks at 410 nm and 426 nm, corresponding to bound ferric and ferrous heme, respectively (fig. 14A). Time course of the heme transfer from NEAT1 to NEAT2 was monitored in a stopped-flow spectrophotometer equipped with a monochromator, mixing apoNEAT2 (2.5 μM final concentration) with different concentrations of holoNEAT1. The time course of the heme transfer was biphasic and best fitted a double exponential process. The fast phase was linearly dependent on the concentration of holoNEAT1. A second-order rate constant of 0.15 ± 0.02 s^{-1} μM^{-1} (R^2 = 0.94) was obtained from the slope of k_{obs1} *vs* holoNEAT1 concentrations (fig. 14B). The slow phase exhibited no significant dependence on NEAT1 concentration and had an average observed rate constant of 0.06 ± 0.01 s^{-1}. In a similar experiment using holoNTD-N1 as heme donor to apoNEAT2, the reaction best fitted a single exponential. The observed rate constants were linearly dependent on holoNTD-N1 concentration. The second order rate constant

for heme acquisition was determined as above and resulted in a value of 0.66 ± 0.05 s^{-1} μM^{-1} (R^2 = 0.99). Therefore, Shr NTD contributes only slightly to the transfer of heme from NEAT1 to NEAT2. To test whether NEAT2 can readily transfer its heme back to NEAT1, time course of the reaction of heme transfer from holoNEAT2 (35 μM) to apoNEAT1 (2.5 μM) was carried out. The spectral changes were monitored at 427 nm. The reaction best fitted a double exponential process, with an observed rate constant at saturating concentration of 1.1 ± 0.2 s^{-1} for the fast phase. The observed rate constant of the second phase was negligible (0.003 ± 0.003 s^{-1}).

Discussion 2

Heme flow between proteins and/or isolated NEAT domains was studied in various Isd-proteins from *S. aureus* and *B. anthracis.* Despite the overall similarity in the organization of the heme relay systems and protein homologies, the transfer process appears to be different in different proteins. In several cases, heme shuttle is mediated by an active process involving protein-protein interactions, as is found in the transfer from IsdA to IsdC [146] and from IsdB to IsdA [149] in *Staphylococcus* and the transfer between bacilli proteins IsdX1 to IsdC [40]. In other examples, including the acquisition of heme by IsdH from Hb in *S. aureus* [116] and the transfer of heme from IsdX2 to IsdC of *B. anthracis* [147], heme transport is suggested to be passive, mediated by heme dissociation and capture from solution. The Sia heme relay system in GAS is different from those characterized in *Bacillus* and *Staphylococcus* by the number and the nature of the interacting proteins. In addition, the mechanism of heme transport was investigated in detail only for the relay between Shp and SiaA, the binding protein of the SiaABC

transporters. Here we carried out analyses of the functional domains in Shr, the first receptor in the relay, and assessed the domains' role in heme acquisition and delivery to Shp.

We previously established that both NEAT1 and NEAT2 could capture free heme from solution [148]. In this study, we found that the measured values of the Soret/280 nm ratio after incubation of apoNEAT2 and apoNEAT1 with metHb and separation by affinity chromatography were ~0.83 and ~2.25, respectively. This absorbance ratio is commonly used as an estimation of heme content [147,164,165] and suggests that the process of heme uptake from metHb is more effective with NEAT1 than it is with NEAT2 (fig. 10A & fig.10B). However, in the stopped-flow experiments conducted with isolated Shr fragments, only the NTD-N1 fragment could efficiently acquire heme from metHb, while NEAT1 and NEAT2 did not (similar observations were made with independent protein preparations). There is no obvious basis for the difference in the capacity to obtain heme from metHb observed with isolated NEAT domains in the static heme transfer, versus the rapid reaction experiments. It seems possible, however, that the higher concentration of NEAT-proteins needed for the heme transfer experiments carried out on a column, in comparison to that needed for the stopped-flow (40 μM and 2.5 μM, respectively), may favor a protein state, much like a certain fold or oligomerization status that is prone for heme uptake. Enzyme concentration was shown to affect reaction kinetics in some cases [166]. The inclusion of the metHb-binding region, NTD, in the NTD-N1 fragment may have increased heme capture by NEAT1 by possibly fostering stable interactions with metHb, or shifting the protein population balance towards the state that favors heme uptake. The suggestion of two protein populations, only one of which participates in heme uptake, is also consistent with the kinetics of heme uptake by NTD-N1 as discussed below.

Heme transfer from metHb to IsdH NEAT3 is ~2-fold faster in the presence of the metHb-binding domain, IsdH NEAT1 [116]. Nevertheless, substantial differences exist between the heme transfer events mediated by Shr NTD-N1 and IsdH. On the one hand, heme transfer from metHb to IsdH NEAT3 in presence of IsdH NEAT1 is a slow biphasic process with rate constants similar to the rate constant of free dissociation of heme from metHb [116]. Conversely, Shr NTD-N1 fragment obtained heme from metHb faster and in a unique three-phase process that was not seen in other characterized heme relays: a rapid first phase with apparent rate constants that decreased hyperbolically with the increase in metHb concentrations (fig. 11B), followed by the second and third phases that did not show linear or hyperbolic dependence on metHb concentrations. While the average rate constant of the third phase does not deviate significantly from that of free dissociation of heme from the β-subunit of metHb (~0.002 s^{-1}) [163], the rate constant of the second phase is ~20-fold higher. The inverse correlation between the apparent rate constants and metHb concentrations observed during the first phase is consistent with the minimal kinetic model proposed in Scheme 1, and is explained by a slow interconversion between two forms of apoNTD-N1 that are present in solution, with only one form that binds metHb in a productive fashion that results in the subsequent heme transfer. The increasing amount of metHb added to the mixture progressively altered the equilibrium, due to the formation of a complex between metHb and the binding form of apoNTD-N1. Formation of different multimeric states is one of the possible explanations for the coexistence of different forms of apoNTD-N1. Dimers formation by NTD-N1 was supported by the analytical gel filtration experiments, and ELISA confirmed that stable interactions between NTD and metHb are formed (fig. S10, S14 and [148]). The first step of Scheme 1 implies that complex formation

without heme transfer results in the spectral changes. This hypothesis was supported by the changes observed in the UV-visible absorbance spectrum of metHb when it was incubated with NTD, but not with MBP. During the second phase, the intermediate complex apoNTD-N1-metHb may facilitate the transfer of heme from the metHb directly to NEAT1 (Scheme 1). The third phase may represent the release of heme in solution from the β-subunit of metHb, as suggested by the low observed rate constants. Alternatively, it may represent the slow dissociation of the holoNTD-N1-apometHb complex.

Like the isolated NTD-N1, the full-length protein acquired heme from metHb in a time course that best fitted a triple exponential equation at all tested metHb concentrations. However, the observed rate constants for the first and second phases were hyperbolically dependent on metHb concentration, whereas the observed rate constants of the third phase did not show an unequivocal dependence on metHb concentration (fig. 12B & C and fig. S15). The fit of k_{obs1} values defines a y intercept of 1 s^{-1}, which corresponds to the reverse of the heme transfer to NEAT1 domain. The first and second phases were ~190 and ~65 times faster, respectively, than the second phase of heme transfer from metHb to apoNTD-N1. We propose that these two phases correspond to the direct heme transfer from metHb to NEAT1 and to NEAT2, respectively (Scheme 2), with the first process ~3 times faster than the second (6.5 ± 0.7 s^{-1} *versus* 2.3 ± 0.6 s^{-1}). The third phase may correspond to the dissociation of the Shr-metHb complex (Scheme 2). Protein-protein interactions involving hemoproteins and cognate partners can result in changes of the absorbance properties of the bound heme ([157-162] and fig S13A). In summary, although both the NTD-N1 fragment and the full-length Shr acquired heme from metHb in a three-phase process, significant differences are found between the mechanisms

involved. The full-length protein, which contains two heme-binding domains, scavenged heme from metHb several fold faster than NTD-N1.

Shp, the adjacent protein to Shr in the Sia system, does not efficiently acquire heme from metHb, but readily scavenges it from Shr [54]. The stopped-flow kinetics experiments in this study revealed that holoNEAT1 transfers heme to apoShp in a two-phase process with second order rate constants of 2.5 ± 0.04 s^{-1} μM^{-1} and 0.017 ± 0.004 s^{-1} μM^{-1}, and with both phases linearly dependent on holoNEAT1 concentrations (fig. 13B and C). This observation is indicative of two heme transfer events occurring simultaneously from two species of holoNEAT1 to apoShp, with one species transferring its heme ~150 times faster than the other species (Scheme 3). Different multimeric states, other protein rearrangements or the presence of a certain fraction of protein not fully competent for heme uptake, may be invoked to explain the presence of two phases here. Similarly, two phases were observed in the transfer reactions between holoNEAT2 and apoShp. The fast phase was dependent on the concentration of holoNEAT2 in a saturable manner, and the slow phase was independent of holoNEAT2 concentrations. The observed limiting value at holoNEAT2 saturation of the fast phase (0.01 ± 0.001 s^{-1}) is comparable to the observed rate constant of the slow phase in the transfer reactions between holoNEAT1 and apoShp. In conclusion, NEAT1 appears to donate heme directly to Shp probably by an active process, whereas heme transfer from NEAT2 to Shp is a slow process that likely relies on the free dissociation of heme in solution. Finally, since the rate constant of the slow phase observed in the transfer reaction between holoNEAT2 and apoShp was nearly equal to zero, it may be an artifact due to damaged or not fully functional protein.

Here we explored the heme flow within Shr using both qualitative and quantitative assays. ApoNEAT2 efficiently acquired heme when mixed in excess with holoNEAT1. The kinetics of heme transfer from holoNEAT1 to apoNEAT2 showed that this reaction was ~17 times slower than the reaction of heme transfer from holoNEAT1 to apoShp, indicating that NEAT1 preferentially transfers its heme to Shp rather than to NEAT2. The reverse heme transfer reaction from holoNEAT2 to apoNEAT1 suggested that NEAT2 transfers heme to NEAT1 faster than it receives heme from NEAT1. This implies that the transfer of heme from NEAT1 to NEAT2 only occurs as an alternative, probably in situations where heme is present in excess. The observed differences in the ability of Shr NEAT domains to obtain and transfer heme illustrate an example of functional diversity of these protein modules when present in multiple copies within a single protein. Another example of NEAT functional diversity is evidenced by the five NEATs of IsdX2 hemophore in *B. anthracis* [147].

Taken together, our results shed light on the intra- and inter-molecular mechanisms of heme acquisition and transfer by Shr. We propose that Shr binds metHb through NTD and forms an intermediate protein complex, which may facilitate direct heme transfer from metHb to NEAT1 and NEAT2, and eventually the release of heme from metHb in solution. Heme scavenged by NEAT1 is rapidly transferred to Shp for delivery into the cell by the SiaABC transporter. Heme acquired by NEAT2 is stored and transferred back to NEAT1 when needed, possibly when heme availability is limiting (fig. 15). The hemolytic GAS can colonize a variety of sites in the human body, including the mucosal membranes in the upper respiratory tract and the skin. This pathogen could also spread via blood and various tissues producing bacteremia, massive necrosis, or both. Therefore, during infection, GAS is confronted with a changing

environment where iron and heme could be highly restricted or toxic in excess. The possible function of Shr as a modulator of heme uptake, as raised by this investigation, could be very important for GAS adaptation during the infection process.

While this manuscript was in preparation, a study [167] was published suggesting that apoShr obtains heme from metHb in a biphasic process with reaction rate constants of 0.027 s^{-1} and 0.0042 s^{-1}. Those measurements were carried out at a single metHb concentration without evaluation of their dependence on metHb concentration [167]. In the present study, we tested heme transfer from metHb to apoNTD-N1 and to apoShr across multiple concentrations of metHb. This comprehensive analysis allows us to establish that heme uptake from metHb involves a three-phase process with reaction rate constanzts of 6.5 s^{-1}, 2.3 s^{-1} and 0.15 s^{-1} under saturating conditions. For the transfer to Shp, we found in this study that while isolated NEAT1 readily gives its heme to Shp, NEAT2 does not. This inefficient transfer of heme from NEAT2 to Shp might explain the partial heme transfer with the full-length Shr (37% of the heme is not transferred) recently reported by Lu et al [167].

Materials and methods 2

The bacterial strains, media and antibiotics

Escherichia coli (*E. coli*) cells were grown aerobically in Luria–Bertani (LB) medium at 37 °C supplemented with 100 μg/ml of ampicillin. The *E. coli* strains used in this study are listed in Table 3.

Recombinant Shr and Shp proteins

The plasmids and primers used in this study are listed in Tables 3 and 4. The cloning of the recombinant Shr proteins, NTD-N1 (pEB11) and NEAT2 (pHSL2), each expressed as N-terminal fusion to the Strep-Xpress® epitope was previously described [148]. Shr NEAT1 fragment is insoluble when expressed as an isolated domain [148]. MBP was previously shown to help in the solubility of recombinant proteins; therefore, an N-terminal fusion of Shr NEAT1 to His-MBP was constructed. Cloning was performed using the Gateway® technology (Invitrogen) according to the manufacture protocol. In brief, NEAT1 region was amplified from NZ131 chromosome with ZE353/354 primer set and was cloned into the entry vector pDONR^{TM}221 by BP Clonase^{TM} II. The resulting entry clone, pYSH5, which carries NEAT1 fragment flanked by the *att*L sites, was then allowed to interact with the destination vector pDEST-His tag-MBP. The produced plasmid, pYSH6, expresses a His-tag-MBP-NEAT1 fusion protein from the TAC promoter. The construction of Shp-His expression vector was accomplished by TOPO® directional cloning according to the manufacturer instruction (Invitrogen, K101-01). The *shp* ORF was amplified from NZ131 chromosome using the

ZE406/ZE407 primer set and introduced into the pET101/D-TOPO vector. The resulting plasmid pOM101 codes for a Shp-His tag fusion protein expressed from the T7 RNA polymerase promoter.

Proteins expression and purification

NTD-N1 and NEAT2 were prepared as previously described [148]. Expression of His-tagged MBP-NEAT1 and His-tagged Shp was induced overnight at 27 °C with 1mM isopropyl β-D-1-thiogalactopyranoside. Cells were harvested and resuspended in an extraction buffer (20 mM Tris pH 8, 100 mM NaCl, 0.1% Triton X-100) with the addition of 0.5 mg/ml and Complete, mini-EDTA-free protease inhibitor cocktail tablets (Roche), then lysed by sonication. The cells' pellet was centrifuged and the cleared lysate was then applied to a 5 ml HisTrap HP affinity column (nickel column) and purified using a FPLC. Purified proteins were dialyzed in PBS buffer (10 mM phosphate-buffered saline, 100 mM NaCl, pH 7.4) prior to their use for experiments. Western blot analysis of recombinant Shp was carried out using anti-His antibodies from mouse (Sigma).

Preparation of apoproteins, measurement of heme and protein concentrations

Preparation of apoproteins and total protein measurements were performed as previously described [148]. Heme concentration was determined by the absorbance at 410 nm using Beer's law (A= εbc, where ε is the molar extinction coefficient at 410 nm of the corresponding heme-

bound protein, b is the path length of the sample and c is the concentration of heme in the sample).

Heme transfer experiments

ApoNEAT1 and apoNEAT2 (200 nmoles of each protein in 2 ml of PBS) were mixed with metHb (100 nmoles in 3 ml of PBS). The final concentrations of apoNEAT proteins and metHb in the 5 ml mixtures were 40 and 20 μM, respectively. After 5 min, the mixtures were then loaded on a HisTrap HP affinity column or *Strep*-Tactin Superflow column, respectively, to separate the Shr fragments from metHb. Trace metHb was removed by washing several times (10 column volumes) with His-tag wash buffer (20 mM sodium phosphate pH 7.4, 500 mM NaCl, 30 mM imidazole) or *Strep-tag* wash buffer (100 mM Tris-HCl pH 8.0, 250 mM NaCl, 1 mM EDTA). Subsequently, the immobilized proteins were eluted with His-tag elution buffer (20 mM sodium phosphate pH 7.4, 500 mM NaCl, 500 mM imidazole) or *Strep*-tag elution buffer (100 mM Tris-HCl pH 8.0, 150 mM NaCl, 1 mM EDTA, 2.5 mM desthiobiotin). Spectroscopic analysis (250-700 nm) of the apoproteins before and after treatment with metHb was carried out using a Varian Cary 50 Bio spectrophotometer. All UV-visible spectra were subtracted from their corresponding background absorbance at 700 nm. The same procedure was used for heme transfer from NEAT1 to NEAT2, with the exception that apoNEAT2 (200 nmoles in 2 ml of PBS) was mixed with holoNEAT1 (100 nmoles) for 5 min and the two proteins were separated using a *Strep*-Tactin Superflow column.

Heme reconstitution, Enzyme-Linked ImmunoSorbent Assays (ELISA)

The heme reconstitution and ELISA experiments were conducted as described in [148].

Stopped-flow analysis

Rapid kinetics was carried out on a Hi-Tech SF-16 stopped-flow spectrophotometer. The reacting apoproteins were mixed individually in PBS at 25 ºC with different concentrations of the corresponding holoprotein. All concentrations of heme-loaded proteins were based on the absorbance of heme bound to the protein. All concentrations used maintained pseudo-first order conditions. Absorbance data were collected over the entire 340-700 nm wavelength span of the diode-array detector. Alternatively, time-courses of the reaction were collected at the wavelength of maximal change with a monochromator. The optical path length for all the stopped-flow experiments was set to 2 mm.

Data analysis

The absorbance traces at individual wavelength were analyzed using KinetAsyst 3 software (Hi-Tech Scientific) and KaleidaGraph (Synergy Software). Transients were fitted using the standard double or triple exponential expression (eq. 1, 2)

$$A = C_1 e^{-kobs1 t} + C_2 e^{-kobs2 t} + b \qquad \text{Eq. 1}$$

$$A = C_1 e^{-kobs1 t} + C_2 e^{-kobs2 t} + C_3 e^{-kobs3 t} + b \qquad \text{Eq. 2}$$

Where A is the absorbance at selected wavelength, k_{obs1}, k_{obs2} and k_{obs3} are the observed rate constants for the different phases, respectively; C1, C2 and C3 are the relative amplitude values for the different phases; and b is an offset value to account for a non-zero baseline.

Table 3: Strains and Plasmids used in this study

Name	Description	Source/Reference
Strains		
E.coli Top10	Host for pOM101 propagation	Invitrogen
E.coli BL21 Star	Host for pOM101 expression	Invitrogen
E.coli One shot Omni Max2-TI	Host for pYSH6 expression	Invitrogen
Plasmids		
pEB11	Expresses Strep tag-NTD-N1 from P_{tet}	[148]
pHSL2	Expresses Strep tag-NEAT2 from P_{tet}-	[148]
pDONR^{TM}221	Gateway® Donor vector with *att*P sites	Invitrogen
pDEST-His tag-MBP	Gateway® Destination vector with *att*R *sites*	[168]
pYSH5	*att*L-NEAT1-*att*L entry vector	This study
pYSH6	Expresses His tag-MBP-NEAT1 from P_{tac}	This study
pET101/D-TOPO	Directional TOPO® TA cloning vector	Invitrogen
pOM101	Expresses Shp-His tag from P_{T7}	This study

Table 4: Primers used in this study

Name	Sequence	Description
ZE353	GAGAACCTGTACTTCCAGTCTTATCAAGCAG GTGAGGTTTCT	Sense primer for Shr NEAT1 domain
ZE354	GGGGACCACTTTGTACAAGAAAGCTGGGTA TTAATCATCAGTTTCTACCTGATAACC	Anti-sense primer for Shr NEAT1 domain
ZE406	GATAAAGGTCAAATTTATGGATG	Sense primer for *shp*
ZE407	GTCTTTTTTAGACCGAAACTTATC	Anti-sense primer for *shp*
ZE139	CCCCGAATTCTTAAATCAAAAACAATTGCGT G	Sense primer for Shr NEAT2 domain
ZE140	AAAAGGTACCTTAGACAACCTTTGCCTTCTC TG	Anti-sense primer for Shr NEAT2 domain

CHAPTER III

DISCOVERY OF HUPZ, THE FIRST STREPTOCOCCAL HEME OXYGENASE

Introduction 3

The restriction of free iron in the mammalian host constitutes a severe limitation to bacterial infections. Most of the biologically available iron in mammalians is bound to protoporphyrin IX in heme molecules, the vast majority of which are sequestered by proteins. Bacterial pathogens overcome this nutritional sequestration using elaborated systems that allow them to scavenge and transport heme from host hemoproteins into the bacterial cell [37,98,144,145]. A few mechanisms then allow bacteria to retrieve iron from the porphyrin center [56]. The most common one relies on oxidative degradation of the porphyrin ring by cytoplasmic enzymes known as heme oxygenases (HO) [57]. When supplied with electron donors, the canonical HOs break down heme to CO, α-biliverdin and free iron [60,169].

The first bacterial HO discovered is HmuO, a homologue of the human HO-1 found in the pathogen *Corynebacterium diphteriae* [72,73]. Subsequently, several other HOs were identified and characterized in *Neisseria meningitides* (HemO) [74], *Clostridium* species (HemO) [75,76] and *Pseudomonas aeruginosa* (PigA or pa-HO and BphO) [77,78]. Like the mammalian HO-1, all of these HOs consist of monomeric α-helices with similar folds and

degrade heme to α-biliverdin [66], with the exception of PigA which produces an unusual mixture of β- and δ-biliverdin [77].

A group of bacterial HOs that are structurally different from the mammalian HO-1 is represented by IsdG and IsdI from *Staphylococcus aureus*. The structure of enzymes from the IsdG family consists of a homodimeric β-barrel with two separate active sites [82,83]. Unlike HmuO-type enzymes, IsdG catalyze the production of staphylobilin, an oxo-bilirubin chromophore and not biliverdin [81]. Members of the IsdG family include HmuD and HmuQ from *Bradyrhizobium japonicum* [84], MhuD from *Mycobacterium tuberculosis* [85] and the IsdG homologues from *Bacillus anthracis* [87] and *Staphylococcus lugdunensis* [86].

A separate group of heme degrading enzymes whose products are not characterized was described in some pathogens including HemS from *Yersinia enterocolitica* [89], ChuS from *Escherichia coli* [88] and HemS homologue from *Bartonella henselae* [90]. Biochemical data supporting heme degradation in the presence of reducing agents was only shown for the last two examples [88,90]. The high sequence homology shared by these three proteins suggests their relatedness. The crystal structure of ChuS revealed a unique structure consisting of two central sets of antiparallel β-sheets, each flanked by two pairs of α-helices [88].

A new family of bacterial HOs with no homology to previously described enzymes was recently uncovered in *Campylobacter jejuni* (Cj1613c) [91], *Helicobacter pylori* (HugZ) [92] and *Vibrio Cholerae* (HutZ) [93]. Members of this family share weak sequence similarities with FMN-binding proteins and form dimers [93,94]. The crystal structure of HugZ was recently resolved; this protein adopts a split β-barrel fold that is characteristics of FMN-binding proteins,

however, actual FMN binding was not demonstrated. [94]. This structure is distinctive from that of HmuO-like or IsdG-like proteins. Interestingly, like PigA, HugZ has a unique δ-meso regiospecificity for cleaving the ring in the heme molecule [92], whereas HutZ is proposed to have both β- and δ-meso regioselectivity [93].

Heme uptake in Group A Streptococcus (GAS) is mediated by a conserved ten-gene operon, *sia* (streptococcal iron acquisition system) that is directly repressed by the iron-dependent regulator MtsR [45,47]. Shr, the product of the first gene in the *sia* locus is a complex surface receptor. It contains two heme-binding NEAT domains separated by a series of leucin-rich repeats, a calcium binding EF hand and a unique N-terminus region (NTD) which harbors two uncharacterized DUF1533 modules [148,150]. Shr is attached to the cytoplasmic membrane by a hydrophobic tail located at its C-terminus and is exposed at the bacterial surface by protruding through the peptidoglycan layer [48]. Different regions of the protein recognize and interact with various ligands including heme, methemoglobin (metHb), hemoglobin-haptoglobin complex and some ECM proteins [45,48,148]. The full-length Shr and a fragment of the protein that includes NTD and NEAT1 (NTD-N1) obtain heme from metHb in vitro [54,148]. Heme acquired by Shr is efficiently transferred to Shp, the protein encoded by the second gene in the *sia* operon, which in turn transfers it to the SiaABC (HtsABC) transporter [152]. Recent kinetic and spectroscopic analyses indicate that Shr and NTD-N1 fragment scavenge directly heme from metHb by two distinct and unprecedented three-phase processes. Additionally, NEAT1 efficiently transfers its heme to Shp in a biphasic process, whereas NEAT2 does not and may serve as temporary heme storage on the bacterial surface. Furthermore, a reversible heme

exchange occurs between NEAT1 and NEAT2, constituting the first example of intra-molecular heme transfer between NEAT domains.

The fate of the imported heme inside the streptococcal cell remains unknown, as to date, a heme oxygenase has not been identified in Streptococci. Herein, we report the identification of the first heme oxygenase described in the *Streptococcus* genus. We provide biochemical evidences for heme binding and degradation by the enzyme and we show that it is the representative of a new family of heme oxygenases.

Results 3

Heme binding by HupZ

GAS utilizes host heme containing proteins as iron source during infection [44]. This implies that the bacterium possesses mechanisms that allow it to retrieve iron from heme. This function is commonly carried out by HOs which catalyze the enzymatic cleavage of the porphyrin ring releasing free iron, CO and biliverdin [60]. Homologues of HOs are absent from the streptococcal genome, raising an intriguing mystery regarding heme utilization by GAS. Microarray analysis of MtsR-regulated genes identified putative gene (Spy49_0662) that was overexpressed in the *mtsR* mutant strain, suggesting its implication in iron or heme metabolism [170]. Spy49_0662 translates into a small protein of about 18.5 kDa with no secretion signal indicating that the protein likely functions in the cytoplasm. *In silico* analysis showed that this protein contains a module that belongs to the superfamily of the signature domain of the

pyridoxamine 5'-phosphate oxidase (PNPOx). The PNPOx domain is found in FMN binding enzymes.

To test its role in iron utilization, we cloned and expressed Spy49_0662 from M49 GAS in *E. coli* as a C-terminal fusion to hexa-histidine tag. The recombinant protein was purified on an affinity column using FPLC. The cell lysate had a yellow color that was retained in the affinity column during purification. However, the yellow substance was separated from the protein and was eluted out of the column in different protein-free fraction. SDS-PAGE analysis confirmed the presence of a single protein band that migrated to the expected size of 18.5 kDa (fig. S18A). Subsequently, UV-visible spectroscopic analysis was conducted on the different fractions and revealed that the absorbance spectrum of the yellow fraction is consistent with that of oxidized FMN (fig. S18B). In contrast, the spectrum of the purified recombinant protein included bands at 334 and 405 nm (fig. S18C) which suggest that it is co-purified with reduced FMN [171]. Heme titration experiments were then carried out to test whether the Spy49-0662 protein binds heme. Various concentrations of hemin chloride were added to 40 μM of the purified protein in 20 mM sodium phosphate buffer, pH 7.4. Upon hemin addition, a Soret peak appeared at 414 nm and increased with incremental addition of hemin. The peak at 414 nm progressively shifted toward 420 nm and this shift coincided with the appearance of two bands at 530 and 560 nm, consistent with the characteristic spectrum of bound ferrous heme (fig. 16A). The plot of the differential absorbance at 414 nm as a function of hemin concentration indicated that the protein bound heme to saturation at 40 μM of hemin, suggesting a 1:1 binding ratio (fig. 16B). On the other hand, the characteristic peaks of bound heme were absent when various concentrations of hemin were added to the buffer without the protein (fig 16C). Taken together,

these data established that Spy49-0662 expresses a new heme binding protein in GAS. The protein was therefore named HupZ (for heme utilization protein). The molar extinction coefficient for heme-bound HupZ was determined at 414 nm using the pyridine hemochromogen method and resulted in $\varepsilon_{414\ nm} = 110000\ M^{-1}\ cm^{-1}$ (fig. S19).

Heme degradation by HupZ

Heme degradation by HOs requires a source of reducing equivalent which is provided in mammals by the combined action of NADPH and cytochrome P450 reductase (CPR) [60,66]. While the native redox partner for the bacterial HOs is mostly unknown, CPR and ascorbic acid are typically used for *in vitro* heme degradation studies. HoloHupZ was prepared by mixing the apoprotein with hemin chloride at a concentration ratio of 1:1.5 (protein to hemin). After 30 min incubation on ice, the mixture was dialyzed then gel filtered to separate the holoprotein from excess free heme. Catalase at a final concentration of 2 μM was added to 20 μM holoHupZ in 20 mM sodium phosphate buffer to prevent non enzymatic oxidation of the heme by hydrogen peroxide. Surprisingly, the Soret peak of the protein, as well as the bands at 530 and 560 nm decreased over time as the protein solution was incubated at room temperature. This observation suggested enzymatic heme degradation (fig. 17A). The decrease of the Soret peak and of the band at 560 nm isosbestically generated growing bands at 360 and 630 nm respectively, showing the formation and accumulation of an intermediate with maximum absorbance at the corresponding wavelengths (fig. 17A and inset). As a control, a similar experiment was conducted using holoShp, another characterized heme-binding protein in GAS. Interestingly, the

Soret peak as well as the β- and α-bands of holoShp did not decrease over time, indicating that heme degradation was not taking place (fig. 17B).

We hypothesized that the observed heme degradation by HupZ in presence of catalase was supported by electrons from a reduced cofactor that might have copurified with the protein. To test this hypothesis, 2 ml of 20 μM holoHupZ was incubated overnight at 4 °C, with 1 mM of potassium ferricyanide. Following gel filtration to remove the ferricyanide, the protein was diluted to 10 μM and catalase was added to it to a final concentration of 2 μM. The UV-visible absorbance spectrum of the protein solution was subsequently monitored for heme degradation. Unlike the untreated protein, the Soret peak of the ferricyanide treated holoHupZ did not significantly decrease, indicating that heme degradation was inhibited by the oxidizing agent (fig. 17C).

CPR-NADPH as a source of electrons for heme degradation by HupZ

Heme degradation by HupZ was further assessed in a reaction containing 20 μM of the holoprotein, 2 μM of catalase, 25 μg of CPR and 1 mM of NADPH. The spectral changes of the reaction were recorded between 350 and 700 nm at room temperature for 1 hour. The peak at 414 nm and the bands at 530 and 560 nm characterizing heme bound to HupZ decreased significantly in the first 30 min then became stagnant. These variations in the spectral features substantiated that the bound heme was degraded over time and that the reaction reached it rate-limiting step or was completed within 30 min. Heme degradation in this reaction was accompanied by a slow shift of the Soret peak toward 420 nm and generated a growing peak at 670 nm (fig. 18A and

inset). In addition, the color of the reaction turned from red to green, suggesting biliverdin production (fig. S20). When the reaction was carried out in the absence of CPR or NADPH, the spectral changes were similar to that of the holoprotein alone described in fig. 17A (fig. 18B and 18C). An additional control reaction was carried out using a solution containing 20 μM of heme-bound NEAT2 (a characterized heme-binding protein in GAS), 2 μM catalase, 25 μg of CPR and 1 mM of NADPH. No changes in the spectral features of the holoprotein were observed after 1 hour (fig. 18D). This clearly, showed that NEAT2 does not degrade heme even in the presence of the CPR-NADPH system, and that the heme degradation observed in the reaction containing holoHupZ was imputable to the enzymatic activity of the latter.

Ascorbic acid as reducing partner for HupZ-catalyzed heme degradation

The ability of HupZ to degrade heme using ascorbic acid as an electron donor was tested. For that, 20 mM of ascorbic acid and 2 μM of catalase were added to 20 μM of holoHupZ and the absorbance spectra of the reaction were recorded between 350 and 700 nm for one hour. The spectral variations observed for this reaction did not differ significantly from that of the holoprotein without addition of a reducing agent (fig. 19A), suggesting that ascorbic acid does not significantly contribute to HupZ heme oxygenase activity. The addition of ascorbic acid to holoShp did not change the spectral features of the holoprotein over time (fig. 19B). Here again the data indicate that the decrease in the characteristic peaks of heme-bound HupZ was catalyzed by the protein. Unlike with ascorbic acid, an observable reduction of the bound heme iron

precedes an important decrease of the Soret in presence of CPR-NADPH as a source of electrons.

Sequence comparison of HupZ and other bacterial heme degrading enzymes

Bacterial HOs are classified in four major groups based on their structural similarities. Representatives of these different groups include, HmuO from *C. diphteriae*, IsdG from *S. aureus*, ChuS from *E. coli* and HugZ from *H. pylori*. To determine whether HupZ belongs to one of the characterized HOs families, a multiple sequence alignment was conducted using the web-based tool, ClustalW2 (EMBL-EBI). The amino acids sequence of HupZ was aligned against the sequences of three representatives of each of the four bacterial HOs families. The proteins members of each family grouped into a single or two linked clades showing their phylogenetic relatedness as expected (fig. 20). Interestingly, HupZ defines a monophyletic group by itself, suggesting that it is the prototype of a new family of bacterial HOs (fig. 20). In spite of being members of different monophyletic groups, HupZ, MhuD and PigA are at similar evolutionary distance from the root with estimated 43%, 42% and 44% evolution respectively. On the other hand, the evolutionary distances of the human HO-1 (36%), HmuO (34%) and HugZ (35%) from the common ancestor are also very similar. HutZ, HmuZ and PhuS evolved between 26 and 30 % from the common ancestor, whereas IsdG, IsdI, HemS and ChuS were the least evolved with evolutionary distances between 16 and 18%.

Discussion 3

During infection, GAS obtain and utilize iron from the mammalian host hemoproteins [44]. Heme is scavenged from host heme containing proteins by Shr, which subsequently transfers its heme to Shp. The latter then conveys heme to a dedicated transporter (SiaABC) for its transportation through the thick peptidoglycan layers to the cytoplasm [45,53,54,148,152,167]. In the cytoplasm, the imported heme must be degraded through an enzymatic process to release iron from the porphyrin center [57]. In most bacteria, HOs carry out this function by catalyzing the oxidative cleavage of the *meso* carbon bridges of the porphyrin at the positions α, β, γ or δ [57,59]. In GAS however, the process of heme degradation has not been reported since homologues of HOs were not found in the genome of these bacteria.

In this study we characterized the protein encoded by *hupZ*, a gene from GAS that is up-regulated in low iron conditions. The protein lacks a secretion signal, indicating its localization in the cytoplasmic compartment. The recombinant HupZ expressed and purified from *E. coli* bound heme to saturation at 1:1 ratio (fig. 16). Thus, it is a novel heme binding protein in GAS with potentially an intracellular function. We hypothesized that HupZ is involved in heme metabolism and therefore tested its ability to degrade heme. *In vitro* heme degradation experiments require the presence of a suitable reducing equivalent and are typically carried out with CPR-NADPH or ascorbic acid as electron donors.

Heme bound-HupZ, incubated without the addition of an external reducing partner, surprisingly degraded heme even in the presence of catalase to prevent non enzymatic oxidation of heme by hydrogen peroxide (fig. 17). The inherent heme degradation activity of HupZ was

inhibited when the protein was incubated with the oxidizing agent, potassium ferricyanide. These results suggested that HupZ was purified with a reduced cofactor serving as a source of electrons for heme degradation by the protein. Sequence analysis of HupZ showed that the protein harbors a PNPOx-like module which is found in FMN-binding proteins. In addition, the cell lysate of *E. coli* overexpressing HupZ contained a substantial amount of oxidized FMN that was separated from the protein during purification (Fig. S18B). Together these observations indicate that the reduced cofactor that might have purified with HupZ is FMN hydroquinone ($FMNH_2$). The *E coli* chorismate synthase, is another example of protein which does not bind oxidized FMN when purified aerobically but stably binds $FMNH_2$ with high affinity [171,172].

Furthermore, when ascorbic acid was used as an electron source for heme degradation by HupZ, no difference was observed compared to the activity of the protein by itself. This clearly indicates that ascorbic acid is not an efficient reducing partner for HupZ function. On the other hand, heme degradation by HupZ was considerably enhanced when CPR-NADPH was used as reducing equivalent. The first step of the catalytic mechanism of heme oxygenases is the reduction of ferric heme to ferrous heme [66]. The spectral shift (from 414 nm to 420 nm) observed shortly after NADPH addition indicates the formation of ferrous heme, possibly followed by O_2 binding. The reaction produced a green color indicative of biliverdin production, which was confirmed by the spectral features of the product. In fact, the characteristic peaks of bound heme progressively decreased while generating isosbestically new peaks that are consistent with biliverdin absorbance spectrum. Heme degradation by HupZ using its reduced cofactor or ascorbic acid produced a growing peak at 630 nm while the reaction with CPR-NADPH generated a growing peak at 670 nm. This suggests that the products generated by these

reactions may be different biliverdin isomers, or a mixture of isomers in one case or the other, as seen with PigA and HugZ [77,92]. Though, further biochemical and chemical analyses are necessary to unequivocally characterize all the products generated by HupZ catalyzed heme degradation, as well as its regiospecificity.

Sequence comparison between HupZ and several HOs from different structural families showed that this enzyme is not related to any previously characterized HO, although it is at similar evolutionary distance as PigA and HmuD from *P. aeruginosa* and *M. tuberculosis* respectively (fig. 20). A more conclusive structural comparison of HupZ with other HOs will be carried out in the near future, as the resolution of the protein's structure by crystallography is underway.

In conclusion, we identified and characterized for the first time, a heme oxygenase in the *Streptococcus* genus which was named HupZ. Orthologs of the protein are found in other important pathogens such as *Streptococcus agalactiae* and *Streptococcus dysgalactiae*. It is the representative of a new family of flavoenzymes capable of catalyzing heme degradation using electrons from their reduced flavin cofactor.

Materials and methods 3

The bacterial strains, media and antibiotics

Escherichia coli (*E. coli*) cells were grown aerobically in Luria–Bertani (LB) medium at 37 °C supplemented with 100 µg/ml of ampicillin. The *E. coli* strains used in this study are listed in Table 5.

Recombinant HupZ, NEAT2 and Shp proteins

The plasmids and primers used in this study are listed in Tables 5 and 6. The cloning of the recombinant Shp expressed as a C-terminus fusion to the His-tag was previously described (Chapter 2). The construction of HupZ-His and NEAT2-His expression vectors was accomplished by TOPO® directional cloning according to the manufacturer instruction (Invitrogen, K101-01). The *hupZ* and *shr NEAT2* ORFs were amplified from NZ131 chromosome using the ZE437/ZE438 and ZE427/ZE428 primer sets respectively and introduced into the pET101/D-TOPO vector. The resulting plasmids, pZZ2 and pOM102, code for a HupZ-His tag and NEAT2-His tag fusion proteins respectively, expressed from the T7 RNA polymerase promoter.

Proteins expression and purification

Expression of the recombinant His-tagged proteins was induced overnight at 27 °C with 1mM isopropyl β-D-1-thiogalactopyranoside. Cells were harvested and re-suspended in an extraction buffer (20 mM Tris pH 8, 100 mM NaCl, 0.1% Triton X-100) with the addition of 0.5 mg/ml and Complete, mini-EDTA-free protease inhibitor cocktail tablets (Roche), then lysed by sonication. The cells' pellet was centrifuged and the cleared lysate was then applied to a 5 ml HisTrap HP affinity column (nickel column) and purified using a FPLC. Purified proteins were dialyzed in sodium phosphate buffer (20 mM sodium phosphate, 500 mM NaCl, pH 7.4) prior to their use for experiments. Western blot analysis of the recombinant His-tagged proteins was carried out using anti-His antibodies from mouse (Sigma).

Heme reconstitution

The heme reconstitution experiments were conducted as described in [148]. All the spectra were normalized by sustracting the absorbance at 700 nm.

Heme degradation assays

Heme-HupZ complex was prepared at a hemin:protein ratio of 1.5:1 and excess heme was removed by filtration through a PD-10 column (GE Healthcare). Degradation of bound heme by HupZ was carried out without electron donor and with two electron donor systems (ascorbic acid and NADPH-CPR). Ascorbic acid was added to a final concentration of 20 mM. In the NADPH-

CPR system, heme-HupZ protein (20 μM) was added to 25 μg of recombinant human NADPH-cytochrome P450 reductase (CPR). The reaction was initiated by adding NADPH to 1 mM and spectra were recorded from 350 nm to 700 nm every 10 min for 1 h. Catalase (bovine liver, Sigma-Aldrich) was added to the reaction systems at a final concentration of 2 μM. All reaction systems were in 1 ml total volume.

Table 5: Strains and Plasmids used in this study

Name	Description	Source/Reference
Strains		
E.coli Top10	Host for pOM101 and pZZ2 propagation	Invitrogen
E.coli BL21 Star	Host for pOM101 and pZZ2 expression	Invitrogen
Plasmids		
pOM102	Expresses NEAT2-His tag from P_{T7}	This study
pET101/D-TOPO	Directional TOPO® TA cloning vector	Invitrogen
pOM101	Expresses Shp-His tag from P_{T7}	Chapter 2
pZZ2	Expresses HupZ-His tag from P_{T7}	This study

Table 6: Primers used in this study

Name	Sequence	Description
ZE427	ATGAATCAAAAACAATTGCGTG	Sense primer for Shr NEAT2 domain
ZE428	AACCTTTGCCTTCTCTGTTGTAAGG	Anti-sense primer for Shr NEAT2 domain
ZE437	ATGATAACACAAGAAATGAAA	Sense primer for *hupZ*
ZE438	GTTACTTTCACTGTTTATTTCTT	Anti-sense primer for *hupZ*

GENERAL DISCUSSION

The novel Hb binding motif in Shr NTD

Hb binding is the first and probably the most important step in the process of heme uptake. It is mediated in the vast majority of Gram-negative bacteria by a consensus protein motif FRAP/NPNL [1] and by a NEAT domain in most Gram-positive hemoproteins receptors [2-6]. Interestingly, the two NEAT domains of Shr do not participate in Hb binding by the protein; rather, this function is carried out by an uncharacterized region of Shr NTD. The Hb binding NEAT domains of *Staphylococcus aureus* IsdH and IsdB contain an aromatic motif consisting of YYHY or YYHFF [2]. These aromatic motifs as well as the consensus motif found in Gram-negatives are absent from Shr NTD, suggesting that the latter contains a novel alternative Hb binding motif, which is yet to be identified and characterized [7]. On the other hand, NTD contains two copies of a domain of unknown function (DUF1533) that can be legitimately hypothesized as the possible Hb binding domains of Shr.

One possibility for identifying the precise region and amino acid residues required for Hb binding by Shr is to conduct partial deletions in order to determine the minimal NTD sequence capable of carrying the function. Subsequently, site directed mutagenesis targeting various residues may be employed to identify a critical motif. Alternatively, a DNA library from Shr NTD's sequence may be used to achieve a phage display, which will allow for the selection of NTD subdomains that show Hb binding. A successful identification of this novel Hb binding motif may also serve as the basis for identifying and studying the function of other bacterial

proteins in which it can be found. Moreover, an emerging strategy to counter bacterial adaptation to antibiotics is the development of molecules that target the iron metabolism of bacteria. One approach is the use of chelators and antagonists to inhibit the binding of iron or iron complexes such as Hb to their receptors [8]. The kinetic studies herein, demonstrate that Shr must bind Hb to efficiently scavenge heme from it. Therefore, the Hb binding motif in Shr constitutes a good target for the development of novel therapeutic molecules against GAS.

Significance of heme reduction by Shr

Shr is copurified with a mixture of ferric and ferrous heme and has the capacity to acquire and reduce ferric heme from solution [7,9]. On the other hand, isolated NEAT2 contains mostly ferrous heme whereas NEAT1 domain is purified with ferric heme. The data from the kinetic studies of heme transfer show that heme is passed from metHb to both NEAT1 and NEAT2 domains in a direct process, but only NEAT1 efficiently transfers its heme to Shp. This observed functional difference may relate to the oxidation status of the heme iron. Examples that support this hypothesis and where the redox state of the iron in bound heme affects the properties of the hemprotein were reported. In IsdC NEAT domain, the reduction of ferric heme causes heme loss by the protein [10]. In addition, the iron axial ligand of IsdA switches from tyrosine to histidine when the ferric heme is reduced. A mechanism of closing/opening of the heme binding pocket, depending on the oxidative state of the heme iron, was therefore suggested for IsdA [10,11]. Moreover, porphyrin with a ferric center binds with higher affinity and stability to IsdH NEAT3 than porphyrin a ferrous center [12].

In the Shr heme reconstitution assay, ferric heme reduction by the protein was more pronounced with increasing amounts of bound heme, suggesting that excess of heme may favor the process. It is therefore plausible to hypothesize that in high heme conditions, NEAT2 binds and reduces ferric heme for storage in the ferrous form, and in low heme situations ferric heme is regenerated then passed to NEAT1 for export to Shp. The storage of ferrous heme which is supposedly less stable and weakly bound is probably rendered possible by the association of ferrous heme with gaseous ligands such as O_2, CO or NO in the context of the host environment [13,14]. This hypothesis can be tested by conducting comparative kinetic studies of heme transfer using stopped-flow spectrophotometer in both aerobic and anaerobic conditions. Rates comparisons between reactions using fully reduced and fully oxidized proteins, as well as between aerobic and anaerobic transfer reactions, will provide direct evidence of the importance for maintaining a certain redox status to achieve an efficient heme transfer.

Basis for the heme degradation by HupZ alone

We identified for the first streptococcal HO (HupZ), which does not relate in sequence and in mechanism to any previously studied HO. HoloHupZ is capable of degrading its bound heme without externally supplied reducing partner. This inherent HO activity is inhibited when the protein is treated with potassium ferricyanide. These observations suggest that HupZ is copurified with a reduced cofactor serving as the electrons donor for heme degradation. *In silico* analysis of HupZ, shows that the protein contains a module from the superfamily of the signature domain of the pyridoxamine 5'-phosphate oxidase (PNPOx). The latter is a FMN flavoprotein

that catalyzes the oxidation of pyridoxamine-5-P (PMP) and pyridoxine-5-P (PNP) to pyridoxal-5-P (PLP). In addition to the presence of a PNPOx domain in HupZ, cell lysate of *E. coli* overexpressing the protein displays a yellow color that is retained in the affinity column during purification. However, the yellow substance is eluted out of the column in a fraction, which is protein-free and separate from that of HupZ. UV-visible spectroscopic analysis shows that the absorbance spectrum of the yellow fraction is consistent with the absorbance spectrum of FMN.

A similar situation is seen with *E coli* chorismate synthase, which does not bind oxidized FMN when purified aerobically [15]. Addition of chorismate synthase to oxidized FMN solution did not quench the fluorescence of the cofactor and ultracentrifugation recovered almost all of the FMN in the filtrate [16]. This underlines the weak binding of oxidized FMN to chorismate synthase and is consistent with the fact that the flavin cofactor is entirely loss during purification [15,16]. The purified chorismate synthase, whose activity requires the reduced form of the flavin cofactor $FMNH_2$, is fully functional in the presence of $FMNH_2$ and dithionite. This suggests that in spite of its inability to associate with oxidized FMN, the protein binds $FMNH_2$, the reduced form of the flavin cofactor and its binding affinity was determined to be more than ten times higher than the estimated affinity for oxidized FMN binding [15,16]. On the other hand, the binding affinity of oxidized FMN to chorismate synthase was increased in the presence of the substrate and analogs of the substrate [17].

It seems possible that like chorismate synthase, HupZ is an FMN binding protein with high affinity to the reduced form of the cofactor. Isolation with some reduced FMN may also explain the heme degradation in the absence of external reducing agent. This hypothesis can be tested by several means. First, as done by Macheroux et al [16], the reduction of FMN and the

binding of the reduced cofactor by HupZ can be simultaneously followed in anaerobiosis, by monitoring the UV-visible spectrum of FMN in presence of HupZ and the xanthine/xanthine-oxidase couple as a reducing partner. Second, the kinetics of inherent heme degradation by HupZ alone, and by HupZ in the presence of dithionite and FMN can be conducted in a stopped-flow spectrophotometer to assess whether reduced FMN increases the rate of heme degradation. In the same experiments, the formation of the flavin-quinone intermediates characterizing passage from one oxidative state to another can be monitored and correlated with heme degradation. Finally, resolving the crystal structure of HupZ in the presence and in the absence of FMN will reveal the presence or not of the reduced flavin cofactor.

Potential in vivo reducing partners of HupZ

The catalytic action of HOs requires reducing equivalents that are provided in mammals by CPR-NADPH [18,19]. CPR is a flavoprotein that contains one FAD and one FMN prosthetic groups. In plants, cyanobacteria and some eubacteria, the redox system composed of NADPH, ferredoxin reductase (FNR) and ferredoxin is suggested to be the reducing partner of the HOs [20-22]. A recent study showed that pa-HO (PigA), a HO from *P. aeruginosa* can efficiently degrade heme using FNR, a FAD-containing flavoprotein, as a reducing partner without the requirement for ferredoxin [23]. Though, additional FNR mediated heme oxygenation has not been shown for any other bacterial system and may not represent the general mechanism for bacteria.

Studies associating flavins with the catalytic mechanisms of HOs are on the rise. Like HupZ, several bacterial HOs were recently described as potentially FMN-binding proteins [24,25]. FMN-containing heme enzymes such as flavocytochrome b_2 have been extensively studied and have been shown to oxygenate the heme substrate using electrons from the flavin hydroquinone ($FMNH_2$) [26]. This suggests that the reduced cofactor by itself may be sufficient to sustain heme degradation by this class of enzymes *in vivo*. However, because of the lack of experimental evidence so far for FMN binding by these HOs, it cannot be ruled out that HupZ may rely on an intracellular reducing partner to carry out its catalytic activity. Therefore, several approaches can be used to identify possible reducing partners of HupZ. One perspective is to conduct genome mining for flavin-dependent oxidases/reductases in GAS and express the recombinant proteins for characterization. Another possibility is to perform a cross-linking in GAS cell lysate followed by immunoprecipitation. Alternatively, purified HupZ may be incubated with GAS cell lysate to allow for possible complex formation. Subsequent separation of the complex from the lysate may allow fishing out and identifying a putative HupZ partner protein.

HupZ heme degradation products

Heme degradation by the conical HO produces CO, α-biliverdin and free iron [27]. However, several bacterial HOs that generate unconventional products were reported. For example, along with CO and free iron, IsdG catalyzes heme degradation to produce an oxo-bilirubin (staphylobilin), whereas PigA and HugZ generate β- and δ-biliverdins [28-30]. On the

other hand, the products of heme degradation by HupZ are yet to be characterized. The spectroscopic analysis of the heme catabolism reactions showed that the decrease of the Soret peak and of the α- and β-bands is accompanied by a concomitant increase around 360 nm and 630 nm respectively. These spectral features are different from those of all the HOs mentioned above and suggest that the product generated may be an unprecedented isomer of biliverdin (such as γ-biliverdin) or a mixture of isomers. Furthermore, the reaction of heme degradation by HupZ using CPR-NADPH as electrons donor turns from red to green after one hour of incubation, consistent with the production of biliverdin.

Further studies to characterize and unequivocally identify the products generated by HupZ-catalyzed heme degradation are underway. For that, the final product will be extracted with organic solvents then lyophilized in order to concentrate the products in a minimal volume. Additional purification steps will be applied as needed prior to separation of the products by HPLC. UV-visible spectroscopy and mass spectrometry will be conducted on the samples collected from the HPLC separation. More analyses such as NMR or ENDOR (Electron-Nuclear Double Resonance) spectroscopy may be necessary to determine the chemical structures of the products.

In mammals, biliverdin produced by HO-catalyzed heme degradation is reduced into bilirubin by a biliverdin-reductase (BVR) [31]. The fate of the biliverdin in bacteria is unknown in most cases. A homologue of mammalian biliverdin reductase has been identified only in cyanobacteria [32,33]. In *Pseudomonas aeruginosa*, a bacterial phytochrome BphP, removes biliverdin from the catalytic site of PigA and BphO. However, a subsequent transformation of the removed biliverdin by BphP was not shown and its physiological relevance is still unclear

[22]. Therefore, the fate of biliverdin in non-photosynthetic bacteria remains an intriguing question which constitutes the focus of several ongoing investigations.

It is conceivable that, like in *Pseudomonas aeruginosa*, a dedicated protein in GAS removes the bound biliverdin from HupZ active site and eventually delivers it to a putative enzyme for further conversion. Alternatively, a single protein may carry out the dual function of biliverdin removal and transformation, in which case it would mechanistically resemble the mammalian BVR. Strategies like those suggested in the section above may be adopted to look for proteins involved in biliverdin conversion or excretion from the cell.

In summary, this study explored the role of Shr in heme acquisition by GAS and established the protein as a new type of composite NEAT-containing receptor. It also deciphered the molecular mechanism of heme scavenging and transfer by Shr from metHb, providing the first example of intra-molecular heme exchange between NEAT domains. In addition, this work solved a long-standing enigma by identifying and characterizing for the first time a heme oxygenase in the *Streptococcus* genus (HupZ). Importantly, this study provided new direct evidence that associates flavins with heme metabolism in bacteria, thus setting a new direction in the field of heme acquisition and utilization by pathogens.

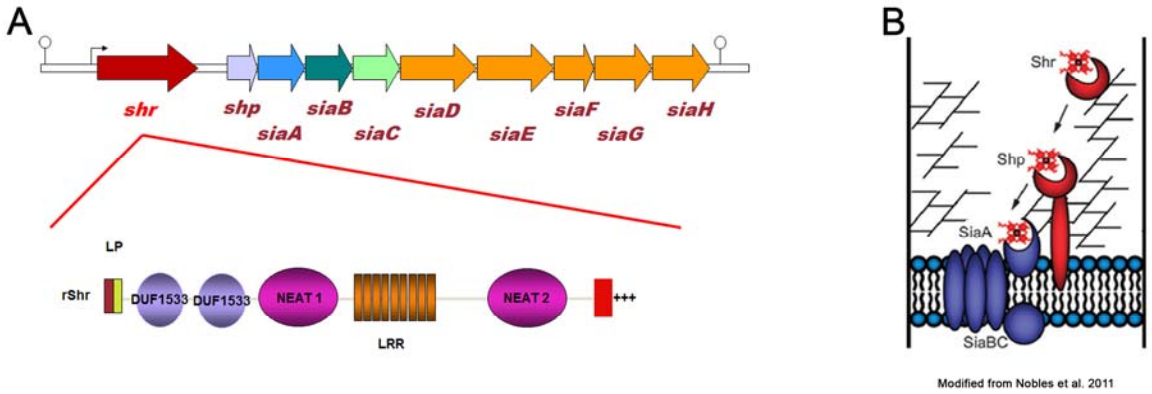

Figure 1: (A) Schematic representation of the *sia* operon and the Shr protein. (B) Heme relay in Group A Streptococcus.

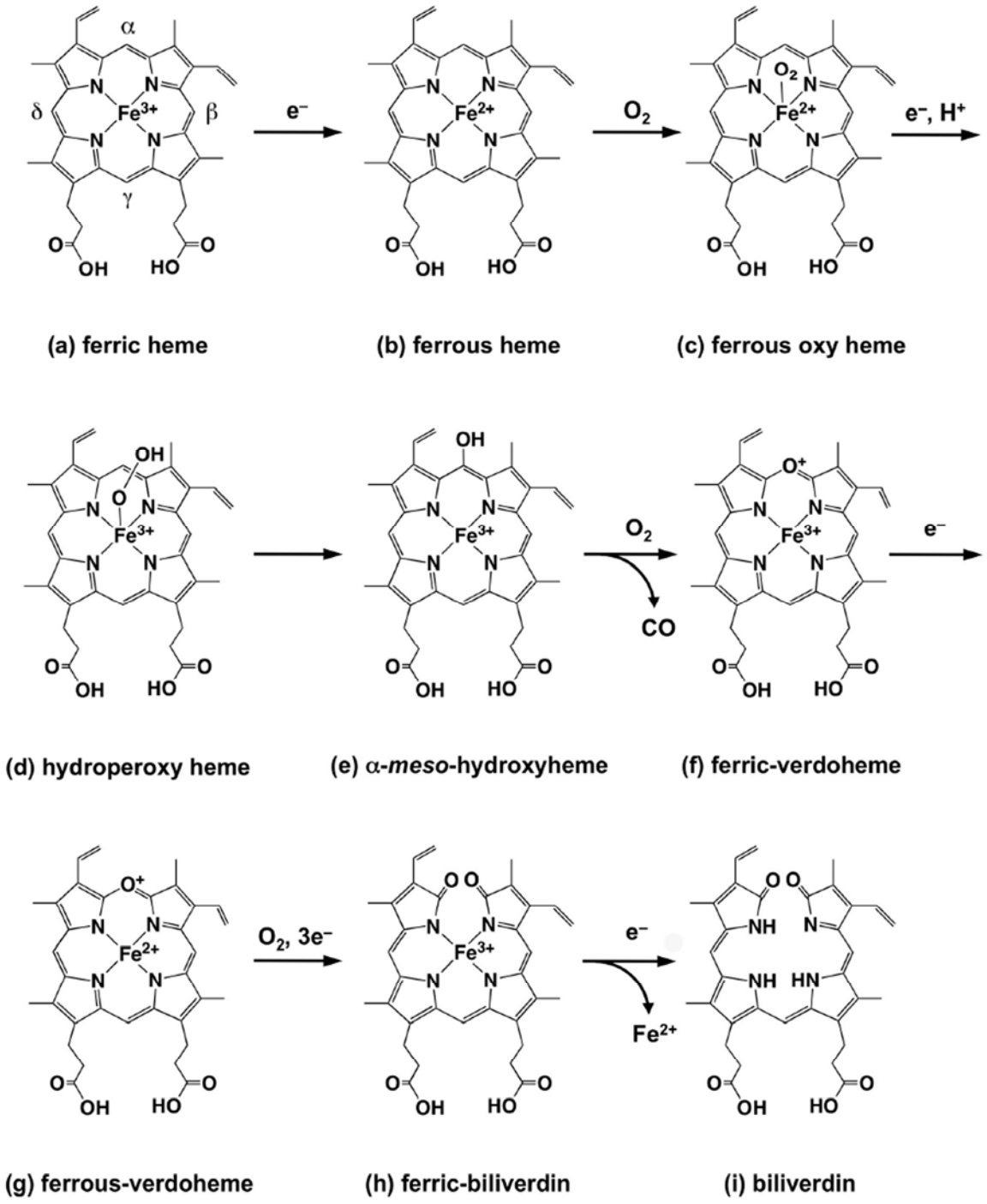

Figure 2: Catalytic mechanism of heme oxygenases [1].

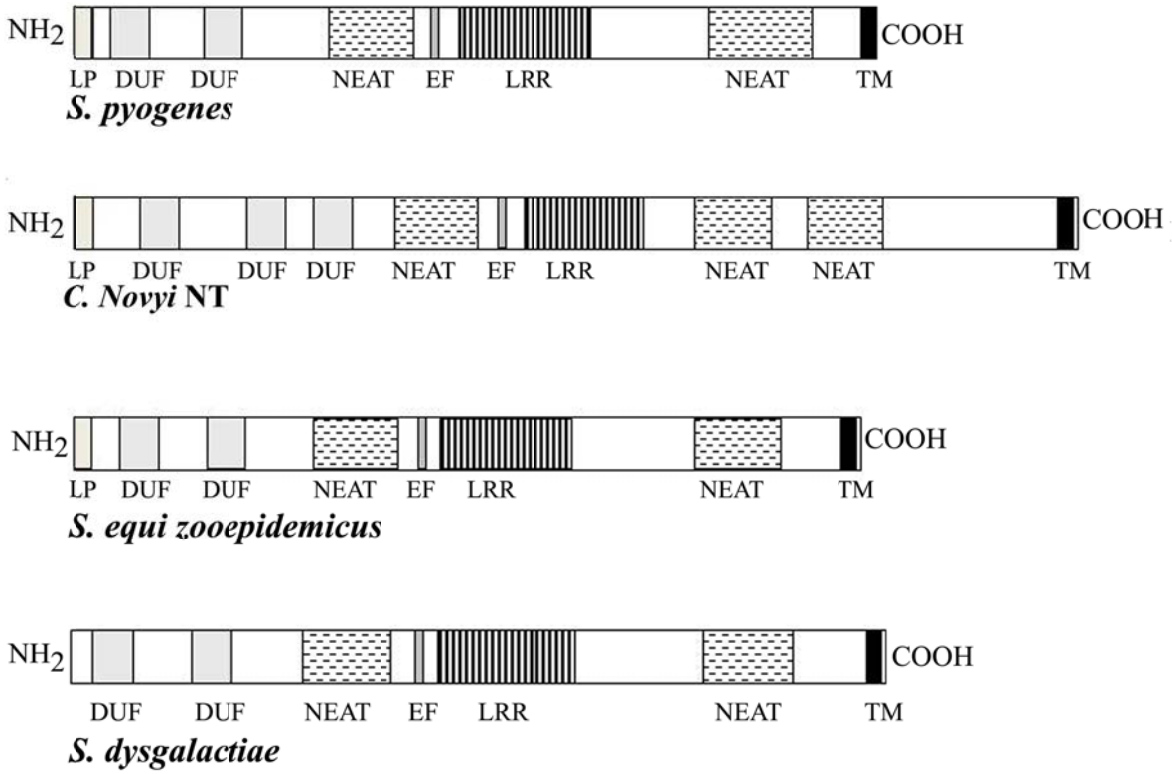

Figure 3: Shr proteins in pyogenic Streptococci and *Clostridium novyi*. LP: Leader Peptide; DUF: Domain of Unknown Function 1533; NEAT: NEAr Transporter domain; EF: EF-hand motif; TM: TransMembrane domain.

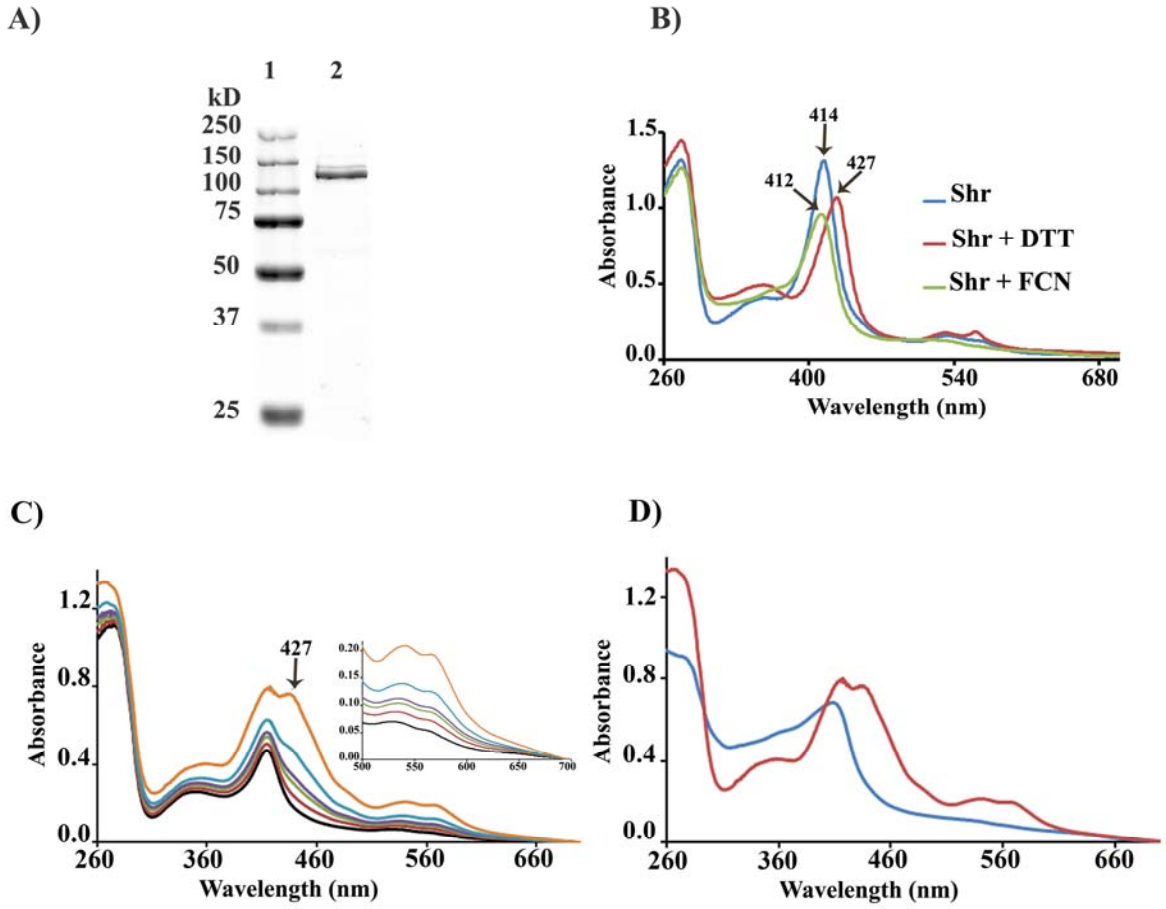

Figure 4: Hemin binding and reduction by rShr. (A) SDS-PAGE showing purified rShr. **(B)** 9 μM Shr (blue line) was treated with 10 mM of DTT (red line) or 30 μM ferricyanide (FCN) (green line). Histag elution buffer containing 10 mM DTT was used as a blank for DTT-treated Shr spectrum and excess ferricyanide was removed from the protein sample by dialysis in phosphate buffer. **(C)** An increase of heme bound to Shr (3 μM) as increasing concentrations (1 μM, red; 3 μM, green; 5 μM, purple; 10 μM, blue; or 20 μM, orange) of hemin were added to

the protein is shown by the sharp peak at 414 nm. Hemin reduction is indicated by the growing absorbance at 427 nm and at ~540 and ~564 nm. The corresponding hemin chloride concentrations in Histag elution buffer served as blanks for the UV-visible scans (see figure S2). The insert magnifies the 500 nm – 700 nm region. **(D)** UV-visible spectra of rShr following the addition of 20 μM hemin (red line) and treatment with ferricyanide (blue line). Hemin reduction shown by the presence of a Soret peak at 427 nm and by the peaks at ~540 and ~564 nm (red spectrum) is reversed by the addition of ferricyanide (blue spectrum).

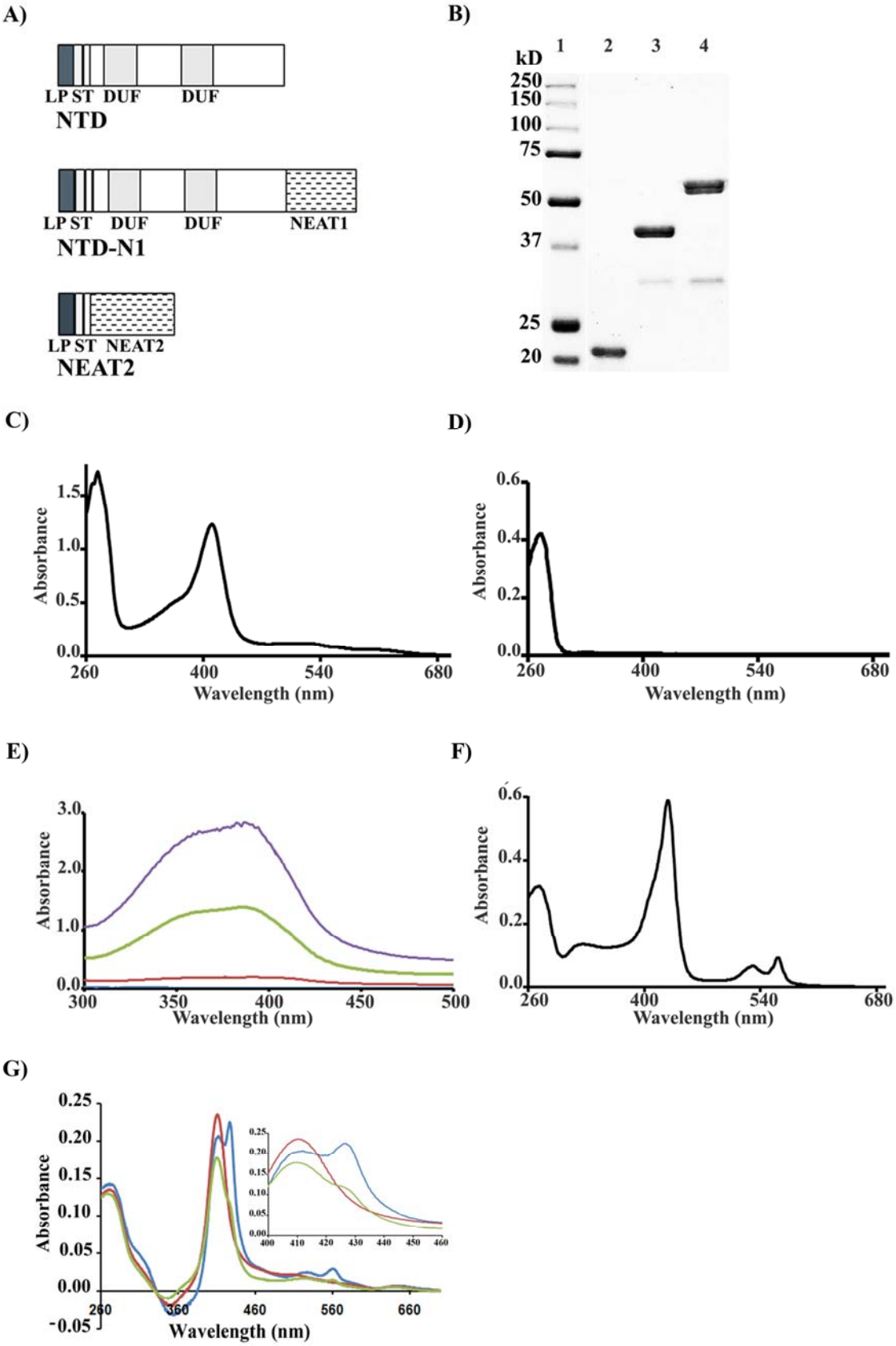
A)
LP ST DUF DUF
NTD
LP ST DUF DUF NEAT1
NTD-N1
LP ST NEAT2
NEAT2
B)
kD
1 2 3 4
250
150
100
75
50
37
25
20
C)
Absorbance
Wavelength (nm)
D)
Absorbance
Wavelength (nm)
E)
Absorbance
Wavelength (nm)
F)
Absorbance
Wavelength (nm)
G)
Absorbance
Wavelength (nm)

Figure 5: **Heme binding by Shr fragments. (A)** Schematic representation of NTD, NTD-N1 and NEAT2. LP: Leader Peptide; ST: *Strep*-Tag; DUF: Domain of Unknown Function 1533; NEAT: NEAr Transporter domain; **(B)** SDS-PAGE showing purified recombinant Shr fragments (1) Molecular weight marker, (2) NEAT2, (3) NTD, (4) NTD-N1. The UV-visible spectra of NEAT1 **(C)**, NTD **(D),** NTD with additions of hemin chloride (1 μM, red; 5 μM, green; or 10 μM, purple) **(E)** and NEAT2 **(F). (G)** UV-visible spectra of NEAT2 following titration with 20 μM hemin (blue). The red and green lines, respectively, represent the spectrum 5 min and 24 h, after addition of 6 μM ferricyanide. The insert magnifies the 400 nm – 460 nm region, showing the shifts in the Soret peaks. The *Strep*-tag wash buffer alone was treated exactly the same way as the protein solution, and used as blank for UV-visible scan.

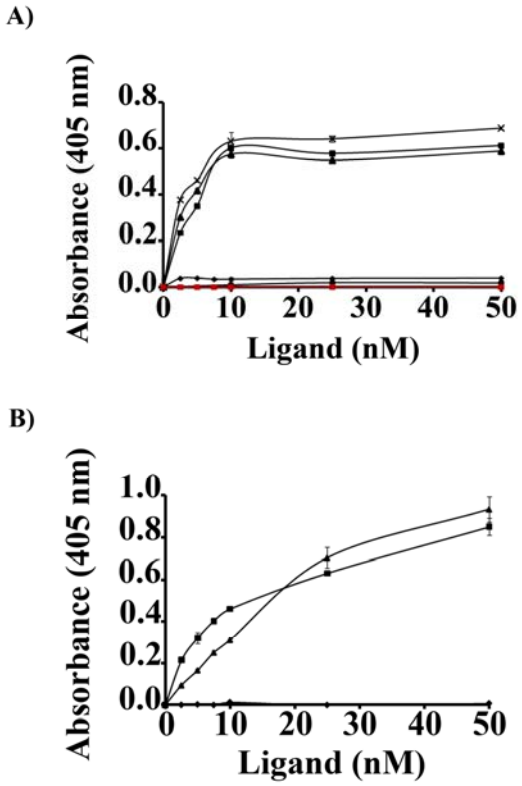

Figure 6: (A) Methemoglobin binding by Shr fragments. ELISA showed methemoglobin binding by rShr (crosses), NTD (black squares), and NTD-N1 (triangles). In contrast, NEAT2 (dots) or BSA (diamonds) did not bind methemoglobin. ELISA testing apohemoglobin binding by NTD (Red squares) showed no binding. The plates were coated with rShr or the Shr fragments and subsequently reacted with increasing concentrations of methemoglobin or apohemoglobin. Protein binding was detected with anti-hemoglobin antibodies as described in Materials and Methods. **(B)** Direct detection of immobilized holohemoglobin (triangles) and apohemoglobin (squares) with anti-hemoglobin antibodies. Uncoated wells (diamonds) were used as a negative control. Each datum point in sections A and B represents the mean ± SD (represented by the error bars) from data from at least two independent experiments done in triplicates.

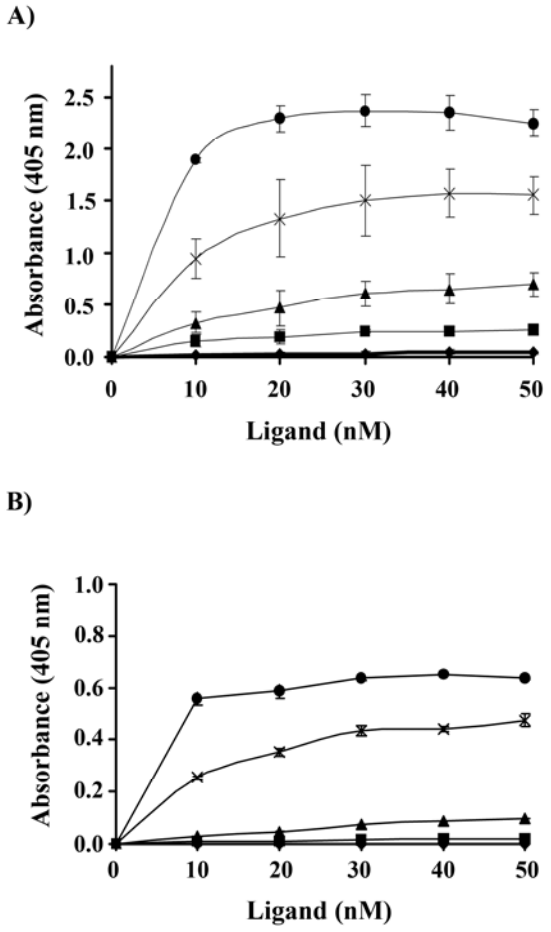

Figure 7: Binding of extracellular matrix proteins by Shr. Elisa assay showing fibronectin **(A)** and laminin **(B)** binding by rShr (crosses) and NEAT2 (dots). NTD-N1 (triangles) slightly bound fibronectin but did not bind laminin. In contrast, NTD (squares) or BSA (diamonds) did not bind fibronectin or laminin. The plates were coated with rShr or Shr fragments and subsequently reacted with increasing concentrations of fibronectin or laminin as described in Materials and Methods. Each datum point in panels A and B stands for the mean ± SD (shown by the error bars) of three independent experiments done in triplicates.

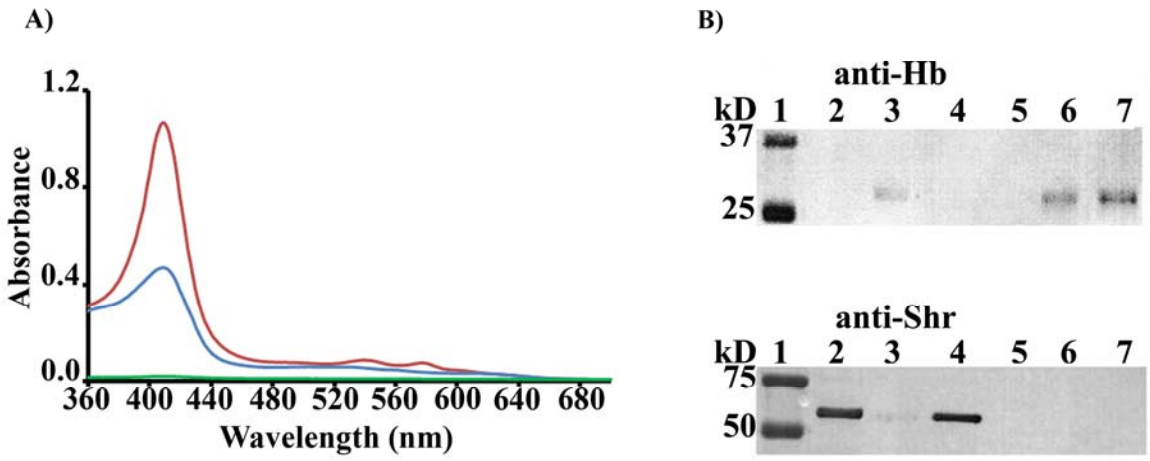

Figure 8: **Heme transfer from methemoglobin to apoNTD-N1**. **(A)** UV-visible spectra of 10 μM apoNTD-N1 after contact with methemoglobin (red) or hemin chloride (blue) and 10 μM apoNTD-N1 (green). **(B)** Western blot analysis of the fraction containing the Hb washes and NTD-N1 elution. Proteins (50 ng/well) were detected with anti-Hb (**upper panel**) or anti-Shr (**lower panel**) antibodies. (1) MW Marker; (2) purified apoNTD-N1; (3) Hb fraction; (4) NTD-N1 after Hb flow; (5) Empty lane; (6) Hb 50 ng ; (7) Hb 100 ng.

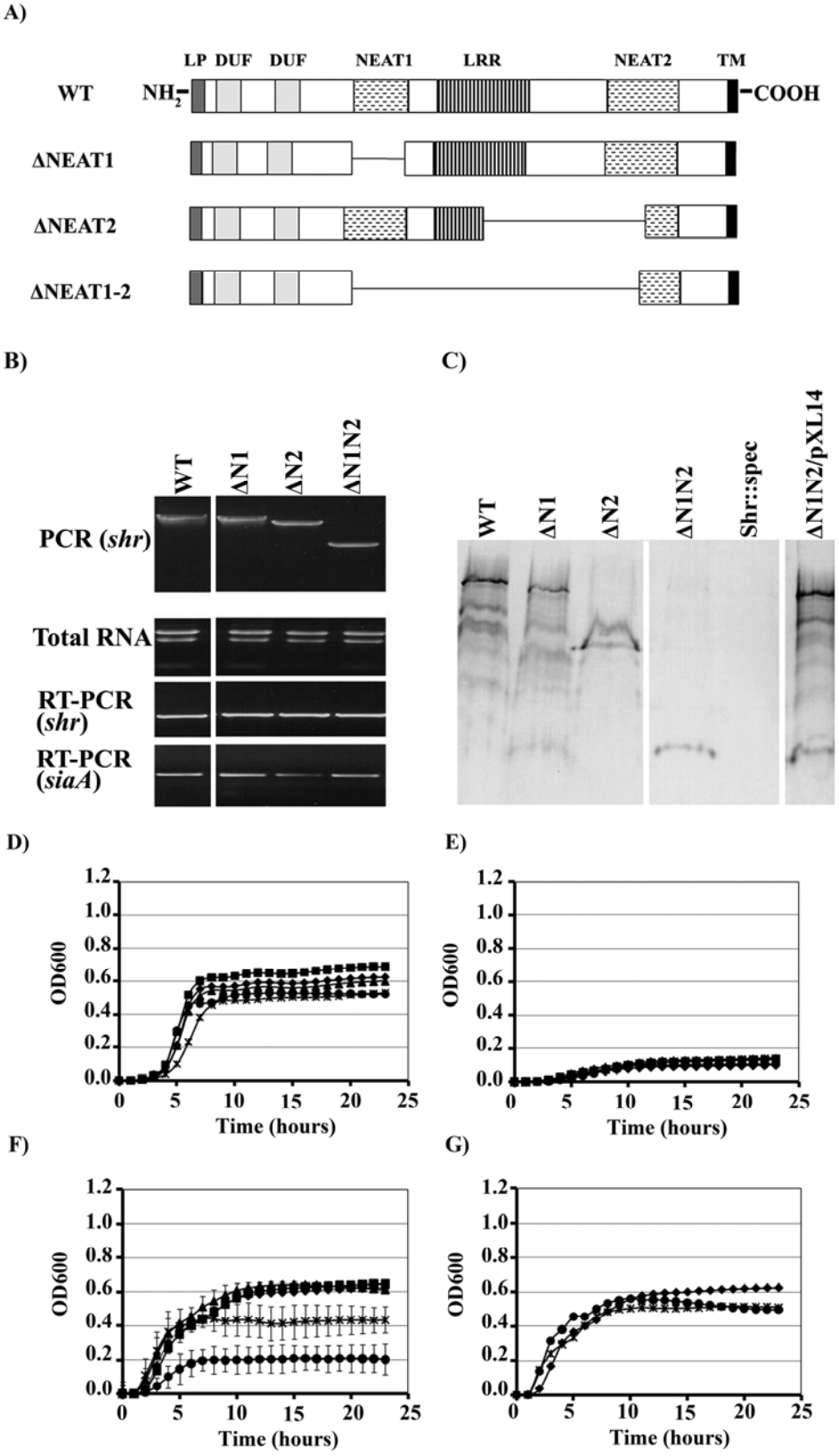
A)
LP DUF DUF NEAT1 LRR NEAT2 TM
WT
NH2
COOH
ΔNEAT1
ΔNEAT2
ΔNEAT1-2
B)
WT
ΔN1
ΔN2
ΔN1N2
PCR (shr)
Total RNA
RT-PCR (shr)
RT-PCR (siaA)
C)
WT
ΔN1
ΔN2
ΔN1N2
Shr::spec
ΔN1N2/pXL14
D)
E)
F)
G)
OD600
Time (hours)

Figure 9: Growth analysis of *shr* deletion mutants. (A) Schematic representation of the in frame deletions created in Shr. WT: wild type; ΔNEAT1: a deletion of the NEAT1 domain; ΔNEAT2: a deletion of the NEAT2 domain; ΔNEAT1-2: a deletion of both NEAT1 and NEAT2 domains. Panels B-E describe the characterization of the constructed GAS mutants **(B)** The first panel shows PCR analysis of the chromosomal *shr* gene. Total RNA from each strain is shown in the second panel. The third and fourth panels respectively show RT-PCR analysis of the expression of *shr* (ZE106/126 primers) and *siaA* (204A-Fwd/Rev primers) genes. **(C)** Western blot showing the expression of the corresponding Shr protein variants. WT: wild type GAS (strain NZ131); ΔN1: NEAT1 mutant (strain ZE4925); ΔN2: NEAT2 mutant (strain ZE4926); ΔN1N2: NEAT1-2 mutant (strain ZE4929); Shr::spec: non polar null *shr* mutant (strain ZE4912); ΔN1N2/pXL14: NEAT1-2 mutant complemented with *shr* (strain ZE4924). A 1 ml volume of each culture at OD_{600} = 1 was processed and 20 μl of the prepared samples were loaded per well. **(D)** Growth in CDM in the presence of 20 μM of iron. **(E)** Growth in CDM with 2 mM dipyridyl and no additional source of iron. **(F)** Growth in CDM with 2 mM dipyridyl and 20 μM of methemoglobin, as the sole source of iron. Diamonds: wild type GAS (strain NZ131); Squares: ΔNEAT1 mutant (strain ZE4925); Triangles: ΔNEAT2 mutant; Crosses: ΔNEAT1-2 mutant; Dots: null *shr* mutant. **(G)** Growth of wild type and Shr complemented strains in CDM with 2 mM dipyridyl and 20 μM of hemoglobin as the sole source of iron. Diamonds: wild type GAS; Crosses: ΔNEAT1-2 mutant complemented with *shr*; Dots: Null *shr* mutant (*shr::aad9*) complemented with *shr* (strain ZE4924). Cells were grown in a 96 well microplate at 37 °C for 24 h and growth was monitored at OD_{600}. Each datum point in all of the panels represents the mean of at least two independent experiments performed in triplicates. For clarity purpose the

SD (represented by the error bars) is shown only in panel F (in which significant growth differences are found between the strains).

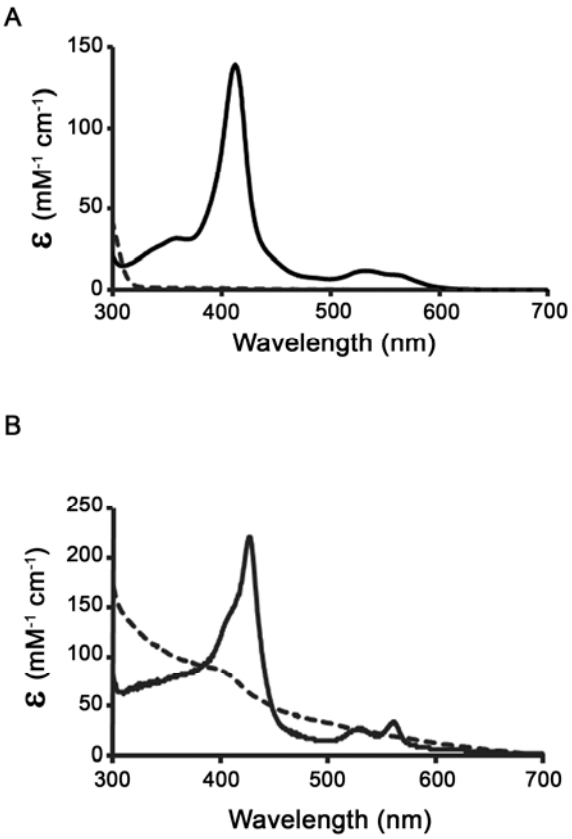

Figure 10: Heme acquisition from MetHb. (A) UV-visible absorbance spectra of apoNEAT1 before (dashed line) and after incubation with metHb (smooth line). The Soret peak at 412 nm indicates ferric heme binding by NEAT1. **(B)** UV-visible absorbance spectra of apoNEAT2 (dashed line) and apoNEAT2 after incubation with metHb (smooth line). A major Soret peak at 426 nm along with peaks at 410 nm, 530 and 560 nm indicate a mixture of bound ferric and

ferrous heme. All the absorbance spectra were corrected by subtracting their corresponding background absorbance at 700 nm.

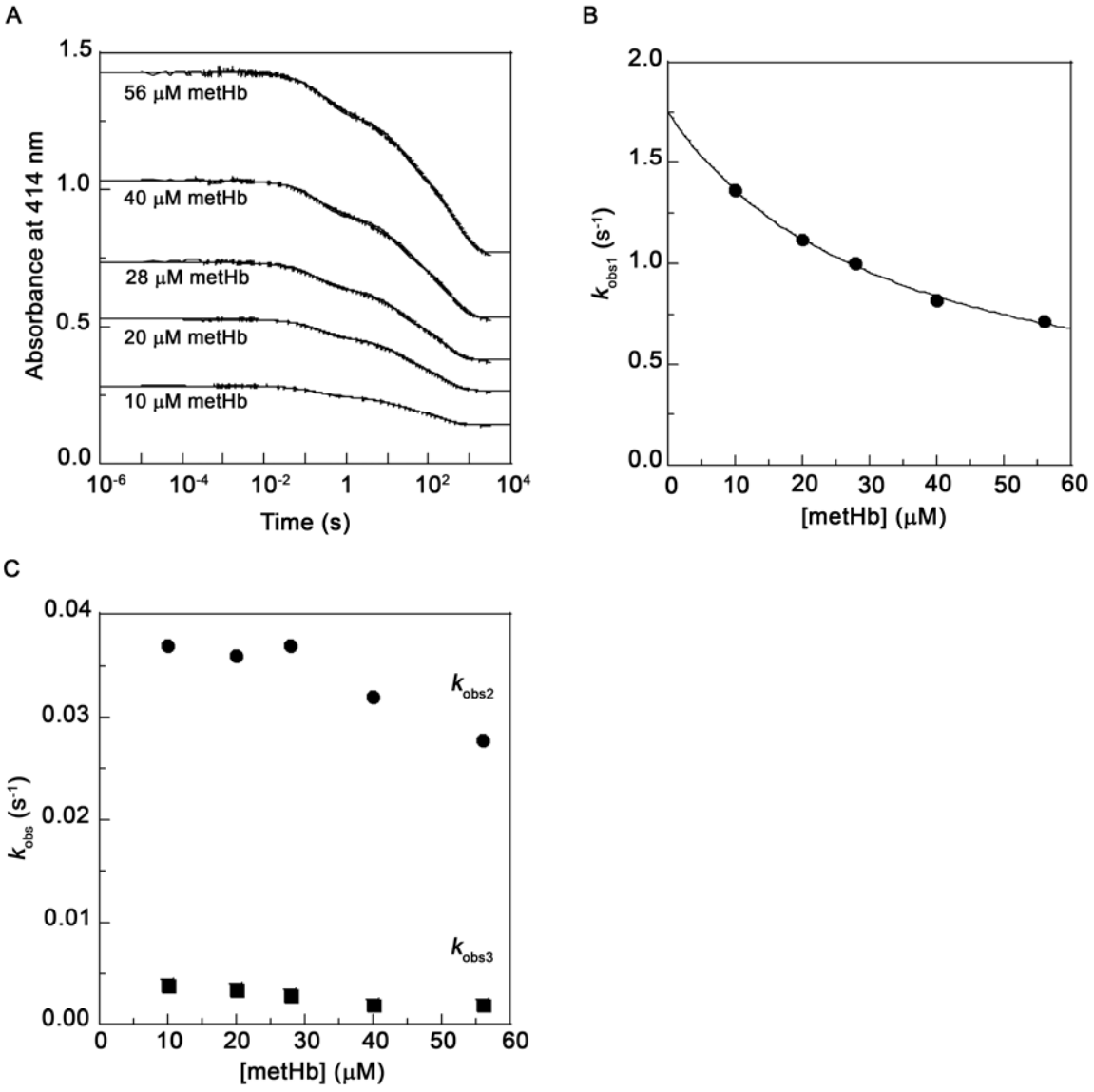

Figure 11: Kinetics of heme transfer from metHb to apoNTD-N1. (A) Traces of the absorbance at 414 nm of the reaction containing 2.5 μM of apoNTD-N1 and various concentrations of metHb recorded as a function of time. Absorbance variations at 414 nm as a function of time best fitted a triple exponential at all concentrations of metHb tested (equation 2).

(B) Observed rate constants for the first phase of heme transfer from metHb to apoNTD-N1 plotted as a function of metHb concentration and fitted using the equation: $k_{obs1} = k_1 + k_2 * (K_{eq} / (K_{eq} + x))$ ($R^2 = 0.99$). **(C)** The observed rate constants for the second (k_{obs2}) and third (k_{obs3}) phases as functions of metHb concentration. All concentrations of metHb were based on heme bound absorption.

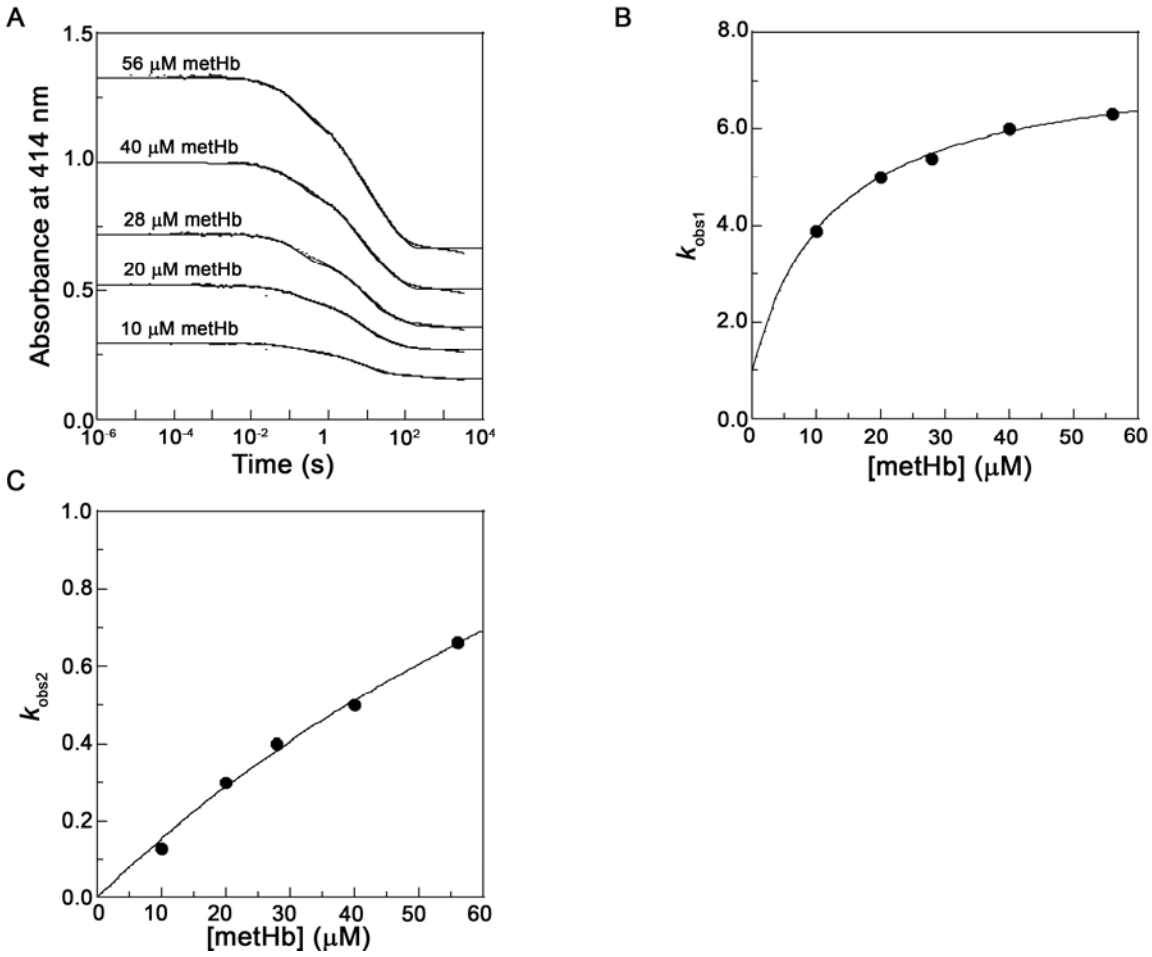

Figure 12: Kinetics of heme transfer from metHb to the full-length Shr. (A) Traces of the absorbance at 414 nm of the reaction containing 2.5 μM of apoShr and various concentrations of metHb recorded as a function of time. Absorbance variations at 414 nm as a function of time best

fitted a triple exponential at all concentrations of metHb tested (equation 2). **(B)** Observed rate constants for the first phase of heme transfer from metHb to apoShr plotted as a function of metHb concentration. k_{obs1} was fitted using the equation: $k_{obs1} = 1+[6.5x / (12 + x)]$ ($R^2 = 0.99$). **(C)** The observed rate constants for the second (k_{obs2}) phase were fitted using the equations: $k_{obs2} = 2.3x / (138 + x)$ ($R^2 = 0.99$).

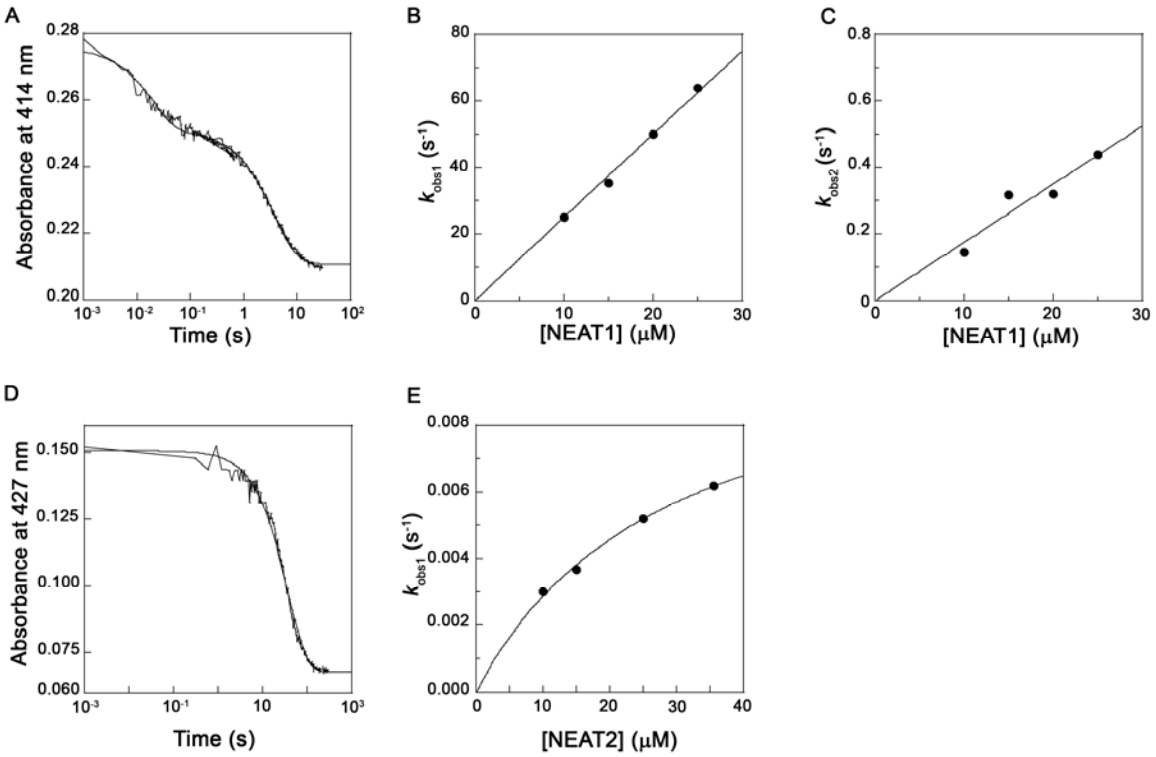

Figure 13: Kinetics of heme transfer from Shr NEAT domains to apoShp. Various concentrations of holoNEAT1 or holoNEAT2 were mixed with apoShp (2.5 μM). **(A)** Representative trace of the time course of heme transfer from holoNEAT1 to apoShp. **(B)** The observed rate constants for the fast phase of heme transfer from holoNEAT1 to apoShp plotted as a function of [holoNEAT1] was fitted using the equation: $y = 2.5x$ ($R^2 = 0.99$). **(C)** The

observed rate constants for the slow phase of heme transfer from holoNEAT1 to apoShp plotted as a function of [holoNEAT1] was fitted using the equation: y = 0.017x. (R^2 = 0.89). **(D)** Representative trace of the time course of heme transfer from holoNEAT2 to apoShp. **(E)** The plot of the observed rate constants of the heme transfer from holoNEAT2 to apoShp as a function of [holoNEAT2] fitted using the equation: y = 0.01x / (x+25). (R^2 = 0.99)

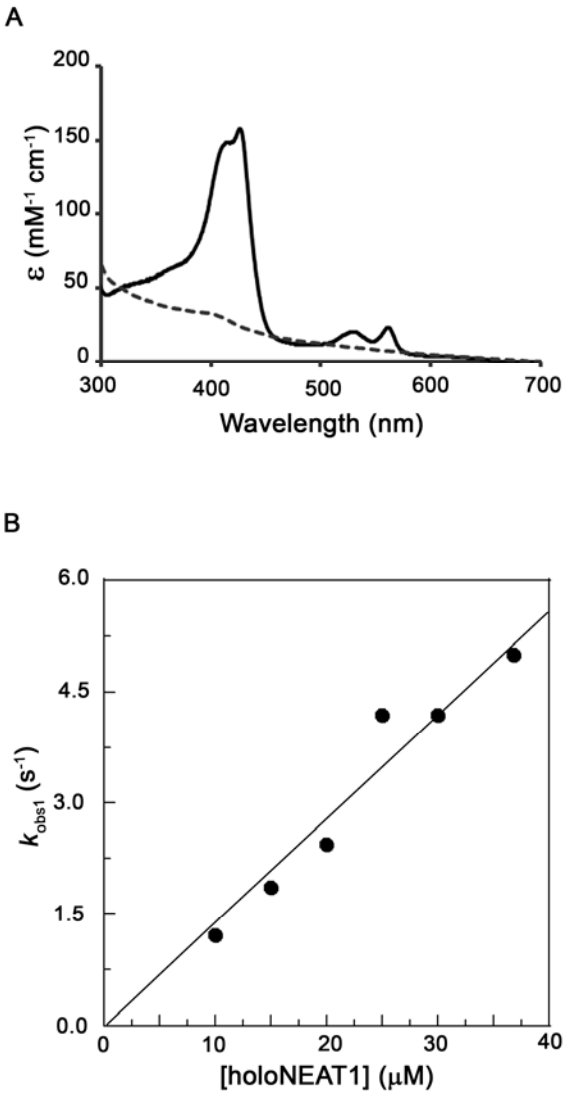

Figure 14: Heme transfer from holoNEAT1 to apoNEAT2. (A) UV-visible absorbance spectra of apoNEAT2 before (dashed line) and after incubation with holoNEAT1 (smooth line). ApoNEAT2 upon incubation with holoNEAT1 showed Soret peaks at 411 and 426 nm as well as peaks at 530 and 560 nm, indicating a mixture of bound ferric and ferrous heme. **(B)** Kinetics of heme transfer from holoNEAT1 to apoNEAT2. The observed rate constants plotted as a function of [holoNEAT1] increased in [holoNEAT1]-dependent manner and was fitted using the equation: $y = 0.14x$ ($R^2 = 0.94$).

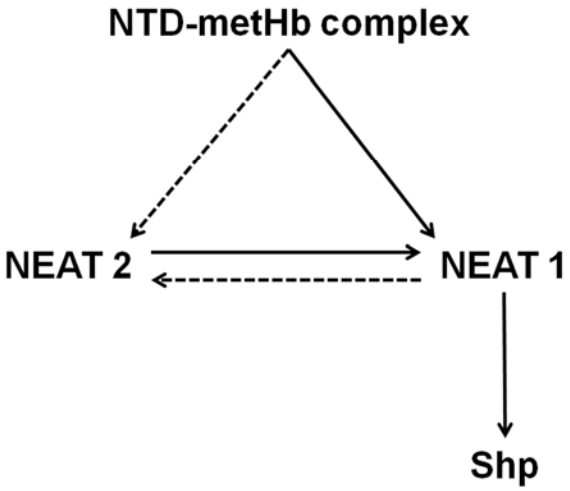

Figure 15: Proposed model of heme acquisition by the *S. pyogenes* Sia system. Shr binds metHb through NTD and forms an intermediate protein complex, which may facilitate direct heme transfer from metHb to NEAT1 and NEAT2 and eventually the release of heme from metHb in solution. Heme scavenged by NEAT1 is rapidly transferred to Shp for delivery into the cell by the SiaABC transporter. Heme acquired by NEAT2 is stored and transferred back to

NEAT1 when needed, possibly when heme availability is limiting. The full and dashed arrows indicate the heme flow under low and high heme availability, respectively.

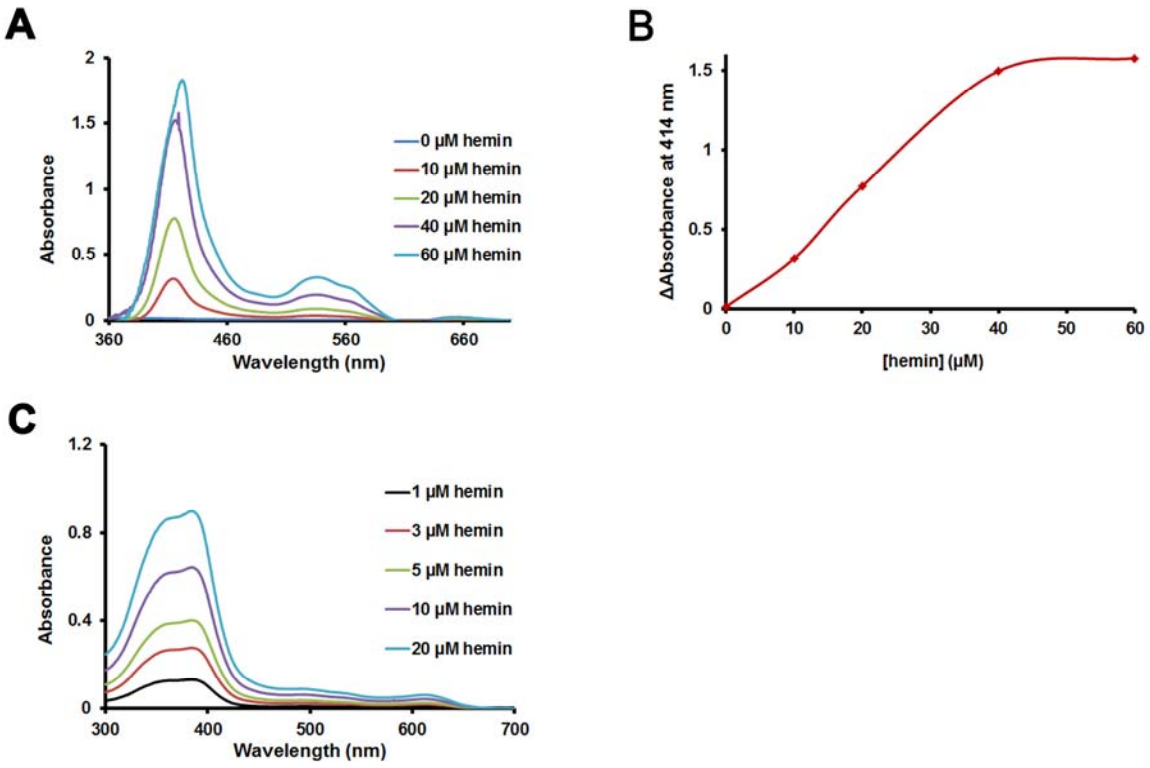

Figure 16: Heme binding by HupZ. Various concentrations of hemin chloride were added to 40 µM HupZ in 1 ml of 20 mM sodium phosphate buffer. The corresponding hemin concentrations in 1 ml of the buffer without protein were used as blanks **(A)**. The differential absorbance at 414 nm plotted as a function of [hemin] shows a binding stoichiometry of 1:1 **(B)**. The spectra of free heme in the buffer **(C)**, showing major differences with those of bound heme seen in **(A)**.

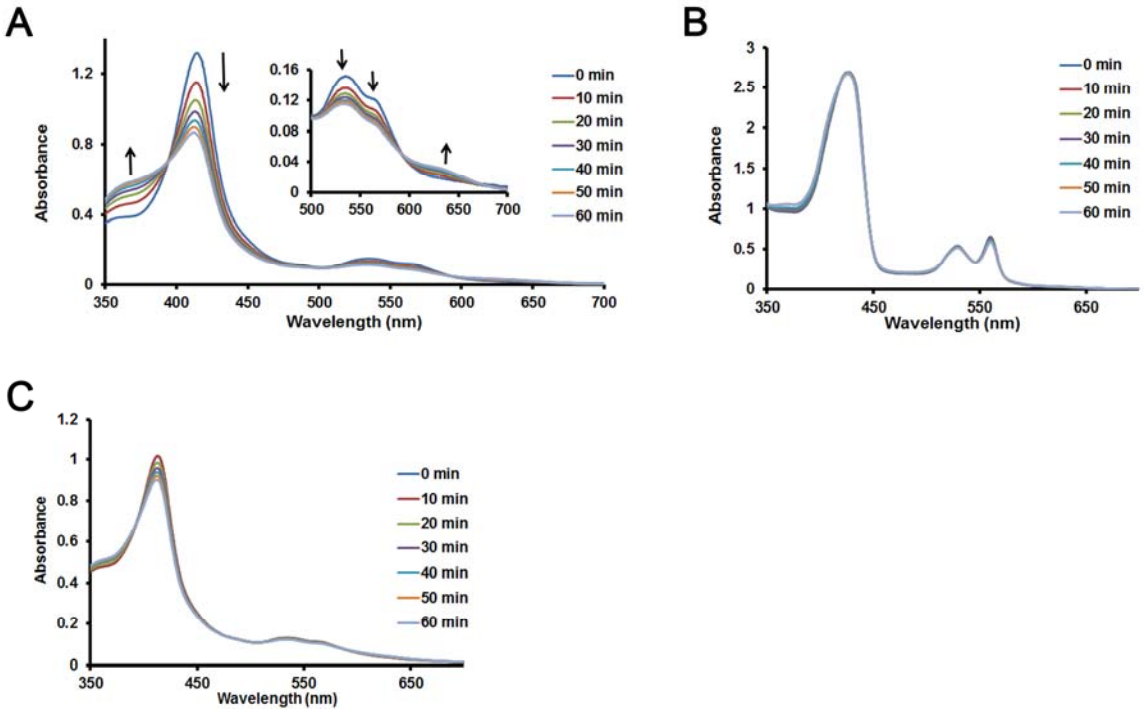

Figure 17: Heme degradation by HupZ without external electron donors. (A) HupZ-catalyzed heme degradation in absence of exogenous reducing equivalent. The inset magnifies the region between 500 and 700 nm showing the decrease of the bands at 530 and 560 nm and the concomitant increase of a band at 630 nm. The arrows indicate the direction of the changes. **(B)** The spectral features of heme bound to Shp did not change over time, indicating absence of heme degradation. **(C)** Inhibition of HupZ catalytic activity by potassium ferricyanide.

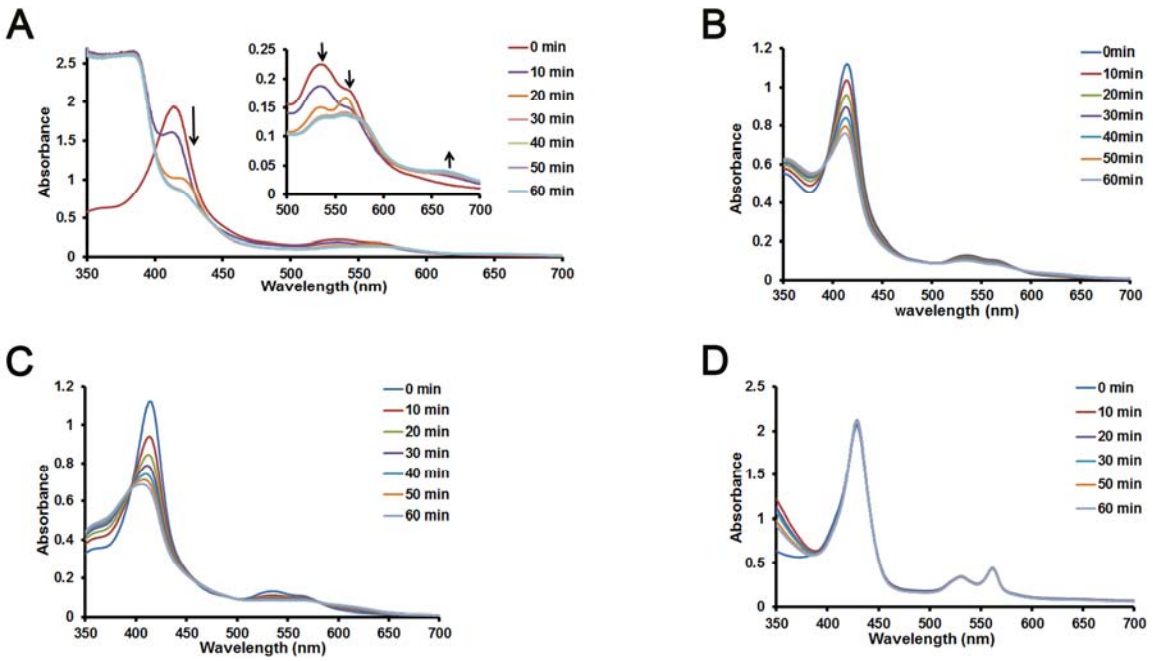

Figure 18: heme degradation by HupZ using CPR-NADPH as reducing equivalent. (A) Heme degradation with CPR-NADPH as source of electrons. The inset magnifies the region between 500 and 700 nm showing the decrease of the bands at 530 and 560 nm and the concomitant increase of a band at 670 nm. The arrows indicate the direction of the changes. The reaction in absence of CPR **(B)** or NADPH **(C)** did not enhance heme degradation by HupZ. **(D)** Control reaction carried out with heme bound NEAT2 and the CPR-NADPH system.

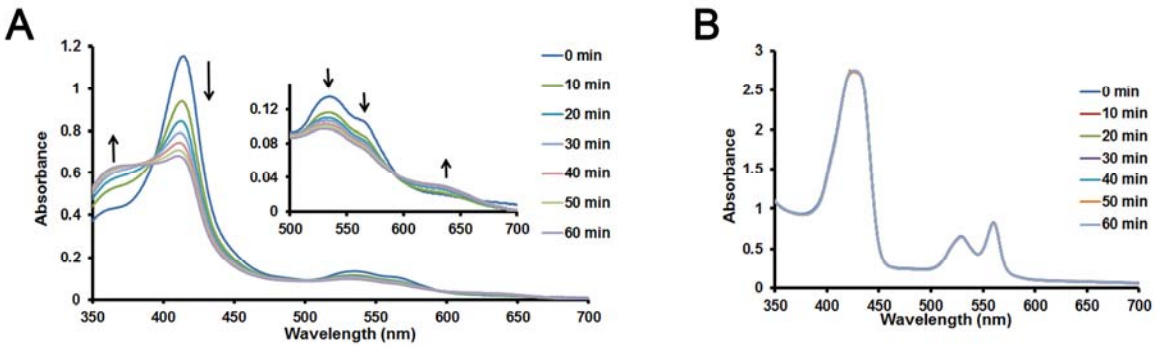

Figure 19: heme degradation by HupZ with ascorbic acid as a source of electrons. (A) Heme degradation by HupZ using ascorbic as a reducing partner. The inset magnifies the region between 500 and 700 nm showing the decrease of the bands at 530 and 560 nm and the concomitant increase of a band at 630 nm. The arrows indicate the direction of the changes. **(B)** Control reaction carried out with heme bound Shp and ascorbic acid.

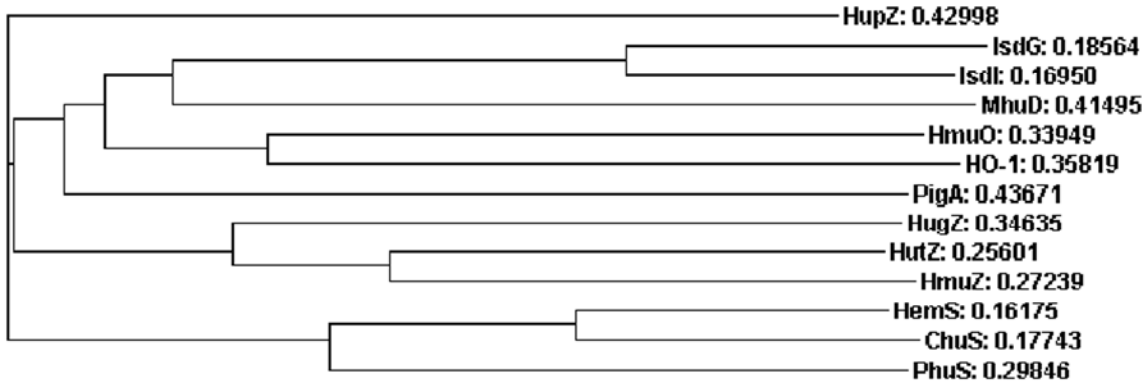

Figure 20: Phylogenetic tree of bacterial heme oxygenases generated from ClustalW2 (EMBL-EBI). The number displayed for each HO represents its evolutionary distance from the root.

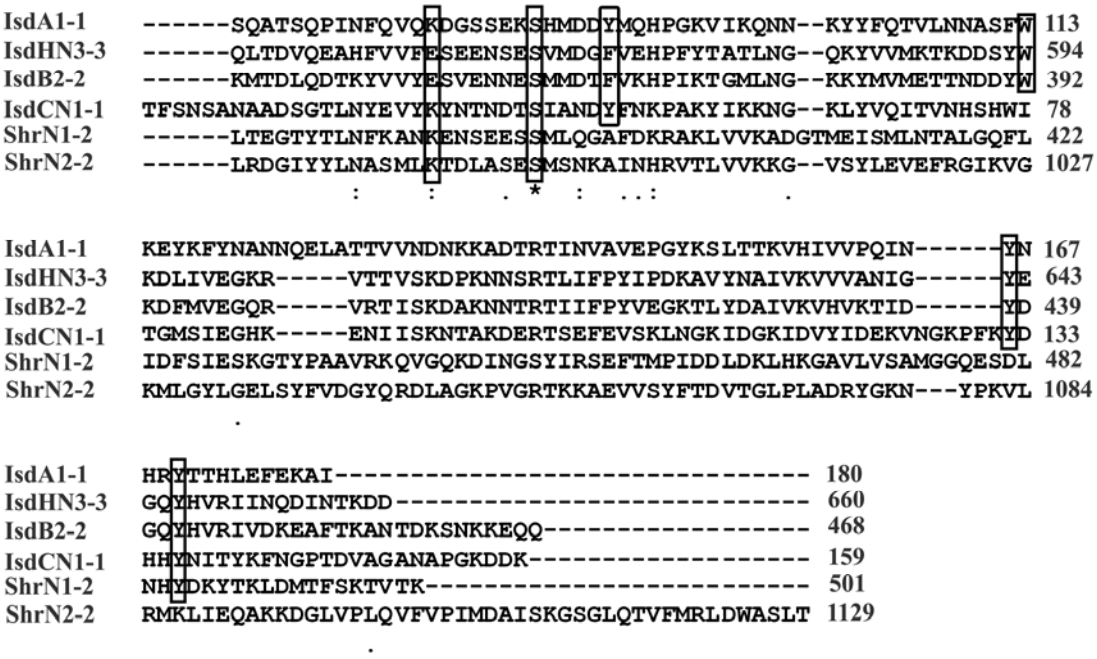

Figure S1: NEAT alignment. Sequence alignment of the heme-binding NEAT domains of IsdA, IsdH, IsdB, IsdC, and the two NEAT domains of GAS Shr. Alignment was generated using the ClustalW program. Important residues found in the heme-binding pocket are indicated by the black frames [2]. The residues corresponding to K75 and S82 of IsdA heme binding pocket are conserved in Shr NEAT1 and NEAT2. The conserved iron-coordinating Y166 in Isd, however, is absent from Shr NEAT domains and the Isd-conserved Y170 is present in Shr NEAT1 only. The aromatic residues at position 87 and 113 are present in Isd but not in Shr.

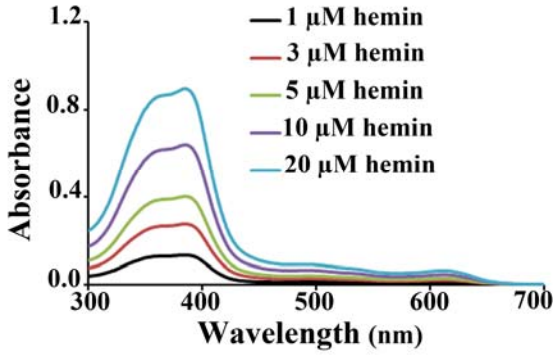

Figure S2: UV-visible spectra of hemin chloride. Increasing concentrations of hemin chloride were added to Histag elution buffer and the spectra were determined as described in Material and methods.

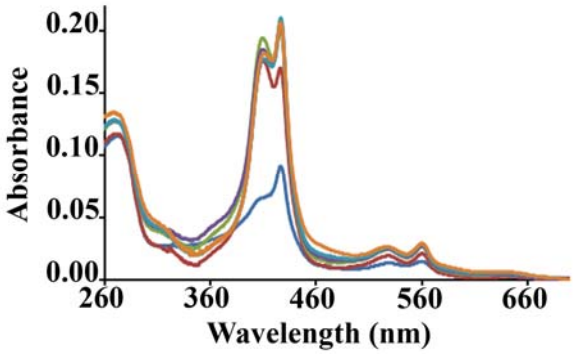

Figure S3: Heme reconstitution of NEAT2 protein fragment. Increasing concentrations (1 µM, red; 3 µM, green; 5 µM, purple; 10 µM, light blue and 20 µM, orange) of hemin chloride were added to NEAT2 protein in Strep-tag elution buffer. The corresponding hemin chloride concentrations were added to Strep-tag elution buffer and used as blanks for the UV-visible scans.

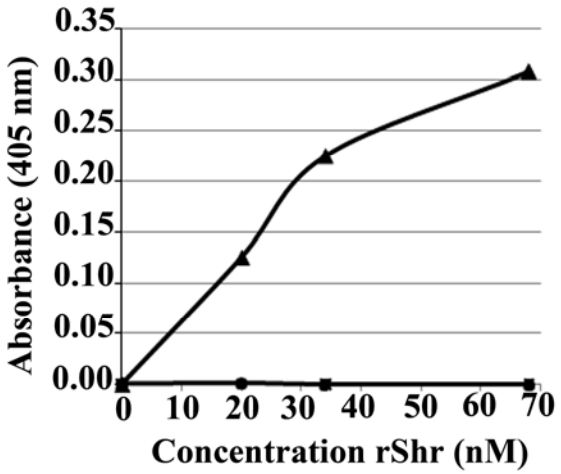

Figure S4: Binding of rShr to holo and apo hemoglobin. Binding of rShr to microtiter plate wells coated with 200 nM Goat IgG (circles), 200 nM apohemoglobin (squares), and 200 nM holohemoglobin (triangles). Increasing concentrations of rShr were incubated in wells overnight at 4 ºC. Bound protein was detected with polyclonal anti-Shr antibodies and anti-rabbit AP conjugated antibodies. The experiments were repeated twice and the values are derived from the means of triplicate wells.

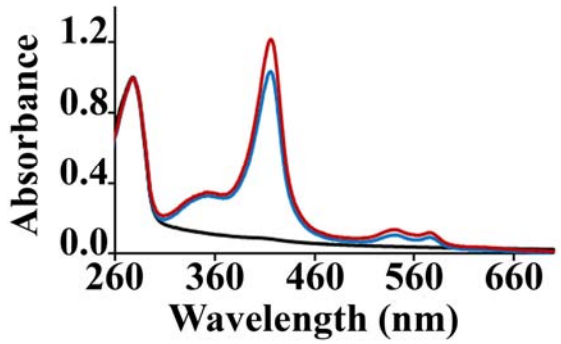

Figure S5: Heme transfer from methemoglobin to apoNTD-N1. UV-visible spectra of apoNTD-N1 (black), apoNTD-N1 after 5 min incubation with methemoglobin (blue) and apoNTD-N1 after 75 min incubation with methemoglobin (red). ApoNTD-N1 (100 nmoles in 2 ml *Strep*-tag wash buffer) was incubated with methemoglobin (50 nmoles in phosphate buffer solution). NTD-N1 was separated from methemoglobin through a *Strep*-Tactin column following an extensive wash with *Strep*-tag wash buffer.

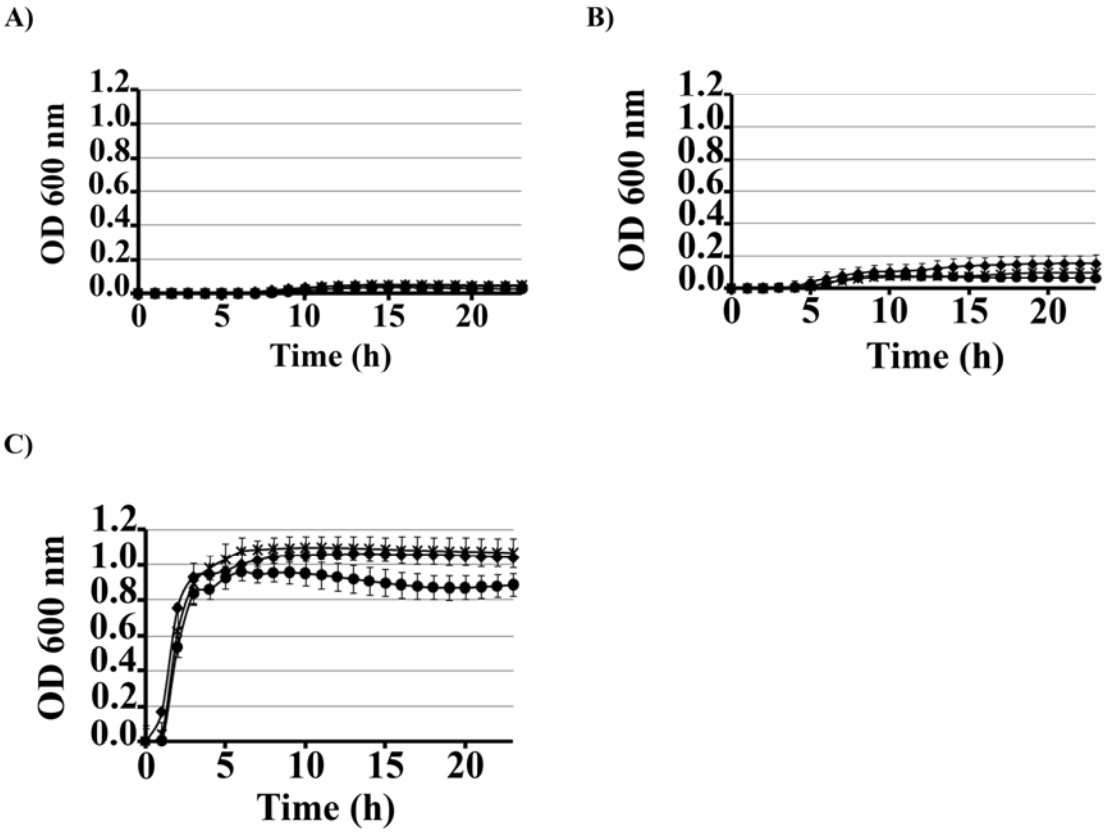

Figure S6: Growth phenotype of wild type GAS and Shr mutants. (A) In presence of 2 mM dipyridyl and 5 μM of human hemoglobin as sole source of iron. **(B)** In presence of 2 mM dipyridyl and 10 μM of human hemoglobin as sole source of iron. **(C)** In presence of 2 mM dipyridyl and 60 μM of human hemoglobin as sole source of iron. Cells were grown in a 96 well microplate at 37 °C for 24 h and the growth was monitored at OD_{600}. Diamonds: wild type GAS; Crosses: ΔNEAT1-2 mutant (strain ZE4929); Dots: non polar null *shr* mutant (shr::aad9, strain ZE4912). The vertical bars indicate the standard deviation between triplicates of two repeated experiments.

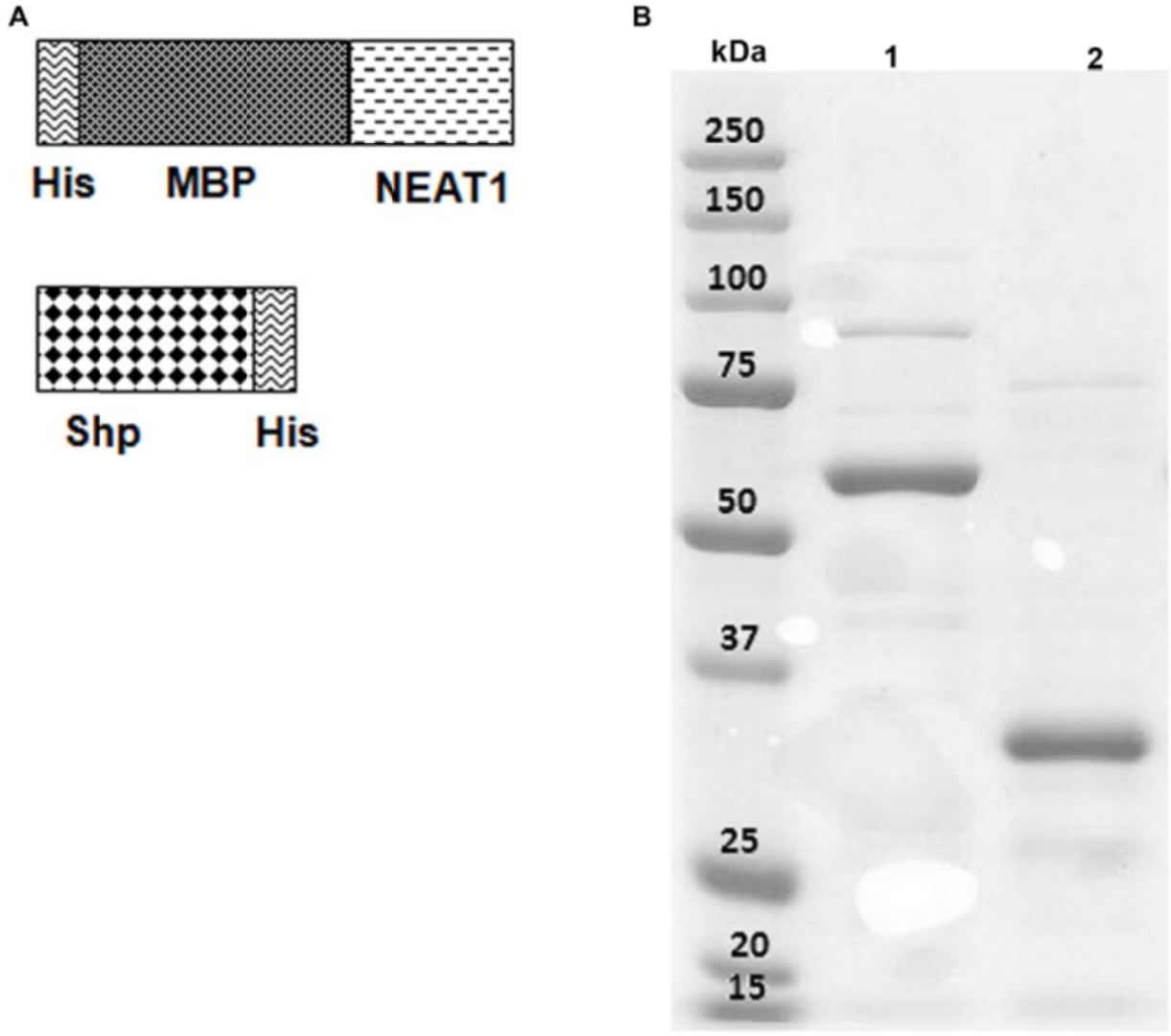

Figure S7: Recombinant His-MBP-NEAT1 and Shp-His proteins. (A) Schematic representation of N-terminal His tagged MBP-NEAT1 fusion and C-terminal His tagged Shp. His: Hexa-histidine; MBP: Maltose Binding Protein. **(B)** SDS-PAGE showing affinity purified His-MBP-NEAT1 (lane 1) and Shp-His (lane 2) proteins. The recombinant proteins migrated according to the expected sizes of 67 kDa (His-MBP-NEAT1) and 29 kDa (Shp-His).

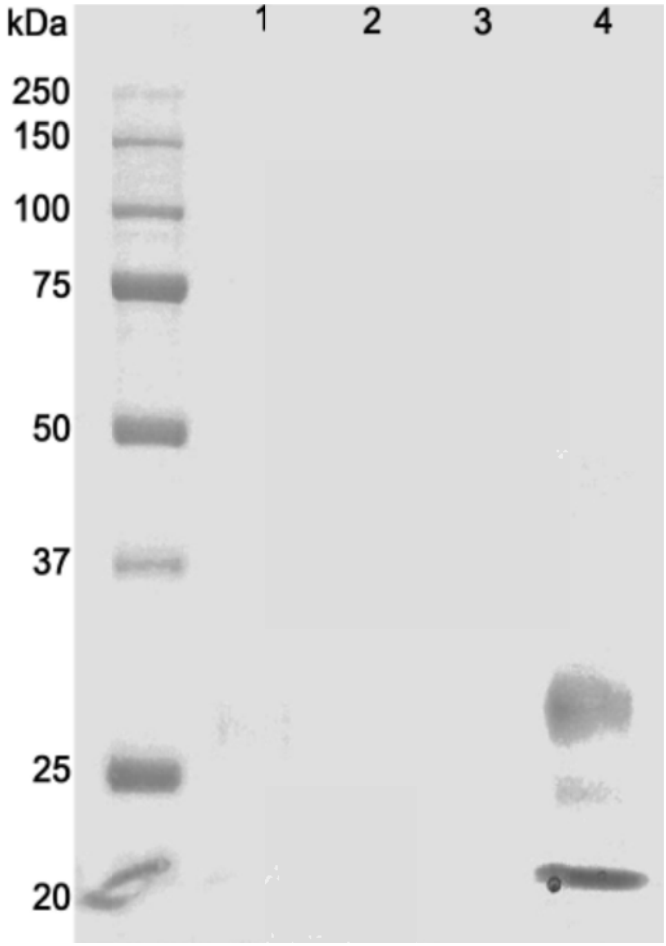

Figure S8: Western blot analysis with anti-Hb antibodies of Shr elution fractions. 20 µl of 1 mg/ml MBP-NEAT1 and NEAT2 eluted from a nickel column after incubation with metHb were analyzed. **(1)** MBP-NEAT1 elution fraction. **(2)** NEAT2 elution fraction. **(3)** Empty lane. **(4)** Control metHb.

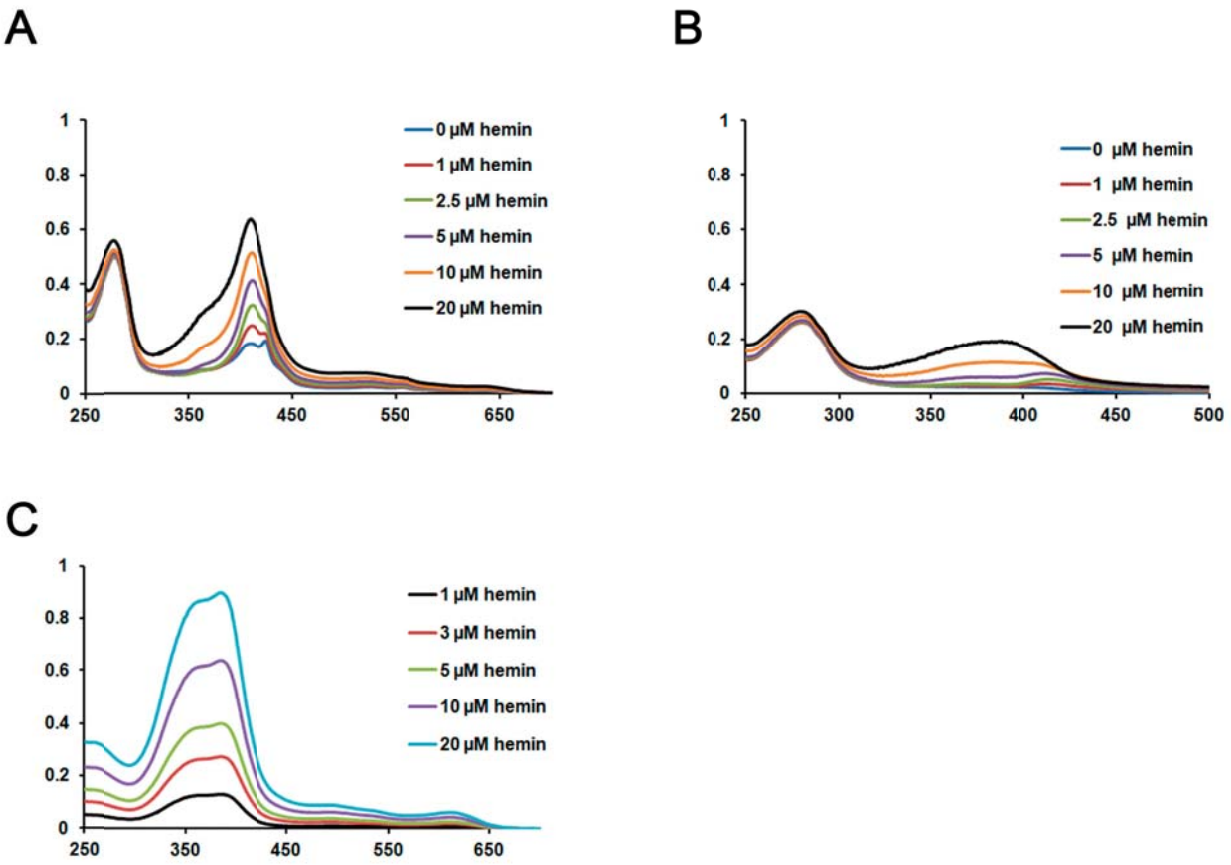

Figure S9: Heme reconstitution spectra of MBP-NEAT1 and MBP. Increasing concentrations of hemin chloride were added to 5 µM MBP-NEAT1 in PBS **(A)** or 5 µM MBP in PBS **(B)**. The UV-visible absorbance of free hemin in PBS **(C)** at each concentration was subtracted from the absorbance of MBP-NEAT1 and MBP. The increase in the Soret peak of MBP-NEAT1 showed that the protein readily acquired heme from solution. In contrast, MBP had a heme reconstitution profile similar to that of free hemin in PBS.

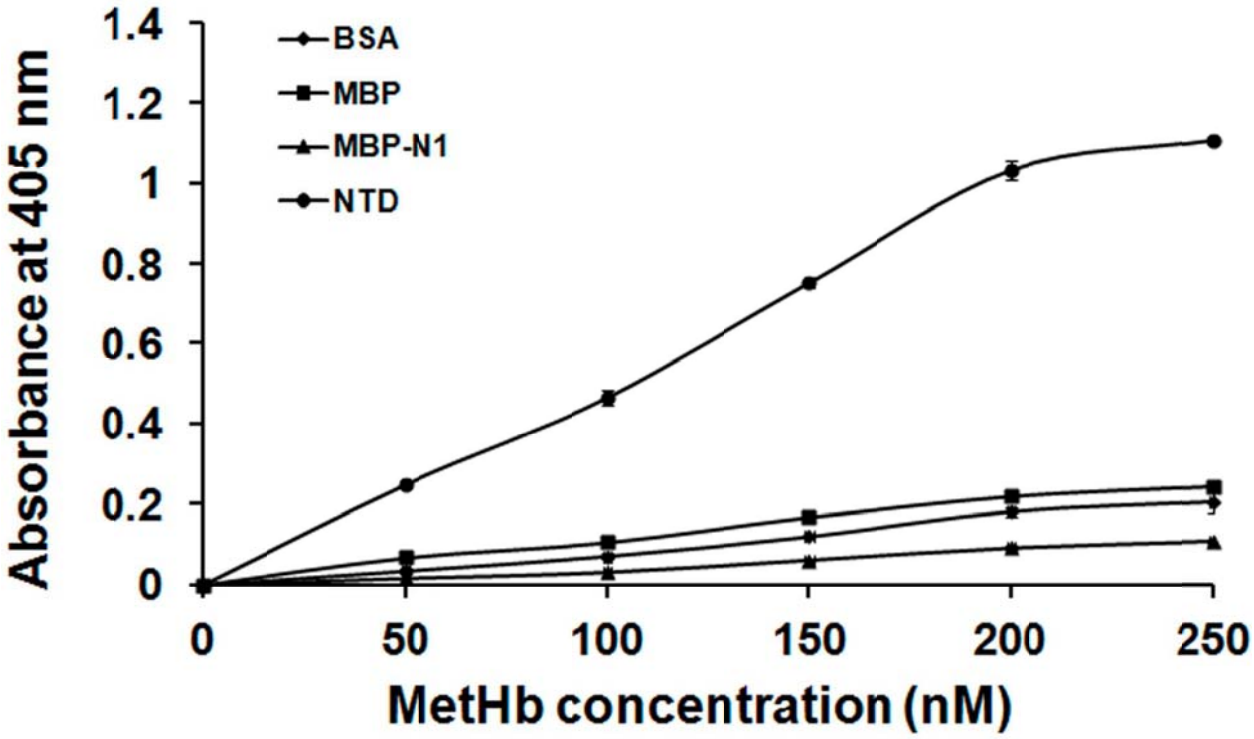

Figure S10: MetHb binding by Shr fragments. ELISA experiments showed a stable metHb binding by NTD (full circles) but not by MBP (squares), MBP-NEAT1 (triangles) or the negative control BSA (diamonds). The 96 wells plates were coated with NTD, MBP, MBP-NEAT1 or BSA, and subsequently reacted with increasing concentrations of metHb. Stable complex formation was detected with anti-hemoglobin antibodies and alkaline phosphatase conjugated secondary antibodies.

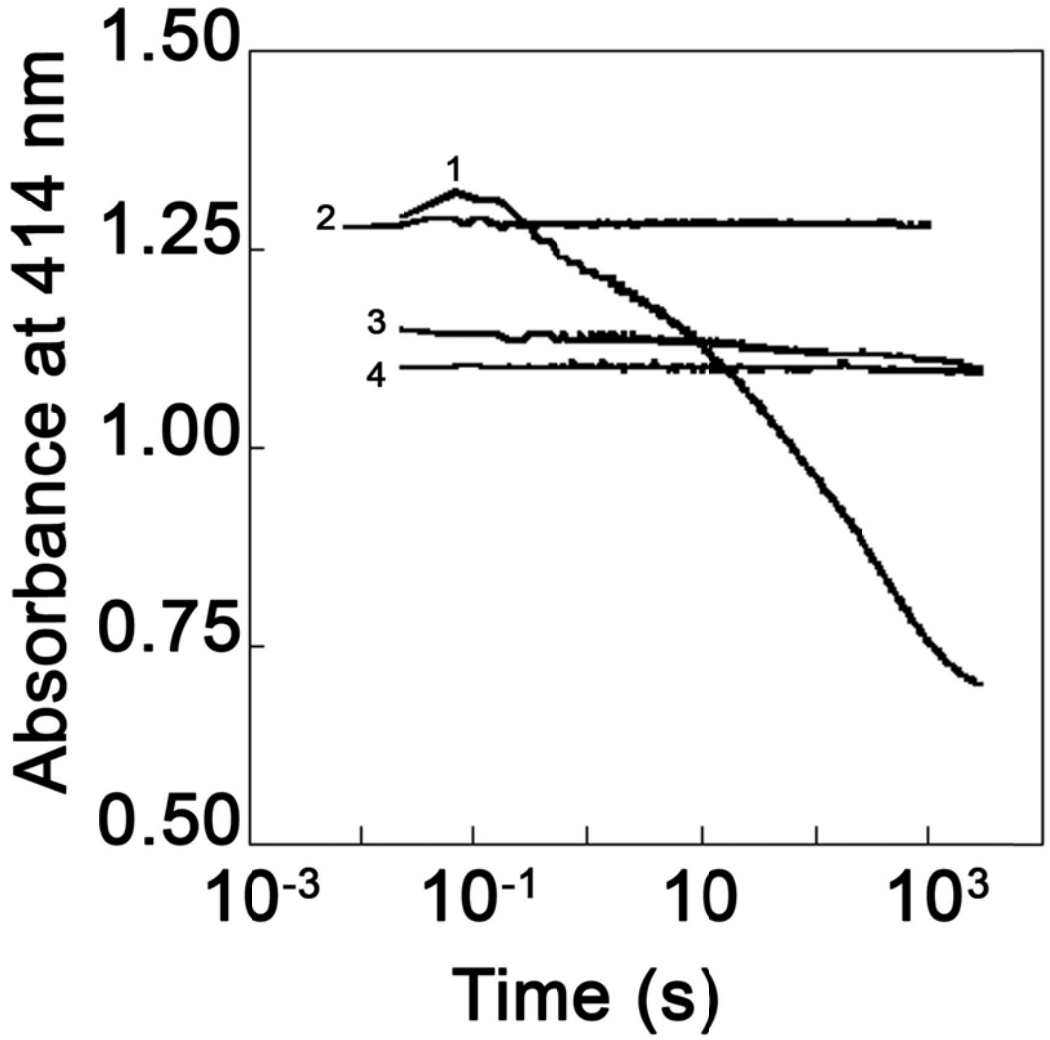

Figure S11: Heme transfer from metHb to Shr fragments. Time course absorbance at 414 nm of the reactions containing, 56 μM of metHb and 2.5 μM of apoNTD-N1 (line 1), 2.5 μM of MBP (line 2), 2.5 μM of apoNEAT2 (line 3) or 2.5 μM of apoNEAT1 (line 4) in PBS pH 7.4 at 25 °C.

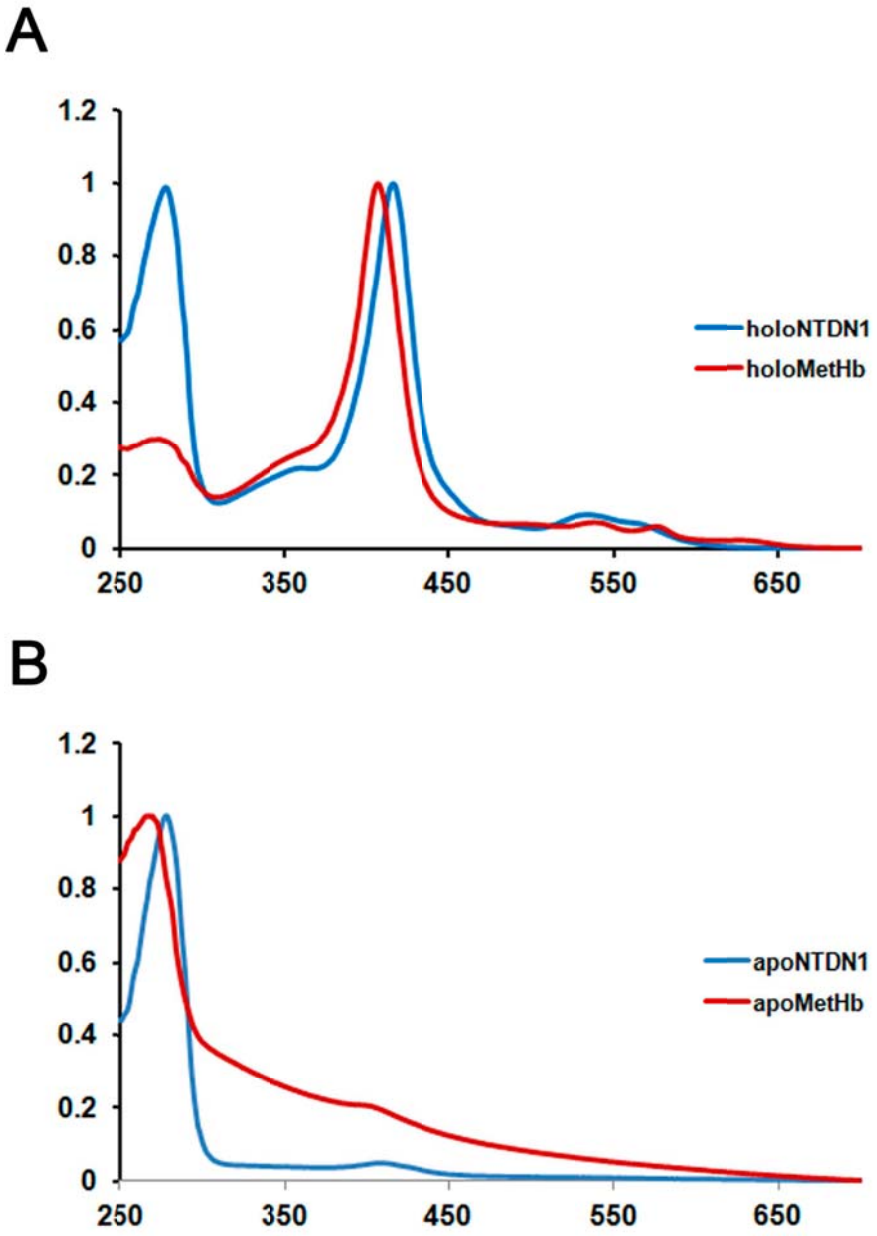

Figure S12: Comparative spectra of NTD-N1 and metHb. (A) UV-visible spectra of holoNTD-N1 and holometHb. **(B)** UV-visible spectra of apoNTD-N1 and apometHb.

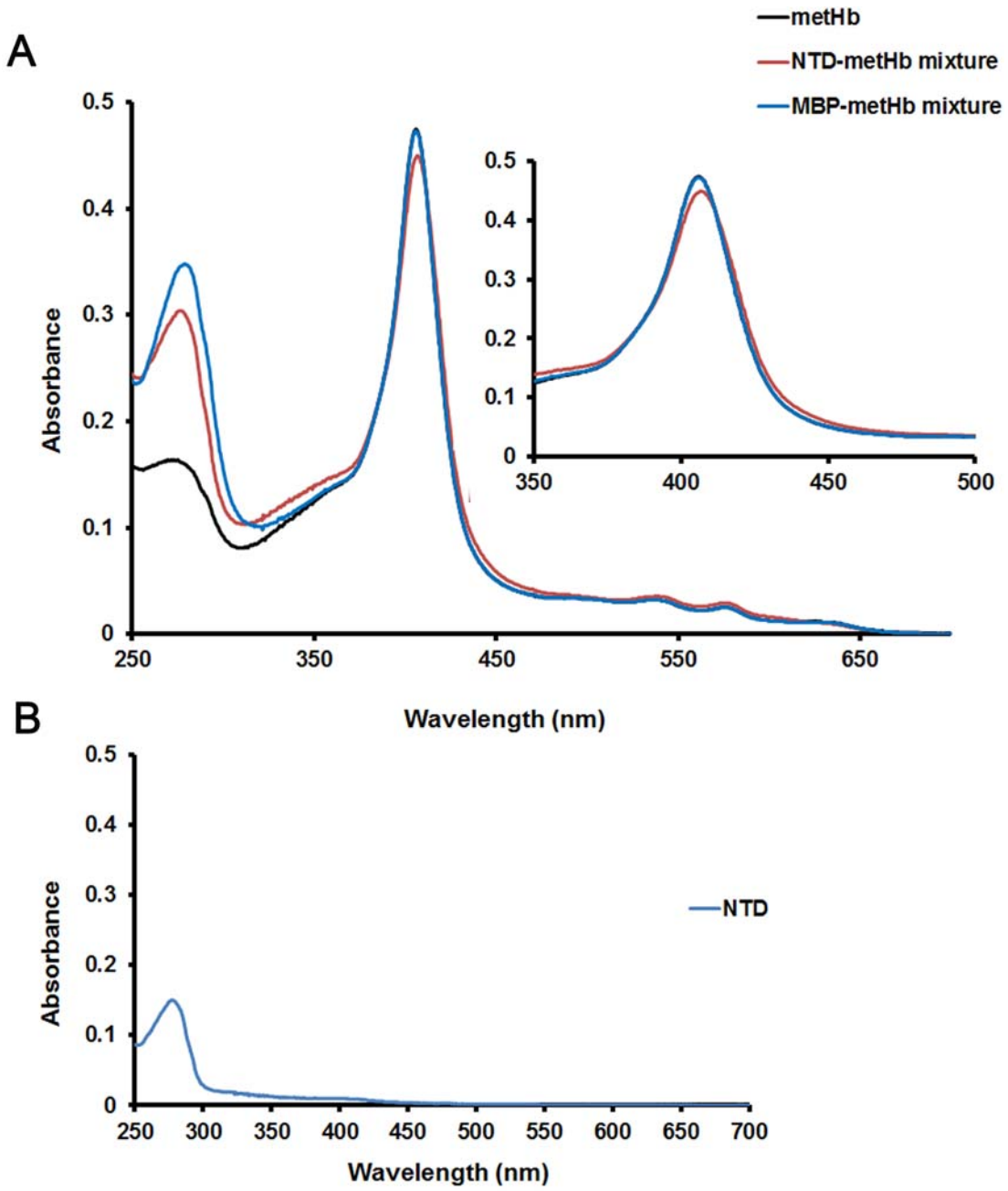

Figure S13: Spectral differences between metHb and NTD-metHb complex. (A) UV-visible spectra of metHb and NTD-metHb, MBP-metHb mixtures. **(B)** UV-visible spectrum of 4.5 μM NTD.

Size exclusion Elution peak of NTD-N1

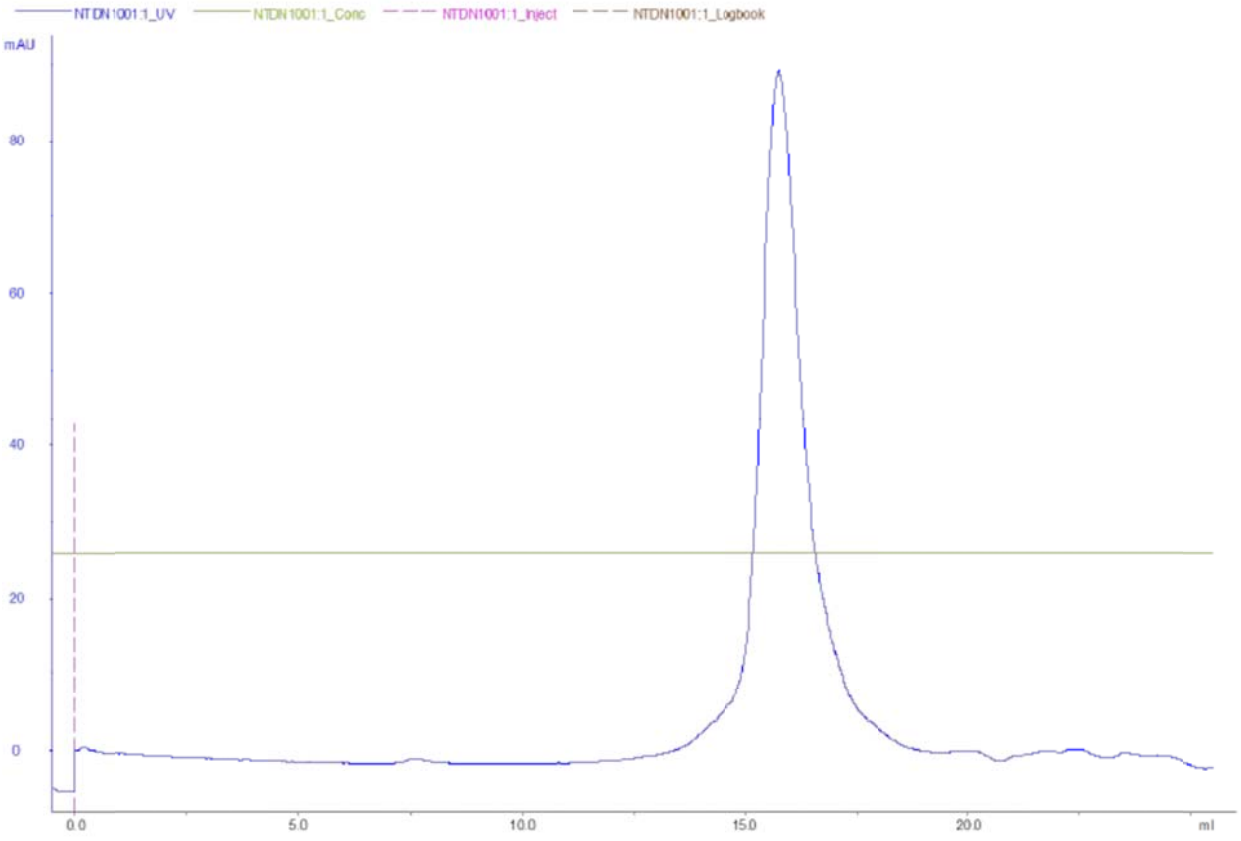

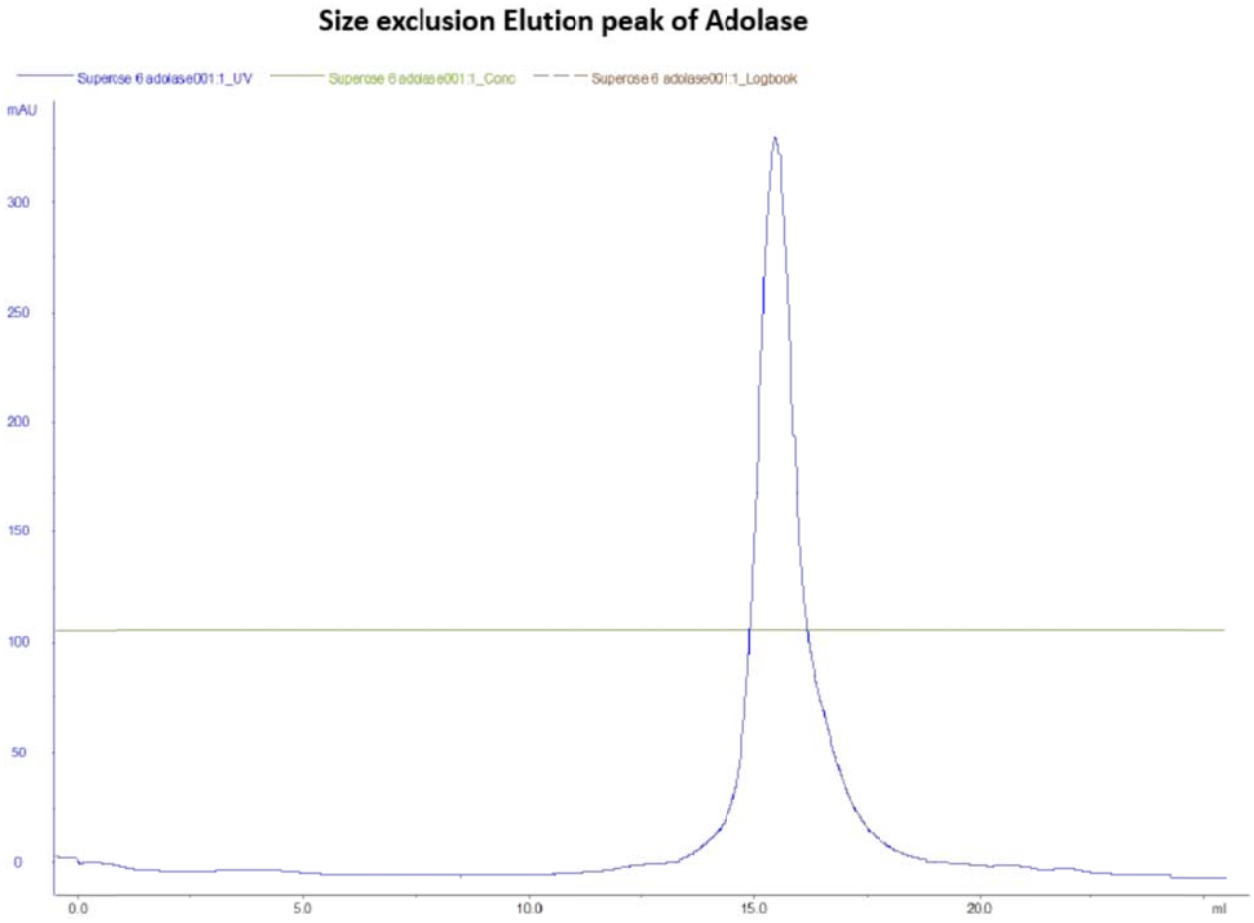

Figure S14: Gel filtration elution profiles of NTD-N1 (A) and aldolase (B).

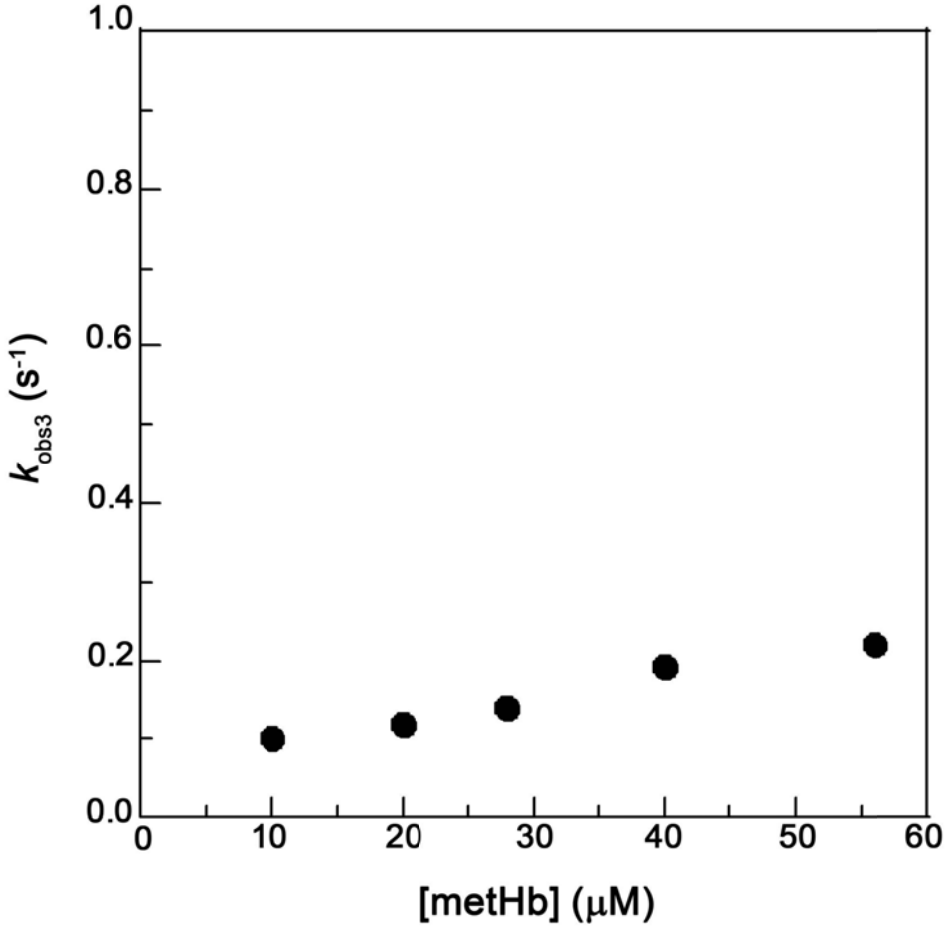

Figure S15: The observed rate constants for the third (k_{obs3}) phase of heme transfer from metHb to Shr.

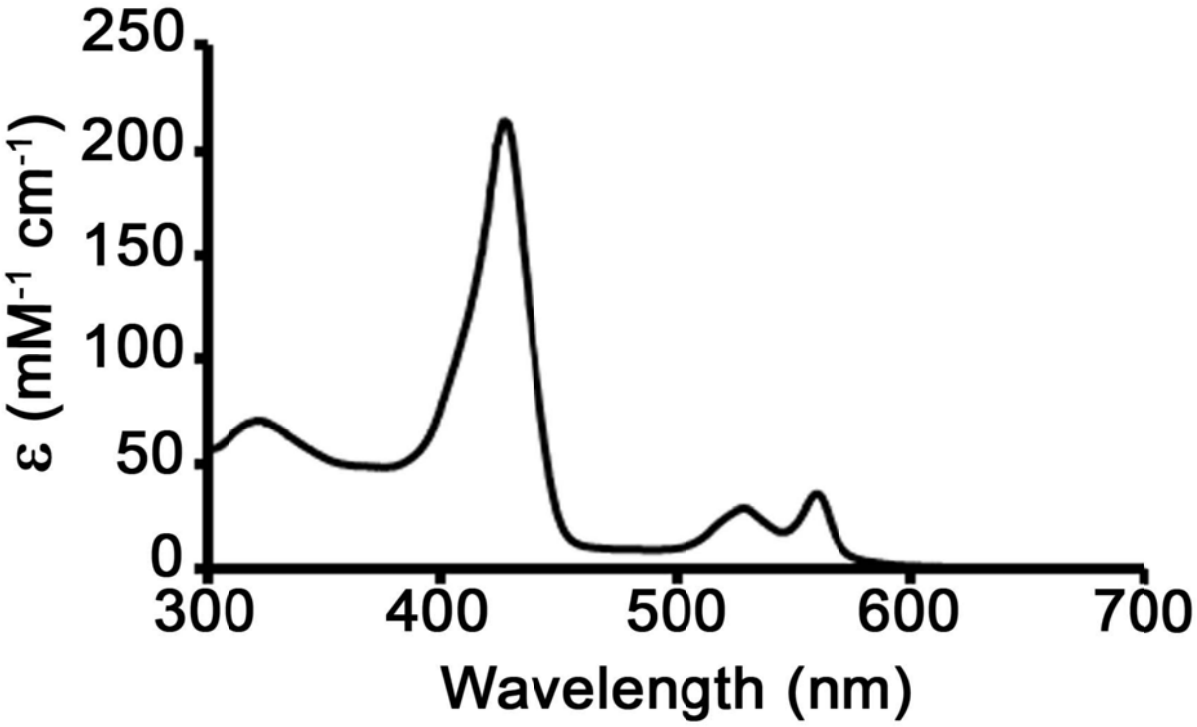

Figure S16: UV-visible spectrum of purified holoShp.

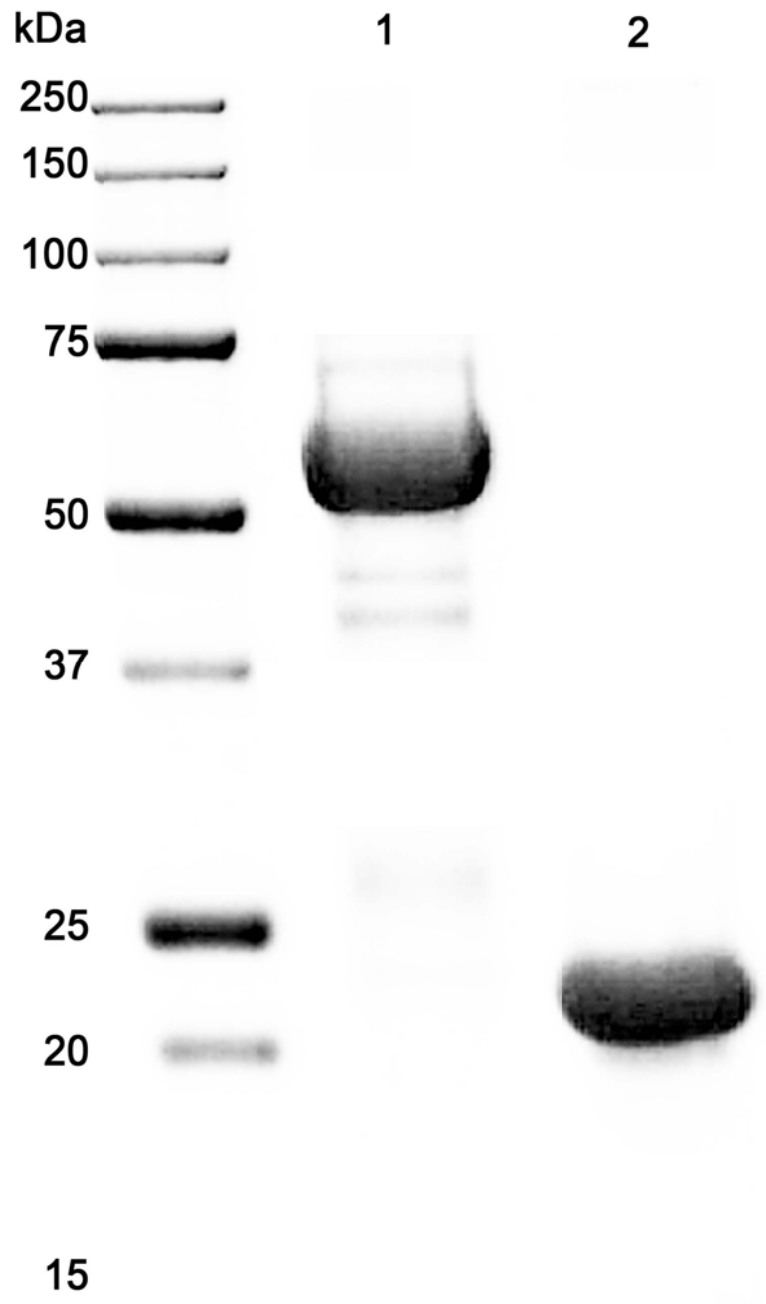

Figure S17: SDS-PAGE analysis of NEAT2 elution fraction after incubation with NEAT1. **(1)** 20 µl of 1 mg/ml control MBP-NEAT1. **(2)** 20 µl of 1 mg/ml NEAT2 eluted from a *Strep*-Tactin Superflow column after incubation with MBP-NEAT1.

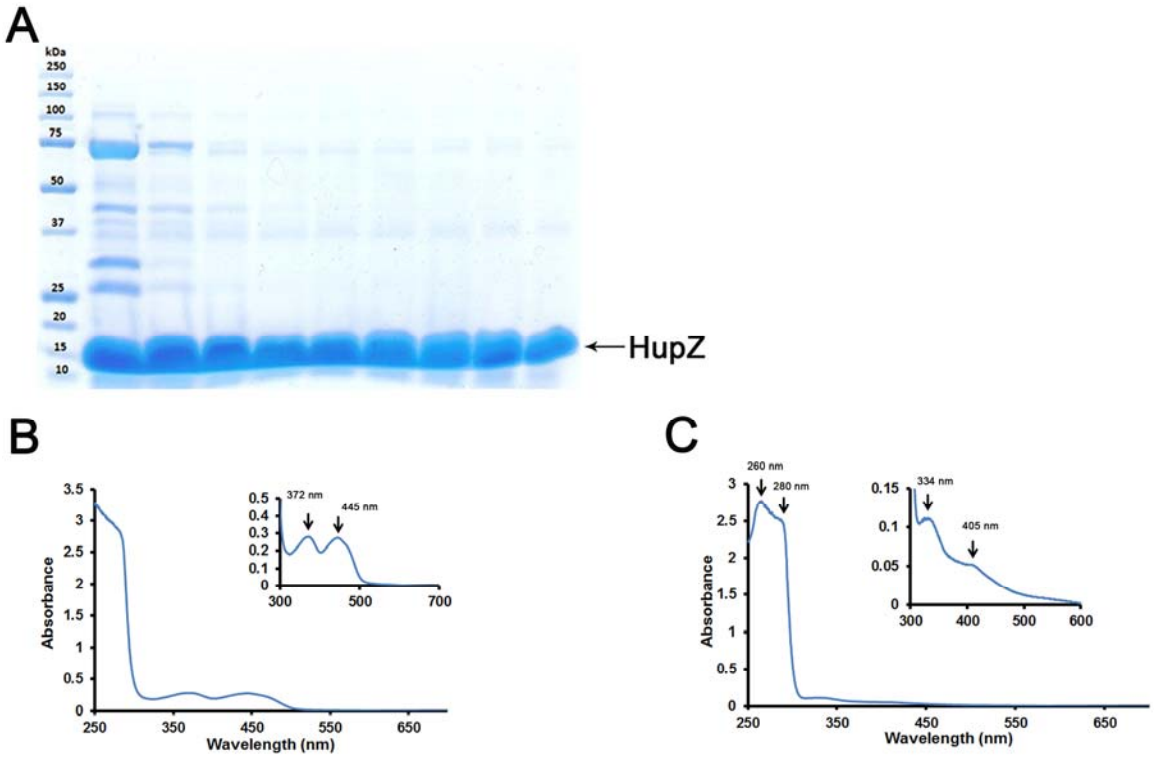

Figure S18: characterization of the purified recombinant HupZ. SDS-PAGE of HupZ elution fractions shows single bands consistent with the expected size of the protein **(A)**. UV-visible absorbance spectra of the yellow eluate showing the characteristic features of oxidized FMN **(B)** and of HupZ as purified **(C)**. The insets show an enlarged scale of the 300-700 nm and 300-600 nm regions, respectively.

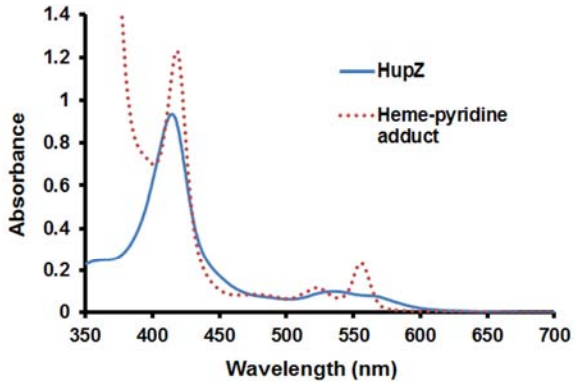

Figure S19: UV-visible absorbance spectra of heme bound HupZ and of the heme-pyridine adduct.

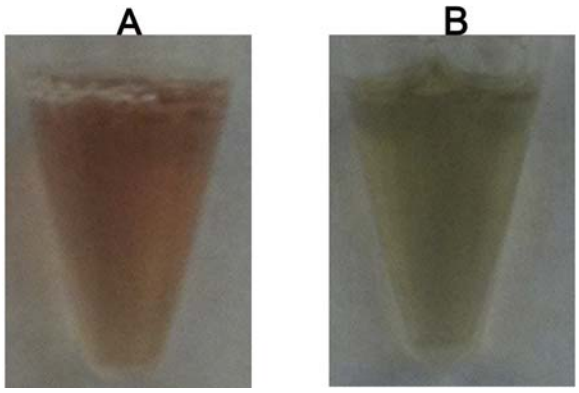

Figure S20: Characteristic color of HupZ-CPR-NADPH heme degradation reaction. The starting color **(A)** and the ending color **(B)** of the reaction showing the change from red to green.

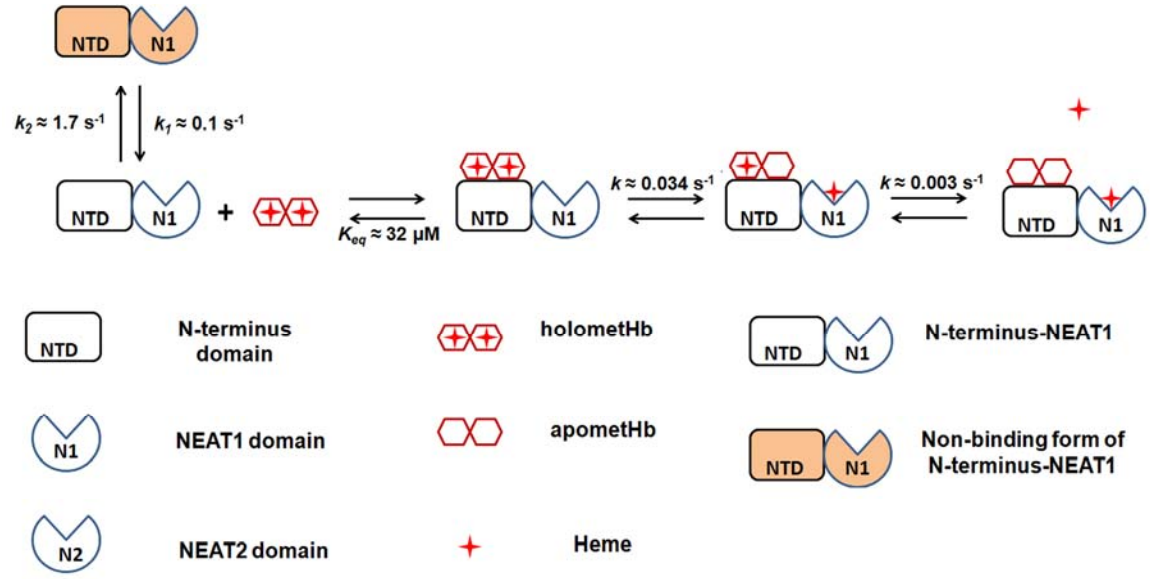

Scheme 1: proposed kinetic model of heme transfer from metHb to apoNTD-N1

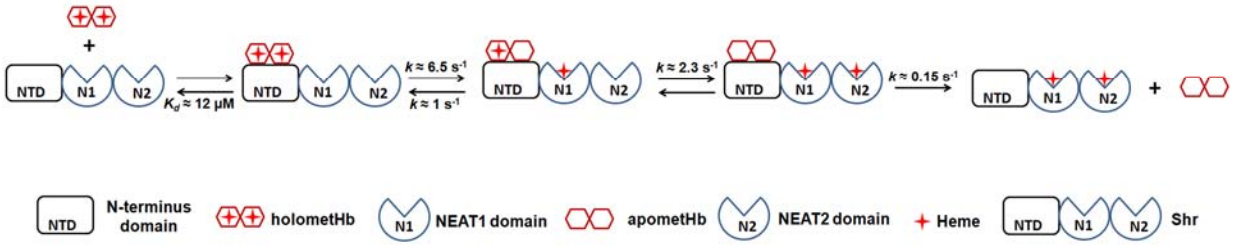

Scheme 2: proposed kinetic model of heme transfer from metHb to apoShr

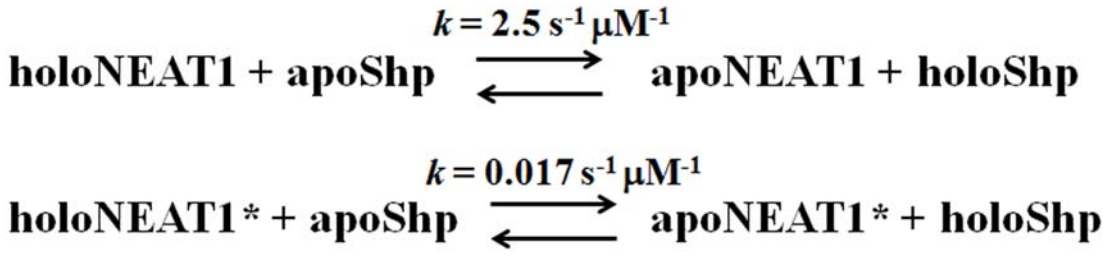

Scheme 3: First and second phases of heme transfer from holoNEAT1 to apoShp HoloNEAT1* and apoNEAT1* represent alternative species of holoNEAT1 and apoNEAT1, respectively.

REFERENCES

1. Carapetis JR, Steer AC, Mulholland EK, Weber M (2005) The global burden of group A streptococcal diseases. Lancet Infect Dis 5: 685-694.
2. Martin JM, Green M (2006) Group A streptococcus. Semin Pediatr Infect Dis 17: 140-148.
3. Lynskey NN, Lawrenson RA, Sriskandan S (2011) New understandings in Streptococcus pyogenes. Curr Opin Infect Dis 24: 196-202.
4. Young MH, Aronoff DM, Engleberg NC (2005) Necrotizing fasciitis: pathogenesis and treatment. Expert Rev Anti Infect Ther 3: 279-294.
5. Cole JN, Henningham A, Gillen CM, Ramachandran V, Walker MJ (2008) Human pathogenic streptococcal proteomics and vaccine development. Proteomics Clin Appl 2: 387-410.
6. Beall B, Facklam R, Thompson T (1996) Sequencing emm-specific PCR products for routine and accurate typing of group A streptococci. J Clin Microbiol 34: 953-958.
7. Bisno AL, Stevens DL (1996) Streptococcal infections of skin and soft tissues. N Engl J Med 334: 240-245.
8. Bisno AL, Gerber MA, Gwaltney JM, Jr., Kaplan EL, Schwartz RH, et al. (2002) Practice guidelines for the diagnosis and management of group A streptococcal pharyngitis. Infectious Diseases Society of America. Clin Infect Dis 35: 113-125.
9. Okada N, Liszewski MK, Atkinson JP, Caparon M (1995) Membrane cofactor protein (CD46) is a keratinocyte receptor for the M protein of the group A streptococcus. Proc Natl Acad Sci U S A 92: 2489-2493.
10. Horstmann RD, Sievertsen HJ, Leippe M, Fischetti VA (1992) Role of fibrinogen in complement inhibition by streptococcal M protein. Infect Immun 60: 5036-5041.
11. Carlsson F, Berggard K, Stalhammar-Carlemalm M, Lindahl G (2003) Evasion of phagocytosis through cooperation between two ligand-binding regions in Streptococcus pyogenes M protein. J Exp Med 198: 1057-1068.
12. Crater DL, van de Rijn I (1995) Hyaluronic acid synthesis operon (has) expression in group A streptococci. J Biol Chem 270: 18452-18458.
13. Dale JB, Washburn RG, Marques MB, Wessels MR (1996) Hyaluronate capsule and surface M protein in resistance to opsonization of group A streptococci. Infect Immun 64: 1495-1501.
14. Buchanan JT, Simpson AJ, Aziz RK, Liu GY, Kristian SA, et al. (2006) DNase expression allows the pathogen group A Streptococcus to escape killing in neutrophil extracellular traps. Curr Biol 16: 396-400.
15. Zinkernagel AS, Timmer AM, Pence MA, Locke JB, Buchanan JT, et al. (2008) The IL-8 protease SpyCEP/ScpC of group A Streptococcus promotes resistance to neutrophil killing. Cell Host Microbe 4: 170-178.
16. Timmer AM, Timmer JC, Pence MA, Hsu LC, Ghochani M, et al. (2009) Streptolysin O promotes group A Streptococcus immune evasion by accelerated macrophage apoptosis. J Biol Chem 284: 862-871.
17. Cole JN BT, Nizet V, Walker MJ. (2011) Molecular insight into invasive group A streptococcal disease. Nat Rev Microbiol 9: 724-736.
18. Ganz T, Nemeth E (2006) Regulation of iron acquisition and iron distribution in mammals. Biochim Biophys Acta 1763: 690-699.

19. Miethke M (2012) Molecular strategies of microbial iron assimilation: from high-affinity complexes to cofactor assembly systems. Metallomics.
20. Wandersman C, Delepelaire P (2004) Bacterial iron sources: from siderophores to hemophores. Annu Rev Microbiol 58: 611-647.
21. Kumar S, Bandyopadhyay U (2005) Free heme toxicity and its detoxification systems in human. Toxicol Lett 157: 175-188.
22. Perutz MF (1960) Structure of hemoglobin. Brookhaven Symp Biol 13: 165-183.
23. Beutler E, Waalen J (2006) The definition of anemia: what is the lower limit of normal of the blood hemoglobin concentration? Blood 107: 1747-1750.
24. Shim BS, Lee TH, Kang YS (1965) Immunological and biochemical investigations of human serum haptoglobin: composition of haptoglobin-haemoglobin intermediate, haemoglobin-binding sites and presence of additional alleles for beta-chain. Nature 207: 1264-1267.
25. Cescau S, Cwerman H, Letoffe S, Delepelaire P, Wandersman C, et al. (2007) Heme acquisition by hemophores. Biometals 20: 603-613.
26. Letoffe S, Ghigo JM, Wandersman C (1994) Iron acquisition from heme and hemoglobin by a Serratia marcescens extracellular protein. Proc Natl Acad Sci U S A 91: 9876-9880.
27. Letoffe S, Nato F, Goldberg ME, Wandersman C (1999) Interactions of HasA, a bacterial haemophore, with haemoglobin and with its outer membrane receptor HasR. Mol Microbiol 33: 546-555.
28. Letoffe S, Delepelaire P, Wandersman C (2004) Free and hemophore-bound heme acquisitions through the outer membrane receptor HasR have different requirements for the TonB-ExbB-ExbD complex. J Bacteriol 186: 4067-4074.
29. Letoffe S, Redeker V, Wandersman C (1998) Isolation and characterization of an extracellular haem-binding protein from Pseudomonas aeruginosa that shares function and sequence similarities with the Serratia marcescens HasA haemophore. Mol Microbiol 28: 1223-1234.
30. Rossi MS, Fetherston JD, Letoffe S, Carniel E, Perry RD, et al. (2001) Identification and characterization of the hemophore-dependent heme acquisition system of Yersinia pestis. Infect Immun 69: 6707-6717.
31. Cope LD, Thomas SE, Latimer JL, Slaughter CA, Muller-Eberhard U, et al. (1994) The 100 kDa haem:haemopexin-binding protein of Haemophilus influenzae: structure and localization. Mol Microbiol 13: 863-873.
32. Henderson DP, Payne SM (1994) Characterization of the Vibrio cholerae outer membrane heme transport protein HutA: sequence of the gene, regulation of expression, and homology to the family of TonB-dependent proteins. J Bacteriol 176: 3269-3277.
33. Torres AG, Payne SM (1997) Haem iron-transport system in enterohaemorrhagic Escherichia coli O157:H7. Mol Microbiol 23: 825-833.
34. Stojiljkovic I, Larson J, Hwa V, Anic S, So M (1996) HmbR outer membrane receptors of pathogenic Neisseria spp.: iron-regulated, hemoglobin-binding proteins with a high level of primary structure conservation. J Bacteriol 178: 4670-4678.
35. Lewis LA, Dyer DW (1995) Identification of an iron-regulated outer membrane protein of Neisseria meningitidis involved in the utilization of hemoglobin complexed to haptoglobin. J Bacteriol 177: 1299-1306.

36. Lewis LA, Gray E, Wang YP, Roe BA, Dyer DW (1997) Molecular characterization of hpuAB, the haemoglobin-haptoglobin-utilization operon of Neisseria meningitidis. Mol Microbiol 23: 737-749.
37. Nobles CL, Maresso AW (2011) The theft of host heme by Gram-positive pathogenic bacteria. Metallomics 3: 788-796.
38. Hammer ND, Skaar EP (2011) Molecular mechanisms of Staphylococcus aureus iron acquisition. Annu Rev Microbiol 65: 129-147.
39. Andrade MA, Ciccarelli FD, Perez-Iratxeta C, Bork P (2002) NEAT: a domain duplicated in genes near the components of a putative Fe3+ siderophore transporter from Gram-positive pathogenic bacteria. Genome Biol 3: RESEARCH0047.
40. Fabian M, Solomaha E, Olson JS, Maresso AW (2009) Heme transfer to the bacterial cell envelope occurs via a secreted hemophore in the Gram-positive pathogen Bacillus anthracis. J Biol Chem 284: 32138-32146.
41. Maresso AW, Garufi G, Schneewind O (2008) *Bacillus anthracis* secretes proteins that mediate heme acquisition from hemoglobin. PLoS Pathog 4: e1000132.
42. Allen CE, Schmitt MP (2011) Novel hemin binding domains in the Corynebacterium diphtheriae HtaA protein interact with hemoglobin and are critical for heme iron utilization by HtaA. J Bacteriol 193: 5374-5385.
43. Tullius MV, Harmston CA, Owens CP, Chim N, Morse RP, et al. (2011) Discovery and characterization of a unique mycobacterial heme acquisition system. Proc Natl Acad Sci U S A 108: 5051-5056.
44. Eichenbaum Z, Muller E, Morse SA, Scott JR (1996) Acquisition of iron from host proteins by the group A streptococcus. Infect Immun 64: 5428-5429.
45. Bates CS, Montañez GE, Woods CR, Vincent RM, Eichenbaum Z (2003) Identification and characterization of a *Streptococcus pyogenes* operon involved in binding of hemoproteins and acquisition of iron. Infect Immun 71: 1042-1055.
46. Montañez GE, Neely MN, Eichenbaum Z (2005) The streptococcal iron uptake (Siu) transporter is required for iron uptake and virulence in a zebrafish infection model. Microbiology 151: 3749-3757.
47. Bates CS, Toukoki C, Neely MN, Eichenbaum Z (2005) Characterization of MtsR, a new metal regulator in group A streptococcus, involved in iron acquisition and virulence. Infect Immun 73: 5743-5753.
48. Fisher M, Huang YS, Li X, McIver KS, Toukoki C, et al. (2008) Shr is a broad-spectrum surface receptor that contributes to adherence and virulence in group A streptococcus. Infect Immun 76: 5006-5015.
49. Aranda Rt, Worley CE, Liu M, Bitto E, Cates MS, et al. (2007) Bis-methionyl coordination in the crystal structure of the heme-binding domain of the streptococcal cell surface protein Shp. J Mol Biol 374: 374-383.
50. Lei B, Smoot LM, Menning HM, Voyich JM, Kala SV, et al. (2002) Identification and characterization of a novel heme-associated cell surface protein made by Streptococcus pyogenes. Infect Immun 70: 4494-4500.
51. Sook BR, Block DR, Sumithran S, Montanez GE, Rodgers KR, et al. (2008) Characterization of SiaA, a streptococcal heme-binding protein associated with a heme ABC transport system. Biochemistry 47: 2678-2688.

52. Sun X, Ge R, Zhang D, Sun H, He QY (2010) Iron-containing lipoprotein SiaA in SiaABC, the primary heme transporter of Streptococcus pyogenes. J Biol Inorg Chem 15: 1265-1273.
53. Lei B, Liu M, Voyich JM, Prater CI, Kala SV, et al. (2003) Identification and characterization of HtsA, a second heme-binding protein made by *Streptococcus pyogenes*. Infect Immun 71: 5962-5969.
54. Zhu H, Liu M, Lei B (2008) The surface protein Shr of *Streptococcus pyogenes* binds heme and transfers it to the streptococcal heme-binding protein Shp. BMC Microbiol 8: 15.
55. Dahesh S, Nizet V, Cole JN (2012) Study of streptococcal hemoprotein receptor (Shr) in iron acquisition and virulence of M1T1 group A streptococcus. Virulence 3.
56. Letoffe S, Heuck G, Delepelaire P, Lange N, Wandersman C (2009) Bacteria capture iron from heme by keeping tetrapyrrol skeleton intact. Proc Natl Acad Sci U S A 106: 11719-11724.
57. Anzaldi LL, Skaar EP (2010) Overcoming the heme paradox: heme toxicity and tolerance in bacterial pathogens. Infect Immun 78: 4977-4989.
58. Dailey HA, Septer AN, Daugherty L, Thames D, Gerdes S, et al. (2011) The Escherichia coli protein YfeX functions as a porphyrinogen oxidase, not a heme dechelatase. MBio 2: e00248-00211.
59. Brown SB (1976) Stereospecific haem cleavage. A model for the formation of bile-pigment isomers in vivo and in vitro. Biochem J 159: 23-27.
60. Maines MD (1997) The heme oxygenase system: a regulator of second messenger gases. Annu Rev Pharmacol Toxicol 37: 517-554.
61. McCoubrey WK, Jr., Huang TJ, Maines MD (1997) Isolation and characterization of a cDNA from the rat brain that encodes hemoprotein heme oxygenase-3. Eur J Biochem 247: 725-732.
62. Schipper HM (2004) Heme oxygenase expression in human central nervous system disorders. Free Radic Biol Med 37: 1995-2011.
63. Abraham NG, Kappas A (2005) Heme oxygenase and the cardiovascular-renal system. Free Radic Biol Med 39: 1-25.
64. Li C, Stocker R (2009) Heme oxygenase and iron: from bacteria to humans. Redox Rep 14: 95-101.
65. Parfenova H, Leffler CW (2008) Cerebroprotective functions of HO-2. Curr Pharm Des 14: 443-453.
66. Unno M, Matsui T, Ikeda-Saito M (2007) Structure and catalytic mechanism of heme oxygenase. Nat Prod Rep 24: 553-570.
67. Ndisang JF, Tabien HE, Wang R (2004) Carbon monoxide and hypertension. J Hypertens 22: 1057-1074.
68. Wong RJ, Zhao H, Stevenson DK (2012) A deficiency in haem oxygenase-1 induces foetal growth restriction by placental vasculature defects. Acta Paediatr 101: 827-834.
69. Molzer C, Huber H, Steyrer A, Ziesel G, Ertl A, et al. (2012) In vitro antioxidant capacity and antigenotoxic properties of protoporphyrin and structurally related tetrapyrroles. Free Radic Res 46: 1369-1377.

70. Stocker R, Peterhans E (1989) Antioxidant properties of conjugated bilirubin and biliverdin: biologically relevant scavenging of hypochlorous acid. Free Radic Res Commun 6: 57-66.
71. Grochot-Przeczek A, Dulak J, Jozkowicz A (2012) Haem oxygenase-1: non-canonical roles in physiology and pathology. Clin Sci (Lond) 122: 93-103.
72. Schmitt MP (1997) Utilization of host iron sources by *Corynebacterium diphtheriae*: identification of a gene whose product is homologous to eukaryotic heme oxygenases and is required for acquisition of iron from heme and hemoglobin. J Bacteriol 179: 838-845.
73. Wilks A, Schmitt MP (1998) Expression and characterization of a heme oxygenase (Hmu O) from *Corynebacterium diphtheriae*. Iron acquisition requires oxidative cleavage of the heme macrocycle. J Biol Chem 273: 837-841.
74. Zhu W, Wilks A, Stojiljkovic I (2000) Degradation of heme in gram-negative bacteria: the product of the hemO gene of Neisseriae is a heme oxygenase. J Bacteriol 182: 6783-6790.
75. Bruggemann H, Bauer R, Raffestin S, Gottschalk G (2004) Characterization of a heme oxygenase of Clostridium tetani and its possible role in oxygen tolerance. Arch Microbiol 182: 259-263.
76. Hassan S, Ohtani K, Wang R, Yuan Y, Wang Y, et al. (2010) Transcriptional regulation of hemO encoding heme oxygenase in Clostridium perfringens. J Microbiol 48: 96-101.
77. Ratliff M, Zhu W, Deshmukh R, Wilks A, Stojiljkovic I (2001) Homologues of neisserial heme oxygenase in gram-negative bacteria: degradation of heme by the product of the pigA gene of Pseudomonas aeruginosa. J Bacteriol 183: 6394-6403.
78. Wegele R, Tasler R, Zeng Y, Rivera M, Frankenberg-Dinkel N (2004) The heme oxygenase(s)-phytochrome system of Pseudomonas aeruginosa. J Biol Chem 279: 45791-45802.
79. Schluchter WM, Glazer AN (1997) Characterization of cyanobacterial biliverdin reductase. Conversion of biliverdin to bilirubin is important for normal phycobiliprotein biosynthesis. J Biol Chem 272: 13562-13569.
80. Frankenberg N, Mukougawa K, Kohchi T, Lagarias JC (2001) Functional genomic analysis of the HY2 family of ferredoxin-dependent bilin reductases from oxygenic photosynthetic organisms. Plant Cell 13: 965-978.
81. Reniere ML, Torres VJ, Skaar EP (2007) Intracellular metalloporphyrin metabolism in Staphylococcus aureus. Biometals 20: 333-345.
82. Skaar EP, Gaspar AH, Schneewind O (2004) IsdG and IsdI, heme-degrading enzymes in the cytoplasm of *Staphylococcus aureus*. J Biol Chem 279: 436-443.
83. Wu R, Skaar EP, Zhang R, Joachimiak G, Gornicki P, et al. (2005) *Staphylococcus aureus* IsdG and IsdI, heme-degrading enzymes with structural similarity to monooxygenases. J Biol Chem 280: 2840-2846.
84. Puri S, O'Brian MR (2006) The hmuQ and hmuD genes from Bradyrhizobium japonicum encode heme-degrading enzymes. J Bacteriol 188: 6476-6482.
85. Chim N, Iniguez A, Nguyen TQ, Goulding CW (2010) Unusual diheme conformation of the heme-degrading protein from Mycobacterium tuberculosis. J Mol Biol 395: 595-608.
86. Haley KP, Janson EM, Heilbronner S, Foster TJ, Skaar EP (2011) Staphylococcus lugdunensis IsdG liberates iron from host heme. J Bacteriol 193: 4749-4757.

87. Skaar EP, Gaspar AH, Schneewind O (2006) Bacillus anthracis IsdG, a heme-degrading monooxygenase. J Bacteriol 188: 1071-1080.
88. Suits MD, Pal GP, Nakatsu K, Matte A, Cygler M, et al. (2005) Identification of an Escherichia coli O157:H7 heme oxygenase with tandem functional repeats. Proc Natl Acad Sci U S A 102: 16955-16960.
89. Stojiljkovic I, Hantke K (1994) Transport of haemin across the cytoplasmic membrane through a haemin-specific periplasmic binding-protein-dependent transport system in Yersinia enterocolitica. Mol Microbiol 13: 719-732.
90. Liu M, Boulouis HJ, Biville F (2012) Heme degrading protein HemS is involved in oxidative stress response of Bartonella henselae. PLoS One 7: e37630.
91. Ridley KA, Rock JD, Li Y, Ketley JM (2006) Heme utilization in Campylobacter jejuni. J Bacteriol 188: 7862-7875.
92. Guo Y, Guo G, Mao X, Zhang W, Xiao J, et al. (2008) Functional identification of HugZ, a heme oxygenase from Helicobacter pylori. BMC Microbiol 8: 226.
93. Uchida T, Sekine Y, Matsui T, Ikeda-Saito M, Ishimori K (2012) A heme degradation enzyme, HutZ, from Vibrio cholerae. Chem Commun (Camb) 48: 6741-6743.
94. Hu Y, Jiang F, Guo Y, Shen X, Zhang Y, et al. (2011) Crystal structure of HugZ, a novel heme oxygenase from Helicobacter pylori. J Biol Chem 286: 1537-1544.
95. Liu X, Gong J, Wei T, Wang Z, Du Q, et al. (2012) Crystal structure of HutZ, a heme storage protein from Vibrio cholerae: A structural mismatch observed in the region of high sequence conservation. BMC Struct Biol 12: 23.
96. Bullen JJ (1981) The significance of iron in infection. Rev Infect Dis 3: 1127-1138.
97. Stojiljkovic I, Perkins-Balding D (2002) Processing of heme and heme-containing proteins by bacteria. DNA Cell Biol 21: 281-295.
98. Tong Y, Guo M (2009) Bacterial heme-transport proteins and their heme-coordination modes. Arch Biochem Biophys 481: 1-15.
99. Drazek ES, Hammack CA, Schmitt MP (2000) *Corynebacterium diphtheriae* genes required for acquisition of iron from haemin and haemoglobin are homologous to ABC haemin transporters. Mol Microbiol 36: 68-84.
100. Hornung JM, Jones HA, Perry RD (1996) The *hmu* locus of *Yersinia pestis* is essential for utilization of free haemin and haem--protein complexes as iron sources. Mol Microbiol 20: 725-739.
101. Thompson JM, Jones HA, Perry RD (1999) Molecular characterization of the hemin uptake locus (*hmu*) from *Yersinia pestis* and analysis of hmu mutants for hemin and hemoprotein utilization. Infect Immun 67: 3879-3892.
102. Allen CE, Schmitt MP (2009) HtaA is an iron-regulated hemin binding protein involved in the utilization of heme iron in *Corynebacterium diphtheriae*. J Bacteriol 191: 2638-2648.
103. Kunkle CA, Schmitt MP (2007) Comparative analysis of *hmu*O function and expression in Corynebacterium species. J Bacteriol 189: 3650-3654.
104. Clarke SR, Wiltshire MD, Foster SJ (2004) IsdA of *Staphylococcus aureus* is a broad spectrum, iron-regulated adhesin. Mol Microbiol 51: 1509-1519.
105. Dryla A, Gelbmann D, von Gabain A, Nagy E (2003) Identification of a novel iron regulated staphylococcal surface protein with haptoglobin-haemoglobin binding activity. Mol Microbiol 49: 37-53.

106. Mazmanian SK, Skaar EP, Gaspar AH, Humayun M, Gornicki P, et al. (2003) Passage of heme-iron across the envelope of *Staphylococcus aureus*. Science 299: 906-909.
107. Torres VJ, Pishchany G, Humayun M, Schneewind O, Skaar EP (2006) *Staphylococcus aureus* IsdB is a hemoglobin receptor required for heme iron utilization. J Bacteriol 188: 8421-8429.
108. Skaar EP, Schneewind O (2004) Iron-regulated surface determinants (Isd) of *Staphylococcus aureus*: stealing iron from heme. Microbes Infect 6: 390-397.
109. Marraffini LA, Schneewind O (2005) Anchor structure of staphylococcal surface proteins. V. Anchor structure of the sortase B substrate IsdC. J Biol Chem 280: 16263-16271.
110. Mazmanian SK, Ton-That H, Su K, Schneewind O (2002) An iron-regulated sortase anchors a class of surface protein during *Staphylococcus aureus* pathogenesis. Proc Natl Acad Sci U S A 99: 2293-2298.
111. Grigg JC, Vermeiren CL, Heinrichs DE, Murphy ME (2007) Haem recognition by a *Staphylococcus aureus* NEAT domain. Mol Microbiol 63: 139-149.
112. Pluym M, Muryoi N, Heinrichs DE, Stillman MJ (2008) Heme binding in the NEAT domains of IsdA and IsdC of *Staphylococcus aureus*. J Inorg Biochem 102: 480-488.
113. Sharp KH, Schneider S, Cockayne A, Paoli M (2007) Crystal structure of the heme-IsdC complex, the central conduit of the Isd iron/heme uptake system in *Staphylococcus aureus*. J Biol Chem 282: 10625-10631.
114. Villareal VA, Pilpa RM, Robson SA, Fadeev EA, Clubb RT (2008) The IsdC protein from *Staphylococcus aureus* uses a flexible binding pocket to capture heme. J Biol Chem 283: 31591-31600.
115. Watanabe M, Tanaka Y, Suenaga A, Kuroda M, Yao M, et al. (2008) Structural basis for multimeric heme complexation through a specific protein-heme interaction: the case of the third neat domain of IsdH from *Staphylococcus aureus*. J Biol Chem 283: 28649-28659.
116. Pilpa RM, Robson SA, Villareal VA, Wong ML, Phillips M, et al. (2009) Functionally distinct NEAT (NEAr Transporter) domains within the *Staphylococcus aureus* IsdH/HarA protein extract heme from methemoglobin. J Biol Chem 284: 1166-1176.
117. Tiedemann MT, Muryoi N, Heinrichs DE, Stillman MJ (2008) Iron acquisition by the haem-binding Isd proteins in *Staphylococcus aureus*: studies of the mechanism using magnetic circular dichroism. Biochem Soc Trans 36: 1138-1143.
118. Dryla A, Hoffmann B, Gelbmann D, Giefing C, Hanner M, et al. (2007) High-affinity binding of the staphylococcal HarA protein to haptoglobin and hemoglobin involves a domain with an antiparallel eight-stranded beta-barrel fold. J Bacteriol 189: 254-264.
119. Pilpa RM, Fadeev EA, Villareal VA, Wong ML, Phillips M, et al. (2006) Solution structure of the NEAT (NEAr Transporter) domain from IsdH/HarA: the human hemoglobin receptor in *Staphylococcus aureus*. J Mol Biol 360: 435-447.
120. Jin B, Newton SM, Shao Y, Jiang X, Charbit A, et al. (2006) Iron acquisition systems for ferric hydroxamates, haemin and haemoglobin in *Listeria monocytogenes*. Mol Microbiol 59: 1185-1198.
121. Gat O, Zaide G, Inbar I, Grosfeld H, Chitlaru T, et al. (2008) Characterization of *Bacillus anthracis* iron-regulated surface determinant (Isd) proteins containing NEAT domains. Mol Microbiol 70: 983-999.

122. Maresso AW, Chapa TJ, Schneewind O (2006) Surface protein IsdC and Sortase B are required for heme-iron scavenging of *Bacillus anthracis*. J Bacteriol 188: 8145-8152.
123. Daou N, Buisson C, Gohar M, Vidic J, Bierne H, et al. (2009) IlsA, a unique surface protein of *Bacillus cereus* required for iron acquisition from heme, hemoglobin and ferritin. PLoS Pathog 5: e1000675.
124. Letunic I, Doerks T, Bork P (2009) SMART 6: recent updates and new developments. Nucleic Acids Res 37: D229-232.
125. Schultz J, Milpetz F, Bork P, Ponting CP (1998) SMART, a simple modular architecture research tool: identification of signaling domains. Proc Natl Acad Sci U S A 95: 5857-5864.
126. Holden MT, Heather Z, Paillot R, Steward KF, Webb K, et al. (2009) Genomic evidence for the evolution of *Streptococcus equi*: host restriction, increased virulence, and genetic exchange with human pathogens. PLoS Pathog 5: e1000346.
127. Makinen MWaC, A. K., editor (1983) Structural and Analytical Aspects of the Electronic Spectra of Hemproteins. Reading, MA: Addison-Wesley Publishing Company, Inc. 141-236 p.
128. Grigg JC, Ukpabi G, Gaudin CF, Murphy ME (2010) Structural biology of heme binding in the *Staphylococcus aureus* Isd system. J Inorg Biochem 104: 341-348.
129. Ascenzi P, Bocedi A, Visca P, Altruda F, Tolosano E, et al. (2005) Hemoglobin and heme scavenging. IUBMB Life 57: 749-759.
130. Umbreit J (2007) Methemoglobin--it's not just blue: a concise review. Am J Hematol 82: 134-144.
131. Asakura T, Minakami S, Yoneyama Y, Yoshikawa H (1964) Combination of globin and its derivatives with hemins and porphyrins. J Biochem 56: 594-600.
132. Francis RT, Jr., Booth JW, Becker RR (1985) Uptake of iron from hemoglobin and the haptoglobin-hemoglobin complex by hemolytic bacteria. Int J Biochem 17: 767-773.
133. Kobe B, Kajava AV (2001) The leucine-rich repeat as a protein recognition motif. Curr Opin Struct Biol 11: 725-732.
134. Michiels J, Xi C, Verhaert J, Vanderleyden J (2002) The functions of Ca(2+) in bacteria: a role for EF-hand proteins? Trends Microbiol 10: 87-93.
135. Rigden DJ, Jedrzejas MJ, Galperin MY (2003) An extracellular calcium-binding domain in bacteria with a distant relationship to EF-hands. FEMS Microbiol Lett 221: 103-110.
136. Zhou Y, Yang W, Kirberger M, Lee HW, Ayalasomayajula G, et al. (2006) Prediction of EF-hand calcium-binding proteins and analysis of bacterial EF-hand proteins. Proteins 65: 643-655.
137. Vermeiren CL, Pluym M, Mack J, Heinrichs DE, Stillman MJ (2006) Characterization of the heme binding properties of *Staphylococcus aureus* IsdA. Biochemistry 45: 12867-12875.
138. Meehan M, Burke FM, Macken S, Owen P (2010) Characterization of the haem-uptake system of the equine pathogen *Streptococcus equi* subsp. *equi*. Microbiology.
139. Genco CA, Dixon DW (2001) Emerging strategies in microbial haem capture. Mol Microbiol 39: 1-11.
140. Eichenbaum Z, Federle MJ, Marra D, de Vos WM, Kuipers OP, et al. (1998) Use of the lactococcal *nis*A promoter to regulate gene expression in gram-positive bacteria:

comparison of induction level and promoter strength. Appl Environ Microbiol 64: 2763-2769.
141. Sambrook J, Fritsch EF, Maniatis T (1989) Molecular Cloning: A Laboratory Manual: Cold Spring Harbor Laboratory Press. 105 p.
142. Brown SB, Lantzke IR (1969) Solution structures of ferrihaem in some dipolar aprotic solvents and their binary aqueous mixtures. Biochem J 115: 279-285.
143. Collier GS, Pratt JM, De Wet CR, Tshabalala CF (1979) Studies on haemin in dimethyl sulphoxide/water mixtures. Biochem J 179: 281-289.
144. Mayfield JA, Dehner CA, DuBois JL (2011) Recent advances in bacterial heme protein biochemistry. Curr Opin Chem Biol 15: 260-266.
145. Pishchany G, Skaar EP (2012) Taste for blood: hemoglobin as a nutrient source for pathogens. PLoS Pathog 8: e1002535.
146. Liu M, Tanaka WN, Zhu H, Xie G, Dooley DM, et al. (2008) Direct hemin transfer from IsdA to IsdC in the iron-regulated surface determinant (Isd) heme acquisition system of *Staphylococcus aureus*. J Biol Chem 283: 6668-6676.
147. Honsa ES, Fabian M, Cardenas AM, Olson JS, Maresso AW (2011) The five near-iron transporter (NEAT) domain anthrax hemophore, IsdX2, scavenges heme from hemoglobin and transfers heme to the surface protein IsdC. J Biol Chem 286: 33652-33660.
148. Ouattara M, Cunha EB, Li X, Huang YS, Dixon D, et al. (2010) Shr of group A streptococcus is a new type of composite NEAT protein involved in sequestering haem from methaemoglobin. Mol Microbiol 78: 739-756.
149. Gaudin CF, Grigg JC, Arrieta AL, Murphy ME (2011) Unique heme-iron coordination by the hemoglobin receptor IsdB of Staphylococcus aureus. Biochemistry 50: 5443-5452.
150. Yanyi C, Shenghui X, Yubin Z, Jie YJ (2010) Calciomics: prediction and analysis of EF-hand calcium binding proteins by protein engineering. Sci China Chem 53: 52-60.
151. Tarlovsky Y, Fabian M, Solomaha E, Honsa E, Olson JS, et al. (2010) A Bacillus anthracis S-layer homology protein that binds heme and mediates heme delivery to IsdC. J Bacteriol 192: 3503-3511.
152. Nygaard TK, Blouin GC, Liu M, Fukumura M, Olson JS, et al. (2006) The mechanism of direct heme transfer from the streptococcal cell surface protein Shp to HtsA of the HtsABC transporter. J Biol Chem 281: 20761-20771.
153. Nygaard TK, Liu M, McClure MJ, Lei B (2006) Identification and characterization of the heme-binding proteins SeShp and SeHtsA of Streptococcus equi subspecies equi. BMC Microbiol 6: 82.
154. Morrison M, Horie S (1965) Determination of heme a concentration in cytochrome preparations by hemochromogen method. Anal Biochem 12: 77-82.
155. Zou J, Hofer AM, Lurtz MM, Gadda G, Ellis AL, et al. (2007) Developing sensors for real-time measurement of high Ca2+ concentrations. Biochemistry 46: 12275-12288.
156. Vogt AD, Di Cera E (2012) Conformational Selection or Induced Fit? A Critical Appraisal of the Kinetic Mechanism. Biochemistry.
157. Andersen CB, Torvund-Jensen M, Nielsen MJ, de Oliveira CL, Hersleth HP, et al. (2012) Structure of the haptoglobin-haemoglobin complex. Nature 489: 456-459.

158. Lambeth JD, Geren LM, Millett F (1984) Adrenodoxin interaction with adrenodoxin reductase and cytochrome P-450scc. Cross-linking of protein complexes and effects of adrenodoxin modification by 1-ethyl-3-(3-dimethylaminopropyl)carbodiimide. J Biol Chem 259: 10025-10029.
159. Tamburini PP, White RE, Schenkman JB (1985) Chemical characterization of protein-protein interactions between cytochrome P-450 and cytochrome b5. J Biol Chem 260: 4007-4015.
160. Rohde KH, Dyer DW (2004) Analysis of haptoglobin and hemoglobin-haptoglobin interactions with the Neisseria meningitidis TonB-dependent receptor HpuAB by flow cytometry. Infect Immun 72: 2494-2506.
161. Hamaguchi H (1969) Purification and some properties of the three common genetic types of haptoglovins and the hemoglobin-haptoglobin complexes. American Journal of Human Genetics 21: 440-456.
162. Smith MJ, and Beck, W.S. (1967) Peroxidase activity of hemoglobin and its subunits: Effects thereupon of haptoglobin. Biochimica and Biophysica Acta - Protein Structure 147: 324-333.
163. Hargrove MS, Whitaker T, Olson JS, Vali RJ, Mathews AJ (1997) Quaternary structure regulates hemin dissociation from human hemoglobin. J Biol Chem 272: 17385-17389.
164. Zhu H, Xie G, Liu M, Olson JS, Fabian M, et al. (2008) Pathway for heme uptake from human methemoglobin by the iron-regulated surface determinants system of *Staphylococcus aureus*. J Biol Chem 283: 18450-18460.
165. Yukl ET, Jepkorir G, Alontaga AY, Pautsch L, Rodriguez JC, et al. (2010) Kinetic and spectroscopic studies of hemin acquisition in the hemophore HasAp from Pseudomonas aeruginosa. Biochemistry 49: 6646-6654.
166. Fitzpatrick PF, Massey V (1982) The kinetic mechanism of D-amino acid oxidase with D-alpha-aminobutyrate as substrate. Effect of enzyme concentration on the kinetics. J Biol Chem 257: 12916-12923.
167. Lu C, Xie G, Liu M, Zhu H, Lei B (2012) Direct heme transfer reactions in the group a streptococcus heme acquisition pathway. PLoS One 7: e37556.
168. Nallamsetty S, Austin BP, Penrose KJ, Waugh DS (2005) Gateway vectors for the production of combinatorially-tagged His6-MBP fusion proteins in the cytoplasm and periplasm of Escherichia coli. Protein Sci 14: 2964-2971.
169. Unno M, Matsui T, Chu GC, Couture M, Yoshida T, et al. (2004) Crystal structure of the dioxygen-bound heme oxygenase from Corynebacterium diphtheriae: implications for heme oxygenase function. J Biol Chem 279: 21055-21061.
170. Toukoki C, Gold KM, McIver KS, Eichenbaum Z (2010) MtsR is a dual regulator that controls virulence genes and metabolic functions in addition to metal homeostasis in the group A streptococcus. Mol Microbiol 76: 971-989.
171. Macheroux P, Petersen J, Bornemann S, Lowe DJ, Thorneley RN (1996) Binding of the oxidized, reduced, and radical flavin species to chorismate synthase. An investigation by spectrophotometry, fluorimetry, and electron paramagnetic resonance and electron nuclear double resonance spectroscopy. Biochemistry 35: 1643-1652.
172. Ramjee MK, Coggins, J. R., Hawkes, T. R., Lowe, D. J., & Thorneley, R. N. F. (1993) The Stoichiometry Of Binding Of Flavin Mononucleotide (FMN) Hydroquinone To

Escherichia Coli Chorismate Synthase. Bioorganic & Medicinal Chemistry Letters 3: 1409-1414.